

A First Proof Sprint

J. Corneli*

Hyperreal Enterprises Ltd

February 11–13, 2026

*Email: joseph.corneli@hyperreal.enterprises

Reproducibility: built February 17, 2026 from `futon6` version-controlled git history (c92a4eb).
Source: <https://github.com/tothedarktowercame/futon6>

Abstract

This monograph reports a multi-agent proof sprint on ten research-level problems, combining rapid draft generation with adversarial verification, targeted repair, and explicit provenance. The workflow uses wiring-diagram decompositions of claim dependencies to localize gaps and coordinate reviewer-driven revisions. Final outcomes are heterogeneous but explicit: the manuscript distinguishes *mathematical status* from *QC-validation status*. In the current ledger, Problems 1, 2, 3, and 8 are treated as mathematically closed with validation-complete records (Problem 2 still depends on the cited newvector/test-vector theorem input); Problems 5 and 7 are mathematically closed with partial QC status (scope-limited closure for Problem 5, and an independent theorem-ledger re-check pending for Problem 7). Problem 4 is partial: proved analytically for $n \leq 3$, and proved for $n = 4$ via the Path 2 algebraic certificate, with higher n open. Problem 6 is partial: the K_n case is proved with $c_0 = 1/3$, while the general-graph bridge remains open (formal $\bar{d} < 1$ bound at $M_t \neq 0$). Problem 9 has strong computational evidence but lacks a clean algebraic closure of the universal converse step. Problem 10 remains conditional under explicitly stated assumptions. The main methodological result is that structure-aware verification and layer-switching strategies improve reliability and calibration in compressed proof sprints.

Contents

Abstract	ii
I Annotated Overview	1
1 Problem 1: Measure Equivalence Under Smooth Shifts of the Φ_3^4 Measure	2
2 Problem 2: Universal Test Vector for Rankin–Selberg Integrals	4
3 Problem 3: Markov Chain with ASEP Polynomial Stationary Distribution	6
4 Problem 4: Root Separation Energy Under Finite Free Convolution ($n = 4$)	8
5 Problem 5: \mathcal{O} -Slice Connectivity via Geometric Fixed Points	10
6 Problem 6: ε -Light Vertex Subsets of Graphs	12
7 Problem 7: Uniform Lattice with 2-Torsion and Rationally Acyclic Universal Cover	14
8 Problem 8: Lagrangian Smoothing of 4-Valent Polyhedral Surfaces	16
9 Problem 9: Polynomial Detection of Rank-1 Scaling for Quadrifocal Tensors	18
10 Problem 10: PCG for RKHS-Constrained Tensor CP Decomposition	20
II Full Proof Drafts	22
Reading Convention	23
11 Problem 1: Equivalence of Φ_3^4 Measure Under Smooth Shifts	24
11.1 Problem Statement	24
11.2 Answer	24
11.3 Solution	24
11.3.1 1. The Φ_3^4 measure	24
11.3.2 2. Absolute continuity with respect to the GFF	25
11.3.3 3. Cameron-Martin theory for the GFF	25

11.3.4 4. Shift of the interacting measure	25
11.3.5 5. Integrability and equivalence	26
11.3.6 6. Alternative argument via the variational approach	27
11.3.7 7. Summary	27
11.4 References	27
12 Problem 2: Universal Test Vector for Rankin-Selberg Integrals	29
12.1 Problem Statement	29
12.2 Answer	29
12.3 Solution	30
12.3.1 1. Rankin-Selberg theory background	30
12.3.2 2. The condition “finite and nonzero for all s ”	30
12.3.3 3. The u_Q twist and the Kirillov model	30
12.3.4 4. Nondegeneracy of the pairing	33
12.3.5 5. Choosing W : the new vector	33
12.3.6 6. The role of u_Q in conductor matching	34
12.3.7 7. Verification in special cases	34
12.3.8 8. Summary	35
12.4 References	35
13 Problem 3: Markov Chain with Interpolation ASEP Polynomial Stationary Distribution	37
13.1 Problem Statement	37
13.2 Answer	37
13.3 Solution	38
13.3.1 1. State space	38
13.3.2 2. Lemma (explicit chain construction)	38
13.3.3 3. Lemma (nontriviality)	38
13.3.4 4. Main theorem (stationary distribution)	39
13.3.5 5. Notation bridge: $F'_{\mu}/P'_{\lambda} = F_{\mu}/P_{\lambda}$	39
13.3.6 6. Sanity check: $n = 2$ reduction	40
13.3.7 7. Conclusion	40
13.4 References	41
14 Problem 4: Root Separation Under Finite Free Convolution	42
14.1 Problem Statement	42
14.2 Answer	42

14.3 Solution	43
14.3.1 Interpreting Φ_n algebraically	43
14.3.2 Connection to the discriminant	43
14.3.3 Finite free convolution and root behavior	44
14.3.4 The inequality via the random matrix model	44
14.3.5 Finite free cumulants and the bilinear structure	44
14.3.6 Complete proof for $n = 3$	45
14.3.7 What the proof requires for $n \geq 4$	46
14.3.8 Verification for small cases	47
14.4 External References	49
15 Problem 5: O-Slice Connectivity via Geometric Fixed Points	50
15.1 Problem Statement	50
15.2 Short Answer	50
15.3 Working Definition (transfer-restricted regular slice)	50
15.4 Characterization Theorem (subgroup-family level)	51
15.5 Proof Sketch	52
15.6 Special Cases	53
15.7 References	54
16 Problem 6: Epsilon-Light Subsets of Graphs	55
16.1 Problem Statement	55
16.2 1. Exact reformulation	56
16.3 2. Complete graph upper bound (rigorous)	56
16.4 3. Random sampling identities (expectation level)	56
16.5 4. Concentration setup (gap-fixed formulation)	57
16.5.1 4a. Star domination with correct counting	57
16.5.2 4b. Freedman/Bernstein martingale parameters	57
16.6 5. Discharging Assumption V via barrier greedy + pigeonhole	58
16.6.1 5a. Heavy edge pruning (Turan)	58
16.6.2 5b. Leverage degree filter (H2')	59
16.6.3 5c. Barrier greedy construction	59
16.6.4 5d. Proof of claim via pigeonhole + PSD trace bound	59
16.6.5 5e. Bounding d_{bar}_t	60
16.6.6 5e'. Additional evidence: Q-polynomial roots	62
16.6.7 5f. Constructing the ϵ -light set	62
16.6.8 Proved results	63

16.6.9	Numerically verified (strong evidence, formal bound in progress)	63
16.6.10	Diagnosis	64
16.6.11	Summary	64
16.7	Key identities and inequalities used	64
16.8	References	65
17	Problem 7: Uniform Lattice with 2-Torsion and Rationally Acyclic Universal Cover	66
17.1	Problem Statement	66
17.2	1. Baseline Geometry	66
17.3	2. Cohomological Structure via Bredon Framework	67
17.4	3. Obligation E2: Finite-CW Realization ($\Gamma \in \text{FH}(Q)$)	67
17.4.1	3a. Fowler's Criterion	67
17.4.2	3b. Concrete Instantiation via Reflection Lattice	67
17.5	4. Obligation S: From Finite Complex to Closed Manifold	68
17.5.1	Available geometric data	68
17.5.2	Approach I: Wall surgery via the $\text{FH}(Q)$ complex	68
17.5.3	Approach IV: Rotation route (resolves the parity tension)	70
17.6	5. Remark: Absence of Smith-Theory Obstruction	71
17.7	6. Theorem	72
17.8	7. Path to Full Closure	72
17.9	References	73
18	Problem 8: Lagrangian Smoothing of Polyhedral Surfaces with 4-Valent Vertices	75
18.1	Problem Statement	75
18.2	Answer	75
18.3	Solution	75
18.3.1	1. Setup: Lagrangian planes in \mathbb{R}^4	75
18.3.2	2. Local structure at a 4-valent vertex	76
18.3.3	3. The symplectic direct sum decomposition (key new argument)	76
18.3.4	4. Maslov index vanishes exactly	78
18.3.5	5. Why 4 is special: the 3-face obstruction	78
18.3.6	5a. Vertex smoothing via the product structure	79
18.3.7	6. Edge smoothing (crease smoothing along edges between vertices)	80
18.3.8	7. Global smoothing	81
18.3.9	8. Topological constraints	82

18.3.10 9. Summary	82
18.4 References	83
19 Problem 9: Polynomial Detection of Rank-1 Scaling for Quadrifocal Tensors	84
19.1 Problem Statement	84
19.2 Answer	84
19.3 Solution	84
19.3.1 1. The quadrifocal tensor as a bilinear form	84
19.3.2 2. The rank-2 constraint and its 3x3 minor formulation	85
19.3.3 3. Effect of rank-1 scaling on the 3x3 minor	85
19.3.4 4. Converse: non-rank-1 λ gives nonzero minors (for generic cameras)	86
19.3.5 5. All matricizations from the same construction	87
19.3.6 6. Construction of F	87
19.3.7 7. Geometric interpretation	88
20 Problem 10: RKHS-Constrained Tensor CP via Preconditioned Conjugate Gradient	89
20.1 Problem Statement	89
20.2 Assumptions Used (explicit)	89
20.3 Solution	89
20.3.1 1. Why naive direct methods fail	89
20.3.2 2. Implicit matrix-vector product in $O(n^2r + qr)$	90
20.3.3 3. Right-hand side	90
20.3.4 4. Preconditioner that matches the corrected algebra	91
20.3.5 5. Convergence (tightened)	92
20.3.6 6. Complexity summary	92
20.3.7 7. Algorithm	93
III Prompt Excerpts and Pivot Moments	95
Part III: The Sprint as Dialogue	96
IV Proof Patterns	107
21 Strategy Patterns Across Ten Problems	108
21.1 Design Pattern: OUTCOME TYPING (Close, Reduce, Map)	108
21.2 Design Pattern: LAYER-SWITCHING (Problem 7)	109

21.3 Design Pattern: CREATIVE REDUCTION (Problem 4)	110
21.4 Design Pattern: STRUCTURAL DECOMPOSITION (Problem 8)	111
21.5 Design Pattern: LAYER SWITCH UNDER COACHING (Problem 6)	111
21.5.1 Phase 1: The TryHarder Loop	112
21.5.2 The coaching intervention	112
21.5.3 Phase 2: The elementary proof	113
21.5.4 Phase 3: The partial averages breakthrough	113
21.5.5 What remains	113
21.5.6 The layer analysis	114
22 Conclusion	115
22.1 Toward Real-Time Argumentation Structure	115
22.2 Cross-Problem Learning	117
22.3 Learning from Success, Not Just Failure	119
22.4 Summary	120
V Color Plates	122

Highlights

- Dependency-graph representations of proofs enabled local gap isolation and targeted repair across all ten problems.
- Node-level verification with predecessor/successor context improved calibration relative to whole-draft review.
- Adversarial critic–responder iteration converted early overclaims into explicit closed, partial, or conditional outcomes.
- Targeted computational stress tests constrained speculative branches, especially in the $n = 4$ branch of Problem 4.
- Structured handoff memos preserved unresolved obligations as named, testable next steps rather than implicit deferrals.

Snapshot

- Ten initial proof attempts drafted in under two hours.
- Over two hundred commits across roughly 55 hours wall-clock (February 11–13, 2026), in addition to earlier infrastructure development.
- A shift in framing over the course of the sprint: from an early “all solved” posture to a clearer partition into proved, conditional, and partial results.
- A methodological lesson: wiring-diagram–based verification localized gaps and inconsistencies more effectively than plain narrative drafting.

Introduction

This monograph records both the mathematical results and the working process behind a compressed, multi-agent proof cycle in `futon6`.¹ The project began as infrastructure—knowledge ingestion, tagging, and wiring-diagram metatheory—and then pivoted into a rapid proof sprint marked by iterative critique and repair.

The working process came to resemble Lakatos’s *Proofs and Refutations* [1] more closely than anticipated. In Lakatos’s dialogue, a conjecture is proposed, counterexamples emerge, the conjecture is revised, and the cycle repeats. Each iteration sharpens both the statement and the participants’ understanding. Our sprint followed a similar rhythm, except that the interlocutors were a human dispatcher, multiple Claude instances (provers), and Codex

¹Source repository: <https://github.com/tothedarktowercame/futon6>

(critic and research assistant). Conjectures were drafted rapidly; adversarial review exposed overclaims and hidden gaps; targeted repair narrowed the remaining obligations.

The wiring-diagram decomposition—representing each proof as a typed graph of claims and dependencies—served as the shared epistemic artefact. Where Lakatos’s fictional classroom had a blackboard, this project had a structured proof graph. That graph made disagreements local and repairable.

The title alludes to the sprint format: ten open problems attempted in roughly 55 hours wall-clock, with both process and outcomes documented. The Lakatosian connection also runs through Pease et al. [2], which formalised Lakatos’s informal logic of mathematical discovery as a dialogue game over argumentation structures, implemented in a system capable of mixed-initiative human–AI collaboration. That paper asked whether computers could participate in mathematical reasoning through conjecture, critique, and reform. The present work can be read as an empirical extension of that question: ten research problems attempted by AI agents under human supervision, with the Lakatosian cycle unfolding at machine speed. In a related strand of work, Corneli et al. [3], developed a computational model of mathematical question-and-answer dialogues using Inference Anchoring Theory + Content (IATC) to annotate MathOverflow threads with performative types (assert, challenge, reform, clarify, etc.). The same vocabulary reappears in this project’s Stage 7 thread-wiring pipeline (see Part III, Act VI), where StackExchange threads are parsed into wiring diagrams whose edges carry the same performative labels. Earlier work on peer-produced mathematical knowledge [5] established the empirical base: PlanetMath as a community-maintained proof ecosystem, studied through the lens of paragogy (peer-produced peer learning). The present sprint can be read as a machine-accelerated instance of the same phenomenon: collaborative, incremental proof construction with explicit argumentation structure.

The working notes reveal a persistent asymmetry: generation is fast; trustworthy validation is slow. Lakatos identified the same imbalance in his classroom: conjectures are cheap, but understanding *why* they fail (or hold) is the real work. In this sprint, the strongest leverage came not from first-pass drafting quality, but from structured verification—tools that made weaknesses visible early, locally, and precisely.

Current Status

Outcome summary (status code $[M|V]$). $M \in \{C, P, ?\}$ with $C =$ closed, $P =$ partial, $? =$ conditional; $V \in \{\checkmark, \sim, ?\}$ with $\checkmark =$ validation-complete, $\sim =$ partial validation, $? =$ not yet fully validated.

- **P1** $[C|\checkmark]$. Mathematical claim is treated as closed, with unified repair checks and canonical node-level verifier alignment in place. See [Status Note P1](#) (p. 2).
- **P2** $[C|\checkmark]$. Local algebraic chain is repaired and node-level verifier outputs are synchronized; the result still depends on the cited newvector/test-vector theorem input. See

[Status Note P2](#) (p. 4).

- **P3 [C|✓]**. Validation-complete existence path under the scoped criterion (current run: 2 verified, 7 plausible, 0 gaps). Uniqueness/irreducibility is treated as optional and out of scope for the core existence claim.
- **P4 [P|?]**. Proved analytically for $n \leq 3$, and proved for $n = 4$ via the Path 2 algebraic certificate; higher n remains open. See [Status Note P4](#) (p. 8).
- **P5 [C|~]**. Closed in the declared local scope for F_O -local connective spectra; indexing-system-level extension remains open. See [Status Note P5](#) (p. 10).
- **P6 [P|?]**. K_n case proved ($c_0 = 1/3$); one technical gap remains in the general-graph argument (formal $\bar{d} < 1$ bound at $M_t \neq 0$). See [Status Note P6](#) (p. 12).
- **P7 [C|~]**. Provisionally closed mathematically via the rotation route; independent theorem-ledger re-check remains the main QC holdout. See [Status Note P7](#) (p. 14).
- **P8 [C|✓]**. Geometric closure is treated as repaired, with unified checks and canonical node-level verifier record now synchronized. See [Status Note P8](#) (p. 16).
- **P9 [P|~]**. Strong computational evidence exists, but the universal converse step is not yet cleanly closed algebraically. See [Status Note P9](#) (p. 18).
- **P10 [?|?]**. Conditional under explicitly stated assumptions; assumption necessity is explicit, while final closure/validation remains open. See [Status Note P10](#) (p. 20).
- Node-level validator outputs and legacy gap flags are tracked under <https://github.com/tothedarktowercame/futon6/tree/master/data/first-proof> (files matching `problem*-codex-results.jsonl`).
- Cross-problem closure-vs-validation inventory.²

Materials and Methods

- **Model/runtime split.** Claude Max runs on a remote Linode host; Codex Pro runs on the local laptop workspace (`/home/joe/code/futon6`).
- **Software/toolchain summary.** Computational checks used Python 3 scripts with NumPy/SciPy for numerical linear algebra and optimization, SymPy for symbolic algebra (resultants, Sturm sequences, Gröbner bases), mpmath for selected high-precision checks, PHCpack via `phcpy` for polynomial-system solving/certification in Problem 4 (Case 3c), and cvxpy for SDP-based sum-of-squares certificate attempts. Proof-structure analysis

²<https://github.com/tothedarktowercame/futon6/blob/master/data/first-proof/closure-validation-audit.md>

used wiring-diagram generators (nine scripts producing JSON and Mermaid flowcharts via the internal `thread_performatives` module) and `validate-ct.py` for classical NER and scope extraction over PlanetMath entries. Pattern tagging and term spotting used Babashka (Clojure) scripts operating on EDN data formats. Document production used L^AT_EX (`pdflatex`) with repository consistency checks via `check-latex-text-truth.py`, `check-latex-syntax-violations.py`, and `check-ratchet-fixedw-typesetting.py`.

- **Codex Pro token accounting (local, log-derived).** From local Codex session telemetry (`~/.codex/sessions/*`, event type `token_count`), over the 50-hour window ending 2026-02-13 21:41 UTC (window start: 2026-02-11 19:41 UTC), there were 333 futon6-related Codex rollout traces out of 334 local rollout traces (99.7%).

Metric	Total	Per rollout (avg)	% of total
Total tokens	965,714,475	2,900,043	100%
Input tokens (all)	961,719,044	2,887,445	99.6%
Cached input	912,686,208	2,740,800	94.5%
Non-cached input	49,032,836	147,246	5.1%
Output tokens	3,995,431	11,997	0.4%
Reasoning-output tokens	2,072,289	6,223	—

Interpretation (inference): the large cached-input share likely reflects repeated reuse of stable local context across rollouts, including processed Math StackExchange/Math-Overflow corpora and derived prompt artifacts such as `se-data/math-processed`, `math-se-processed`, `mo-processed`, and Codex workflows using `--math-se-dir`.

- **Claude Max token accounting (Linode, log-derived).** From Linode session files (`~/.claude/projects/*/`), 9 futon6-related Claude Code sessions were identified; 8 sessions contributed within the 50-hour Codex-comparable window ending 2026-02-13 21:41 UTC.

Metric	Total	Per session (avg)	% of total
Total tokens (50h window)	791,980,382	98,997,548	100%
Input tokens (all)	789,643,774	98,705,472	99.7%
Cached-read input	752,300,790	94,037,599	95.0%
Cache-creation input	37,221,978	4,652,747	4.7%
Non-cached input	121,006	15,126	0.0%
Output tokens	2,336,608	292,076	0.3%

Model: `claude-opus-4-6`; assistant messages: 7,754. Full-window totals (9 sessions, 2026-02-08 through 2026-02-13): total tokens 1,021,665,524; output tokens 2,798,074.

Reader Guide

This document is organized in five parts.

- **Part I (Annotated Overview):** short, citation-rich introductions for Problems 1–10, intended as navigational summaries.
- **Part II (Full Proof Drafts):** expanded writeups imported from the solution files, suitable as the base for a longer manuscript (targeting roughly book-length exposition). Coloured boxes separate the proof proper from process annotations (dead paths, revisions, open obligations).
- **Part III (Prompt Excerpts and Pivot Moments):** curated source excerpts (prompts and dispatch/history snippets) that document key decision points and proof-state transitions.
- **Part IV (Proof Patterns):** a cross-problem analysis of strategy patterns—what worked (layer-switching, creative reduction, structural decomposition), what didn’t (the TryHarder loop), and how a coaching intervention broke a stuck problem open.
- **Part V (Color Plates):** syntax-coloured renderings of the proof files, produced by automated math-mode normalization.

Terminology

AIF

Active Inference Framework—used here as a conceptual lens for agent roles, intervention points, and coordination state; a full AIF policy loop for proof search is proposed future work, not yet implemented in this sprint.

BSS

Batson–Spielman–Srivastava spectral sparsification framework.

IATC

Inference Anchoring Theory + Content—an annotation scheme for mathematical dialogues used here to type dialogue moves and content links within the AIF process model [3].

MSS

Marcus–Spielman–Srivastava interlacing families framework.

PSD

Positive semi-definite (for matrices).

Part I

Annotated Overview

Chapter 1

Problem 1: Measure Equivalence Under Smooth Shifts of the Φ_3^4 Measure

Problem statement

Given the renormalized Φ_3^4 measure μ on \mathbb{T}^3 , and a smooth nonzero shift ψ , determine whether μ and the shifted measure $T_\psi^* \mu$ are equivalent.

Answer

Yes: $\mu \sim T_\psi^* \mu$.

Status Note

Mathematical claim treated as closed, with unified repair checks and the canonical node-level verifier record aligned on the key equivalence chain repairs.

Annotated proof sketch

1. Use absolute continuity of μ with respect to the Gaussian reference measure μ_0 from variational construction results for Φ_3^{41} .
2. Apply Cameron–Martin to the Gaussian part: smooth shifts lie in the relevant Cameron–Martin space and preserve equivalence².
3. Control the interaction change $V(\phi - \psi) - V(\phi)$ using Wick expansion and exponential integrability for the cubic perturbation. This is the renormalized step tied to regularity structures / paracontrolled technology³.

The Radon–Nikodym derivative is strictly positive and integrable in both directions, so mutual absolute continuity follows.

¹Barashkov–Gubinelli, arXiv: <https://arxiv.org/abs/2003.10529>.

²Background discussion: <https://mathoverflow.net/questions/194307/cameron-martin-theorem-non-gaussian-shift>.

³Hairer, arXiv: <https://arxiv.org/abs/1303.5113>; Gubinelli–Imkeller–Perkowski, arXiv: <https://arxiv.org/abs/1210.2684>.

Selected citations

- Variational Φ_3^4 : <https://arxiv.org/abs/2003.10529>
- Regularity structures: <https://arxiv.org/abs/1303.5113>
- Paracontrolled distributions: <https://arxiv.org/abs/1210.2684>
- Cameron–Martin discussion: <https://mathoverflow.net/questions/194307/cameron-martin-theorem-non-gaussian-shift>

Background and prerequisites

Field: Stochastic PDE / Measure Theory.

What you need: Measure theory and Gaussian measures (Cameron–Martin theorem), plus familiarity with either regularity structures or paracontrolled distributions for making sense of the renormalized Φ_3^4 interaction.

Way in: Hairer, “An Introduction to Stochastic PDEs” (lecture notes, arXiv:0907.4178) for the probabilistic side; the Barashkov–Gubinelli variational paper cited below is largely self-contained for the Φ_3^4 -specific machinery.

Chapter 2

Problem 2: Universal Test Vector for Rankin–Selberg Integrals

Problem statement

For generic irreducible admissible representations Π of $\mathrm{GL}_{n+1}(F)$ and π of $\mathrm{GL}_n(F)$ over a non-archimedean local field, ask whether one can fix a single Whittaker vector W in Π such that some V in π makes the twisted local Rankin–Selberg integral finite and nonzero for all complex s .

Answer

Yes: the essential/new Whittaker vector W_0 serves as a universal test vector.

Status Note

Core local algebraic steps are treated as repaired; the result still depends on the cited newvector/test-vector theorem input (HFW). Canonical node-level verifier outputs are now aligned with the repaired lemma chain.

Annotated proof sketch

1. The set of local zeta integrals spans a fractional ideal in $\mathbb{C}[q_F^{\pm s}]$, which is a PID¹. Hence a monomial reduction criterion is available.
2. Evaluate the twisted Kirillov function $\phi_Q(g) = W_0(\mathrm{diag}(g, 1)u_Q)$ at $g = I_n$ to prove nontriviality; this uses the Whittaker transformation law.
3. Use GL_n -equivariance and irreducibility of the Kirillov model restriction to show that fixing any nonzero ϕ (hence ϕ_Q) still generates the full local L -factor ideal.

This yields existence of V with integral equal to a nonzero monomial in q_F^{-s} , so it is finite and nonvanishing for all s .

¹PID refresher: <https://planetmath.org/principalidealdomain>.

Selected citations

- Jacquet–Piatetski-Shapiro–Shalika (Rankin–Selberg local theory): <https://www.jstor.org/stable/2374430>
- Bernstein–Zelevinsky (representations of $GL(n, F)$): <http://mi.mathnet.ru/eng/rm4200>
- MathOverflow reference thread on local test vectors: <https://mathoverflow.net/questions/469865/reference-request-test-vectors-for-local-rankin-selberg-l-factors-in-ramified-c>
- Rankin–Selberg overview thread: <https://mathoverflow.net/questions/223233/jacquet-s-approach-to-rankin-selberg-l-functions>

Background and prerequisites

Field: Automorphic Forms / Representation Theory of p -adic Groups.

What you need: Smooth representations of GL_n over non-archimedean local fields, Whittaker models, and the Rankin–Selberg integral formalism for local L -factors. Graduate-level algebraic number theory assumed.

Way in: Bump, *Automorphic Forms and Representations* (Cambridge, 1997), especially Part II on local theory; Cogdell’s expository article “ L -functions and Converse Theorems for GL_n ” (Fields Institute lectures).

Chapter 3

Problem 3: Markov Chain with ASEP Polynomial Stationary Distribution

Problem statement

Construct a nontrivial Markov chain on permutations of a partition λ whose stationary distribution is the normalized interpolation ASEP polynomial weight at $q = 1$.

Answer

Yes: the inhomogeneous multispecies t -PushTASEP yields the required stationary law.

Annotated proof sketch

1. Define a finite-state continuous-time Markov chain with explicit local transition rates that depend only on (x, t) and species order (not on polynomial values).
2. Invoke the stationary measure theorem identifying the stationary weights with ASEP/-Macdonald objects at $q = 1$ ¹.
3. Use irreducibility (vacancy transport and positive-rate swaps) to conclude uniqueness of the stationary distribution on the finite state space².

Selected citations

- Inhomogeneous multispecies t -PushTASEP: <https://arxiv.org/abs/2403.10485>
- Multiline queues to Macdonald polynomials: <https://doi.org/10.1353/ajm.2022.0007>
- Macdonald polynomial definition page: <https://planetmath.org/macdonaldpolynomials>

¹Ayyer–Martin–Williams, arXiv: <https://arxiv.org/abs/2403.10485>.

²Markov-chain basics: <https://planetmath.org/markovchain>.

Background and prerequisites

Field: Markov Chains / Algebraic Combinatorics / Symmetric Functions.

What you need: Basic Markov chain theory (irreducibility, uniqueness of stationary distributions) and some familiarity with symmetric functions, particularly Macdonald polynomials and their specializations.

Way in: Levin–Peres–Wilmer, *Markov Chains and Mixing Times* (AMS, 2nd ed.) for stochastic foundations; Macdonald, *Symmetric Functions and Hall Polynomials* (OUP, 2nd ed.) for the algebraic-combinatorial side.

Chapter 4

Problem 4: Root Separation Energy Under Finite Free Convolution ($n = 4$)

Problem statement

For monic real-rooted degree- n polynomials, test

$$\frac{1}{\Phi_n(p \boxplus_n q)} \geq \frac{1}{\Phi_n(p)} + \frac{1}{\Phi_n(q)}.$$

Answer

Partial result: proved analytically for $n \leq 3$, and now proved for $n = 4$ via the Path 2 algebraic certificate (3-piece Cauchy–Schwarz with P-convexity of K_{red}); higher n remains open.

Status Note

Problem 4 is proved for $n \leq 3$ analytically (Cauchy–Schwarz), and proved for $n = 4$ via the Path 2 algebraic certificate (3-piece Cauchy–Schwarz + P-convexity of K_{red}). Higher n remains open.

Annotated proof structure

1. Algebraic reduction at $n = 4$: normalize coefficients, derive a polynomial numerator/denominator formulation for the surplus using the exact $\Phi_4 \cdot \text{disc}$ identity¹.
2. Show denominator sign on the real-rooted domain, reducing inequality to nonnegativity of a single polynomial $-N$.
3. Boundary and symmetric-subcase analysis by exact elimination/resultant methods.
4. Path 2 closure for $n = 4$: prove $T_2 + R$ surplus nonnegative via P-convexity/boundary analysis of K_{red} , which supersedes the case-by-case critical-point accounting branch.

¹Discriminant refresher: <https://planetmath.org/discriminantofapolynomial>.

Selected citations

- Finite free convolution (MSS): <https://arxiv.org/abs/1504.00350>
- Interlacing families follow-up: <https://arxiv.org/abs/1507.05020>
- Finite free cumulants perspective: <https://arxiv.org/abs/1707.02443>
- MathOverflow discussion (finite free convolution): <https://mathoverflow.net/questions/375273/finite-free-convolution-of-polynomials>
- PHCpack project page: <https://github.com/janverschelde/PHCpack>

Background and prerequisites

Field: Free Probability / Real Algebraic Geometry / Polynomial Inequalities.

What you need: Real-rooted polynomials and discriminants, the finite free convolution \boxplus_n of Marcus–Spielman–Srivastava, and basic free probability (free cumulants). Computational algebra tools (e.g. resultants, homotopy continuation) appear in the $n = 4$ certification.

Way in: Marcus–Spielman–Srivastava, “Interlacing Families I” (arXiv:1304.4132) for finite free convolution; Nica–Speicher, *Lectures on the Combinatorics of Free Probability* (Cambridge, 2006) for the probabilistic backdrop.

Chapter 5

Problem 5: \mathcal{O} -Slice Connectivity via Geometric Fixed Points

Problem statement

For an incomplete transfer system from an N_∞ operad, define the associated restricted regular slice filtration and characterize \mathcal{O} -slice connectivity using geometric fixed points.

Answer

For $\mathcal{F}_\mathcal{O}$ -local connective G -spectra, one can restrict the Hill–Yarnall connectivity criterion to subgroups in the admissible family $\mathcal{F}_\mathcal{O}$.

Solved in a scope-limited form: the subgroup-family-level characterization is established for $\mathcal{F}_\mathcal{O}$ -local connective spectra; a full indexing-system-level extension is left open.

Status Note

Closed only in the stated local scope ($\mathcal{F}_\mathcal{O}$ -local connective spectra). The indexing-system-level extension remains an explicit open obligation.

Open Gap / Conditional Step. Open obligation (scope extension): move from subgroup-family indexing to full Blumberg–Hill indexing-system data (admissible finite H -sets, not only admissible subgroups). The current result uses $\mathcal{F}_\mathcal{O} = \{H : e \rightarrow H \text{ admissible}\}$ and does not yet encode finer $K \rightarrow H$ admissibility for $K \neq e$. Closing this gap requires a full indexing-system formulation of \mathcal{O} -slice connectivity and, in parallel, a non-local replacement (or discharge) of the $\mathcal{F}_\mathcal{O}$ -locality hypothesis in the reverse direction.

Annotated proof sketch

1. Build $\tau_{\geq n}^\mathcal{O}$ from regular slice cells indexed only by admissible subgroups.
2. Use closure properties of indexing systems to verify that this restriction is stable under conjugation and subgroup passage.
3. Adapt Hill–Yarnall’s geometric fixed-point criterion: for $\mathcal{F}_\mathcal{O}$ -local spectra, no tests are needed outside $\mathcal{F}_\mathcal{O}$ because those geometric fixed points vanish by locality.

Selected citations

- Hill–Yarnall (slice filtration reformulation): <https://arxiv.org/abs/1703.10526>
- Blumberg–Hill (N_∞ operads and indexing systems): <https://arxiv.org/abs/1309.1750>
- HHR monograph context: <https://bookstore.ams.org/surv-346>
- Geometric fixed points background: <https://ncatlab.org/nlab/show/geometric+fixed+points>

Background and prerequisites

Field: Equivariant Stable Homotopy Theory.

What you need: Genuine G -spectra, geometric fixed-point functors, the slice filtration of Hill–Hopkins–Ravenel, and N_∞ operads / indexing systems of Blumberg–Hill. Research-level; assumes graduate coursework in algebraic topology and stable homotopy theory.

Way in: Schwede, *Global Homotopy Theory* (Cambridge, 2018) for equivariant foundations; the Hill–Hopkins–Ravenel Kervaire paper (Annals, 2016) for slice-filtration motivation.

Chapter 6

Problem 6: ε -Light Vertex Subsets of Graphs

Problem statement

Find a universal constant $c_0 > 0$ such that every weighted graph and every $\varepsilon \in (0, 1)$ admit a subset S with

$$|S| \geq c_0 \varepsilon n, \quad L_{G[S]} \preceq \varepsilon L_G.$$

Partial (general case conditional). The K_n case is proved with $c_0 = 1/3$; for general graphs, the remaining issue is the Barrier Maintenance Invariant (BMI): prove the full barrier-degree bound $\bar{d}_t < 1$ when $M_t \neq 0$. The current E/F regime reduction isolates this to two explicit lemmas.

Status Note

Unconditional closure holds for the K_n branch. The general-graph theorem remains conditional on two explicit BMI regime lemmas in the $M_t \neq 0$ branch.

Annotated proof structure

1. Use leverage scores $\tau_e = w_e R_{\text{eff}}(u, v)$ to define the heavy-edge graph and show any ε -light set must be independent there.
2. Apply the leverage-score trace identity and Turan's theorem to extract a large candidate set.
3. Resolve easy branches (independent-in- G and directly bounded spectral sum) unconditionally.
4. Reduce the hard branch to barrier maintenance (BMI), then split by a graph-adaptive E/F regime decomposition; substantial computational evidence is available, but the final general proof still requires two regime lemmas.

Open Gap / Conditional Step. The unresolved step is the full BMI bound in the $M_t \neq 0$ regime. The writeup reduces this to two explicit E/F regime lemmas. Until those lemmas are proved (or replaced by an equivalent closure argument), the universal-constant theorem remains conditional.

Selected citations

- Graph sparsification by effective resistances: <https://arxiv.org/abs/0803.0929>
- Interlacing families II (Kadison–Singer machinery): <https://arxiv.org/abs/1306.3969>
- Twice-Ramanujan sparsifiers: <https://arxiv.org/abs/0901.2698>
- Laplacian matrix definition: <https://planetmath.org/laplacianmatrix>

Background and prerequisites

Field: Spectral Graph Theory / Linear Algebra.

What you need: Graph Laplacians and their spectra, effective resistance and leverage scores, Loewner ordering of positive semidefinite matrices, and matrix concentration inequalities. Turán’s theorem from extremal combinatorics appears in the combinatorial step.

Way in: Spielman, “Spectral and Algebraic Graph Theory” (lecture notes, freely available); Tropp, “An Introduction to Matrix Concentration Inequalities” (Foundations and Trends, 2015).

Chapter 7

Problem 7: Uniform Lattice with 2-Torsion and Rationally Acyclic Universal Cover

Problem statement

Can a cocompact lattice Γ in a real semisimple Lie group, containing an element of order 2, be the fundamental group of a closed manifold whose universal cover is \mathbb{Q} -acyclic?

Provisionally closed via the rotation route ($n = 7$, congruence setting): E2 is discharged and the S-branch is supported by the codim-2 surgery theorem chain documented in the project theorem-number ledger,¹ with final confidence pending independent line-by-line ledger re-check.

Annotated proof structure

1. Use Fowler's fixed-point Euler-characteristic criterion to produce groups in $\text{FH}(\mathbb{Q})$ from suitable $\mathbb{Z}/2$ -extensions².
2. Construct two arithmetic lattice routes:
 - reflection route in even dimension;
 - codimension-2 rotation route in odd dimension (arithmetically cleaner for surgery).
3. Follow the rotation-route S-branch: codimension-2 setup, obstruction chain, and cap/gluing output to a closed manifold model with rationally acyclic universal cover.

Status Note

This monograph treats Problem 7 as provisionally closed via the rotation route. The construction uses Fowler's $\text{FH}(\mathbb{Q})$ criterion and codimension-2 equivariant surgery in the $n = 7$ congruence-lattice setting, with the obstruction-vanishing bridge tracked in the theorem-number ledger.^a Final confidence is contingent on independent ledger re-check. Literature anchors: <https://arxiv.org/abs/1204.4667>, <https://arxiv.org/abs/1705.10909>.

^a<https://github.com/tothedarktowercame/futon6/blob/master/data/first-proof/problem7-g2-theorem-chain.md>

¹<https://github.com/tothedarktowercame/futon6/blob/master/data/first-proof/problem7-g2-theorem-chain.md>

²Fowler: <https://arxiv.org/abs/1204.4667>.

Selected citations

- Fowler criterion: <https://arxiv.org/abs/1204.4667>
- Reflection lattices source used in writeup: <https://arxiv.org/abs/2506.23994>
- Equivariant surgery framework: <https://arxiv.org/abs/1705.10909>
- Davis–Luck obstruction context: <https://arxiv.org/abs/2303.15765>
- G2 theorem-number ledger (project note).³
- Arithmetic lattices (Borel–Harish-Chandra): <https://www.jstor.org/stable/1970362>
- Semisimple Lie group definition: <https://planetmath.org/semisimpleliegroup>
- Related MathOverflow discussion: <https://mathoverflow.net/questions/33545/equivariant-surgery-problem>

Background and prerequisites

Field: Surgery Theory / Geometric Topology / Arithmetic Groups.

What you need: Algebraic topology (homology, fundamental group, covering spaces), surgery theory on manifolds (normal maps, surgery obstructions), and arithmetic lattices in semisimple Lie groups. Research-level; assumes graduate coursework in both topology and Lie theory.

Way in: Lück, *A Basic Introduction to Surgery Theory* (ICTP lecture notes, 2002) for the topological machinery; Raghunathan, *Discrete Subgroups of Lie Groups* (Springer, 1972) for the arithmetic side.

³<https://github.com/tothedarktowercame/futon6/blob/master/data/first-proof/problem7-g2-theorem-chain.md>

Chapter 8

Problem 8: Lagrangian Smoothing of 4-Valent Polyhedral Surfaces

Problem statement

If every vertex of a polyhedral Lagrangian surface in (\mathbb{R}^4, ω) is 4-valent, must the surface admit a Lagrangian smoothing through Hamiltonian isotopy?

Answer

Yes.

Status Note

Current draft treats the geometric argument as closed, with unified repair checks and the canonical node-level verifier record aligned on the main algebraic and Maslov-index repairs.

Annotated proof sketch

1. Analyze a 4-valent vertex: edge vectors span \mathbb{R}^4 , forcing a symplectic splitting into two 2D factors.
2. Write the local model as a product of two planar corners and smooth each corner separately.
3. Check Lagrangian condition factorwise (product of isotropic curves in 2D symplectic factors).
4. Smooth remaining edge creases via exact-graph interpolation and glue local constructions by disjoint supports.
5. Promote to Hamiltonian isotopy using exactness/flux-vanishing in local models and composition closure of compactly supported Hamiltonian isotopies.

Selected citations

- Weinstein neighborhood theorem source paper: <https://www.sciencedirect.com/science/article/pii/000187087190005X>

- McDuff–Salamon textbook page: <https://global.oup.com/academic/product/introduction-to-symplectic-topology-9780198794899>
- Symplectic manifold definition: <https://planetmath.org/symplecticmanifold>
- Lagrangian submanifold definition: <https://planetmath.org/lagrangiansubmanifold>

Background and prerequisites

Field: Symplectic Geometry / Lagrangian Topology.

What you need: Symplectic manifolds, Lagrangian submanifolds, Hamiltonian isotopy, and Weinstein neighborhood theorems. The proof uses only local symplectic techniques (no Floer theory).

Way in: McDuff–Salamon, *Introduction to Symplectic Topology* (OUP, 3rd ed., 2017)—the standard graduate textbook covering all prerequisites.

Chapter 9

Problem 9: Polynomial Detection of Rank-1 Scaling for Quadrifocal Tensors

Problem statement

Given generic camera matrices and quadrifocal tensors $Q^{(\alpha\beta\gamma\delta)}$, construct a polynomial map F of degree bounded independently of n that vanishes exactly on rank-1 separable scaling tensors $\lambda_{\alpha\beta\gamma\delta} = u_\alpha v_\beta w_\gamma x_\delta$.

Answer

Yes: one can use degree-3 determinant constraints (all relevant 3×3 minors).

Status Note

Forward and witness checks are strong, but full closure still hinges on a formal universal converse argument (all non-rank-1 λ , not only tested families). Treat as partial until that algebraic universality step is written cleanly into the proof chain.

Annotated proof sketch

1. For fixed $(\gamma, \delta, k, \ell)$, the determinant pairing defines an alternating bilinear form of rank 2 on \mathbb{R}^4 , so all induced 3×3 minors vanish.
2. If λ is rank-1 separable, Hadamard-diagonal scaling preserves the rank- ≤ 2 property, hence all these minors vanish.
3. Conversely, vanishing of all minors across the three matricization patterns forces each matricization rank to be 1, and compatibility implies full tensor separability.
4. Collect all such minors into F ; each coordinate has degree 3 and no dependence on camera parameters.

Selected citations

- Segre embedding (rank-1 tensor variety): <https://planetmath.org/segreembedding>

- Determinantal varieties: <https://planetmath.org/determinantalvariety>
- Tensor rank definition: <https://planetmath.org/tensorrank>
- Multiple-view geometry reference text: <https://www.robots.ox.ac.uk/~vgg/hzbook/>

Background and prerequisites

Field: Algebraic Geometry / Computer Vision (Multiview Geometry).

What you need: Tensor algebra (rank, matricizations, Segre varieties), determinantal varieties, and the basics of multiview geometry (camera matrices, multi-focal tensors). The algebraic geometry is classical; no scheme theory required.

Way in: Hartley–Zisserman, *Multiple View Geometry in Computer Vision* (Cambridge, 2nd ed.) for the applied setting; Landsberg, *Tensors: Geometry and Applications* (AMS, 2012) for the algebraic underpinnings.

Chapter 10

Problem 10: PCG for RKHS-Constrained Tensor CP Decomposition

Problem statement

Explain why preconditioned conjugate gradient (PCG) solves the mode- k RKHS CP subproblem without $O(N)$ per-iteration cost, where N is the full ambient sample size.

Answer

Use implicit Kronecker/Khatri–Rao matrix–vector products and a Kronecker preconditioner built from expected sampling geometry.

Status Note

This result is **conditional**: it is closed under explicit assumptions ($\lambda > 0$, $K_\tau \succ 0$, and sampling/coherence conditions controlling preconditioned conditioning). Necessity counterexamples are recorded in the full writeup when these assumptions are dropped.

Annotated proof sketch

1. Never form the full system matrix; compute Ax through structured operations: kernel multiplies, sparse sampling/restriction, and Khatri–Rao contractions.
2. Build b by the same structure, again avoiding dense N -scale tensors.
3. Precondition with $P = H \otimes K_\tau$ from replacing sparse sampling by its expectation; invert P via two small Cholesky solves.
4. Apply standard PCG convergence bounds in terms of condition number $\kappa(P^{-1/2}AP^{-1/2})$ and matrix concentration for random sampling.

Selected citations

- Matrix concentration / Freedman-style bound context: <https://arxiv.org/abs/1110.1379>
- FALKON large-scale kernel method: <https://arxiv.org/abs/1705.10958>

- Kronecker product definition: <https://planetmath.org/kroneckerproduct>
- Conjugate gradient method definition: <https://planetmath.org/conjugategradientmethod>

Background and prerequisites

Field: Numerical Linear Algebra / Kernel Methods / Tensor Decomposition.

What you need: Conjugate gradient and preconditioning, Kronecker and Khatri–Rao products, reproducing kernel Hilbert spaces (RKHS), and matrix concentration inequalities for random sampling operators.

Way in: Trefethen–Bau, *Numerical Linear Algebra* (SIAM, 1997) for iterative methods; Rasmussen–Williams, *Gaussian Processes for Machine Learning* (MIT Press, 2006; freely available online) for RKHS context.

Part II

Full Proof Drafts

Reading Convention

This manuscript uses boxed annotations selectively. In the current revision, the full proof chapters are primarily unboxed; process boxes appear only where there is substantive process context to preserve.

- **Unboxed text** is the proof proper. A reader following the five-page-per-problem brief can read only the unboxed text and obtain a self-contained argument (or, where an argument is incomplete, a clearly stated conditional result).
- **Status Note boxes** appear in the annotated overview chapters to summarize closure/QC state for each problem.
- **Process Note boxes** appear in process-facing parts (for example, prompt excerpts) when methodological scope or reviewer context is needed.
- Dead-path / revision / open-obligation semantics are maintained in the tooling vocabulary, but are not instantiated as standalone boxed blocks in the current full-proof chapter text.

Chapter 11

Problem 1: Equivalence of Φ_3^4 Measure Under Smooth Shifts

11.1 Problem Statement

Let T^3 be the 3D unit torus. Let μ be the Φ_3^4 measure on $D'(T^3)$. Let $\psi: T^3 \rightarrow \mathbb{R}$ be a smooth nonzero function and $T_\psi(u) = u + \psi$ the shift map. Are μ and $T_\psi^* \mu$ equivalent (same null sets)?

11.2 Answer

Yes. The measures μ and $T_\psi^* \mu$ are equivalent.

Confidence: Medium-high. The argument combines Cameron-Martin theory with the absolute continuity structure of the Φ_3^4 construction (Barashkov-Gubinelli 2020, Theorem 1.1). The integrability bound is stated for a neighborhood of the required exponent, not for all t , matching the available log-Sobolev technology.

11.3 Solution

11.3.1 1. The Φ_3^4 measure

The Φ_3^4 measure μ on $D'(T^3)$ is the probability measure formally written as:

$$d\mu(\phi) = Z^{-1} \exp(-V(\phi)) d\mu_0(\phi)$$

where μ_0 is the Gaussian free field (GFF) measure with covariance $(m^2 - \Delta)^{-1}$ on T^3 , and the interaction is:

$$V(\phi) = \int_{T^3} (\phi^4 - C \phi^2) dx$$

Here $:\phi^k:$ denotes the k -th Wick power (renormalized product), and C is a mass counterterm that diverges under regularization removal.

The rigorous construction (Hairer 2014, Gubinelli-Imkeller-Perkowski 2015, Barashkov-

Gubinelli 2020) produces μ as a well-defined probability measure on distributions of regularity $C^{-1/2-\epsilon}(T^3)$.

11.3.2 2. Absolute continuity with respect to the GFF

Key fact: The Φ_3^4 measure μ is equivalent to (has the same null sets as) the base Gaussian free field measure μ_0 :

$$\mu \mu_0$$

This equivalence follows from the variational construction of Barashkov-Gubinelli (2020, Theorem 1.1), which establishes $E_{\mu_0}[\exp(-V)] < \infty$ and hence $\mu \ll \mu_0$ with strictly positive density $\exp(-V(\phi))/Z$. Since $\exp(-V(\phi)) > 0$ a.s. (exponential is always positive), the reverse absolute continuity $\mu_0 \ll \mu$ also holds.

11.3.3 3. Cameron-Martin theory for the GFF

For the Gaussian free field μ_0 on T^3 with covariance $C = (m^2 - \Delta)^{-1}$, the Cameron-Martin space is:

$$H = H^1(T^3) \text{ (Sobolev space of order 1)}$$

Since ψ is smooth, $\psi \in C^\infty(T^3)$ subset $H^1(T^3)$, so ψ is in the Cameron-Martin space.

Cameron-Martin theorem: For any $h \in H$, the shifted Gaussian measure $T_h^* \mu_0$ is equivalent to μ_0 , with Radon-Nikodym derivative:

$$dT_h^* \mu_0 / d\mu_0(\phi) = \exp(l_h(\phi) - \|h\|_{H^2}/2)$$

where l_h is the linear functional associated to h . In particular:

$$T_\psi^* \mu_0 \mu_0$$

11.3.4 4. Shift of the interacting measure

To compute $T_\psi^* \mu$, we need the density of the shifted interacting measure:

$$dT_\psi^* \mu / d\mu_0(\phi) = Z^{-1} \exp(-V(\phi - \psi)) * \exp(l_\psi(\phi) - \|\psi\|_{H^2}/2)$$

The shifted interaction $V(\phi - \psi)$ expands (using Wick ordering relative to μ_0):

$$\begin{aligned} V(\phi - \psi) &= V(\phi) - 4 \int \psi : \phi^3 : dx + 6 \int \psi^2 : \phi^2 : dx \\ &\quad - 4 \int \psi^3 : \phi : dx + \int \psi^4 dx \\ &- C \left(\int : \phi^2 : dx - 2 \int \psi : \phi : dx + \int \psi^2 dx \right) + (\text{renorm.corrections}) \end{aligned}$$

Renormalization under shift: The term $6 \int \psi^2 : \phi^2 : dx$ generates an additional logarithmic divergence (from ψ^2 multiplying the Wick square). This is absorbed by shifting the mass counterterm:

$$C \rightarrow C + 6 \|\psi\|_{L^2}^2 * (\log N \text{ correction})$$

The precise counterterm shift is determined by the regularization scheme; see Hairer (2014, Section 9) or Gubinelli-Imkeller-Perkowski (2015, Proposition 6.3) for the explicit formula. For the present argument, only the finiteness of the renormalized difference matters.

After renormalization, $V(\phi - \psi) - V(\phi)$ is a well-defined random variable under μ_0 (and under μ). The dominant fluctuation term is $4 \int \psi : \phi^3 : dx$, which has the right regularity:

- $: \phi^3 : \in C^{-3/2-\epsilon}(T^3)$ (as a distribution)
- $\psi \in C^\infty(T^3)$ (smooth)
- $\int \psi : \phi^3 : dx$ is well-defined (pairing of smooth test function with distribution)

11.3.5 5. Integrability and equivalence

The Radon-Nikodym derivative $dT_{\psi}^* \mu / d\mu$ involves:

$$R(\phi) = \exp(-(V(\phi - \psi) - V(\phi)) + l_\psi(\phi) - \text{const})$$

We need $R \in L^1(\mu)$ and $R > 0$ a.s.

Positivity: $R > 0$ a.s. because it's an exponential. ✓

Integrability: The critical term is $\exp(4 \int \psi : \phi^3 : dx)$ under the Φ_3^4 measure. By the log-Sobolev inequality for Φ_3^4 (Barashkov-Gubinelli 2020), the measure has strong concentration: the tails of $\int \psi : \phi^3 : dx$ are controlled by the quartic interaction. Specifically:

$$E_\mu [\exp(t \int \psi : \phi^3 : dx)] < \infty \text{ for } |t| < t_0$$

where $t_0 > 0$ depends on $\|\psi\|_{C^0}$ and the coupling constant. This exponential integrability follows from the coercivity of the ϕ^4 interaction: the quartic potential dominates the cubic perturbation (Barashkov-Gubinelli 2020, Section 4, exponential integrability from the Polchinski flow). The bound suffices for $R \in L^1(\mu)$ since the exponent in the Radon-Nikodym derivative is bounded by $4 \|\psi\|_{C^0} |\int : \phi^3 : dx|$, and this yields integrability provided the coefficient lies in the admissible exponential-moment range (or after a standard scaling/localization argument). Therefore $R \in L^1(\mu)$ and $1/R \in L^1(T_\psi^* \mu)$, giving:

$$T_\psi^* \mu \text{ (equivalent measures)}$$

11.3.6 6. Alternative argument via the variational approach

Barashkov-Gubinelli (2020) construct the Φ_3^4 measure via the Boué-Dupuis variational formula, which represents:

$$-\log Z = \inf_u E[V(\phi + \int_0^1 u_s ds) + 1/2 \int_0^1 \|u_s\|^2 ds]$$

In this framework, shifting by ψ is equivalent to modifying the variational problem by a shift in the drift, which produces an equivalent measure (the infimum shifts by a finite amount, preserving absolute continuity).

11.3.7 7. Summary

The measures are equivalent because:

1. $\mu \sim \mu_0$ (interacting measure equivalent to Gaussian, by positivity of density)
2. $T_\psi^* \mu_0 \sim \mu_0$ (Cameron-Martin theorem, since $\psi \in H^1$)
3. $V(\phi - \psi) - V(\phi)$ is well-defined after renormalization
4. The exponential of the cubic perturbation is integrable (log-Sobolev / coercivity)
5. Therefore $T_\psi^* \mu \sim \mu$

11.4 References

- N. Barashkov, M. Gubinelli, “A variational method for Φ_3^4 ,” Duke Math J. 169 (2020), 3339-3415. [Theorem 1.1: construction and integrability; Section 4: exponential

integrability from Polchinski flow]

- M. Hairer, “A theory of regularity structures,” *Inventiones Math.* 198 (2014), 269-504. [Section 9: renormalization counterterms]
- M. Gubinelli, P. Imkeller, N. Perkowski, **Paracontrolled distributions and singular PDEs**, *Forum Math. Π* 3 (2015). [Proposition 6.3: explicit counterterm formula]

Process Note — futon6 Corpus References

- PlanetMath: “distribution” — distributions on manifolds
- PlanetMath: “Sobolev space” — Cameron-Martin space is H^1
- PlanetMath: “Gaussian measure” — reference measure μ_0
- PlanetMath: “Radon-Nikodym theorem” — absolute continuity and RN derivatives

Chapter 12

Problem 2: Universal Test Vector for Rankin-Selberg Integrals

12.1 Problem Statement

Let F be a non-archimedean local field with ring of integers \mathcal{o} . Let N_r denote the subgroup of $\mathrm{GL}_r(F)$ consisting of upper-triangular unipotent elements. Let $\psi: F \rightarrow \mathbb{C}^\times$ be a nontrivial additive character of conductor \mathcal{o} , identified with a generic character of N_r .

Let Π be a generic irreducible admissible representation of $\mathrm{GL}_{n+1}(F)$, realized in its ψ^{-1} -Whittaker model $W(\Pi, \psi^{-1})$. Must there exist $W \in W(\Pi, \psi^{-1})$ with the following property? For any generic irreducible admissible representation π of $\mathrm{GL}_n(F)$ in its ψ -Whittaker model $W(\pi, \psi)$, let q be the conductor ideal of π , $Q \in F^\times$ a generator of q^{-1} , and $u_Q := I_{n+1} + QE_{n,n+1}$. Then for some $V \in W(\pi, \psi)$, the local Rankin-Selberg \int

$$\int_{N_n \backslash \mathrm{GL}_n(F)} W(\mathrm{diag}(g, 1)u_Q)V(g)|\det g|^{s-1/2} dg$$

is finite and nonzero for all $s \in C$.

12.2 Answer

Yes. The new vector (essential Whittaker function) of Π serves as a universal test vector, with the u_Q twist compensating for the conductor of π .

Process Note — Confidence

Confidence: Medium-high. The argument combines standard Rankin-Selberg theory (JPSS) with the Bernstein-Zelevinsky theory of the Kirillov model. The key nondegeneracy claim (Section 3a) uses GL_n -equivariance of the $\zeta - \int$ pairing together with irreducibility of the Kirillov model (any nonzero function generates the full module under GL_n -translates) and the PID structure of the fractional ideal ring. The “nonzero for all s ” condition reduces to explicit Laurent polynomial algebra (Section 2).

12.3 Solution

12.3.1 1. Rankin-Selberg theory background

The local Rankin-Selberg $\int I(s, W, V)$ for $\mathrm{GL}_{n+1} \times \mathrm{GL}_n$ is:

$$I(s, W, V) = \int_{N_n \backslash \mathrm{GL}_n(F)} W(\mathrm{diag}(g, 1)) V(g) |\det g|^{s-1/2} dg$$

This converges for $\mathrm{Re}(s) \gg 0$ and extends to a rational function of q_F^{-s} (where $q_F = |\mathrm{o/p}|$). The set of all such integrals as (W, V) vary generates a fractional ideal of $\mathbb{C}[q_F^s, q_F^{-s}]$, whose generator is the local L-factor $L(s, \Pi \times \pi)$.

The problem modifies this by inserting $u_Q = I_{n+1} + QE_{n,n+1}$ into the argument of W , giving the “twisted” Rankin-Selberg \int .

12.3.2 2. The condition “finite and nonzero for all s”

For a rational function $f(q_F^{-s})$ to be finite and nonzero for all $s \in \mathbb{C}$, it must have no poles and no zeros when viewed as a function of $X = q_F^{-s} \in \mathbb{C}^x$. Such a rational function must be $c*X^k = c*q_F^{-ks}$ for some nonzero c and integer k .

So the condition requires: there exists V such that $I(s, W, V) = c*q_F^{-ks}$ for some nonzero constant c and integer k .

By Section 3a below, the integrals over V (for fixed $W = W_0$) generate the full fractional ideal $I = L(s, \Pi \times \pi) * \mathbb{C}[q_F^s, q_F^{-s}]$.

Explicit algebra: I is a free rank-1 module over the ring $R = \mathbb{C}[q_F^s, q_F^{-s}]$, generated by $L(s, \Pi \times \pi)$. We seek an element of I of the form $c*q_F^{-ks}$ (a monomial — no poles or zeros). Write:

$$c*q_F^{-ks} = L(s, \Pi \times \pi) * P(q_F^{-s})$$

where $P = c*q_F^{-ks} * L(s, \Pi \times \pi)^{-1}$. Since $L(s, \Pi \times \pi)^{-1}$ is a polynomial in q_F^{-s} (the local L-factor for $\mathrm{GL}_{n+1} \times \mathrm{GL}_n$ is a product of terms $(1 - \alpha_i q_F^{-s})^{-1}$, so its reciprocal is a polynomial), P is a Laurent polynomial in q_F^{-s} — hence $P \in R$. Therefore $c*q_F^{-ks} \in I$, and by the spanning property, some $V \in W(\pi, \psi)$ realizes this element as its Rankin-Selberg \int against W_0 .

12.3.3 3. The u_Q twist and the Kirillov model

The key role of u_Q : right-translating W by u_Q gives a new Whittaker function $R(u_Q)W \in W(\Pi, \psi^{-1})$. The restriction to the mirabolic subgroup P_{n+1} gives the Kirillov model, and the function:

$$\phi_Q(g) := W(\text{diag}(g, 1)u_Q) = (R(u_Q)W)(\text{diag}(g, 1))$$

lies in the Kirillov model of Π restricted to GL_n .

We need ϕ_Q to be nonzero as a function on GL_n . This requires two separate facts:

Fact 1: $R(u_Q)W$ is nonzero in $W(\Pi, \psi^{-1})$. Right translation by u_Q preserves the Whittaker model (since u_Q lies in the unipotent radical of the standard maximal parabolic, which normalizes ψ). The map $W \rightarrow R(u_Q)W$ is a linear automorphism of $W(\Pi, \psi^{-1})$ (with inverse $R(u_Q^{-1})$), so $R(u_Q)W \neq 0$ whenever $W \neq 0$.

Fact 2: $\phi_Q(g) = W_0(\text{diag}(g, 1)u_Q)$ is nonzero for $W_0 = \text{new vector}$. This is verified by direct evaluation at $g = I_n$:

$$\phi_Q(I_n) = W_0(\text{diag}(I_n, 1) \cdot u_Q) = W_0(u_Q)$$

Now $u_Q = I_{n+1} + QE_{n,n+1}$ is an element of the upper-triangular unipotent subgroup N_{n+1} (its only off-diagonal entry is Q in position $(n, n+1)$). By the Whittaker-model transformation rule:

$$W_0(u_Q) = \psi^{-1}(u_Q) \cdot W_0(I_{n+1})$$

The generic character ψ of N_{n+1} evaluates on superdiagonal entries: $\psi(u_Q) = \psi(Q)$ (the only superdiagonal entry of u_Q is Q in position $(n, n+1)$). With the standard normalization $W_0(I_{n+1}) = 1$:

$$\phi_Q(I_n) = \psi^{-1}(Q) \cdot 1 = \psi^{-1}(Q)$$

Since ψ is a nontrivial character of F and $Q \neq 0$ (Q generates q^{-1}), $\psi^{-1}(Q)$ is a nonzero complex number (it lies on the unit circle). Therefore $\phi_Q(I_n) \neq 0$, so ϕ_Q is nonzero as a function on GL_n . \square

(Note: this argument is specific to $W_0 = \text{new vector}$ with $W_0(I) = 1$. For the universality claim we only need ϕ_Q nonzero for this particular W_0 , so the direct computation suffices.)

Revision — Closing the Universality Gap

The standard JPSS nondegeneracy result (Section 2.7) states that as BOTH W and V vary, the integrals $I(s, W, V)$ generate the full fractional ideal $L(s, \Pi \times \pi) * \mathbb{C}[q_F^s, q_F^{-s}]$. For the universality claim, we need this to hold for FIXED $W = W_0$. This requires the following:

Lemma (fixed-W spanning). Let Π be a generic irreducible admissible representation

of $\mathrm{GL}_{n+1}(F)$, and let ϕ be any nonzero function in the Kirillov model of Π restricted to GL_n . Then the set of integrals

$$\int_{N_n \backslash \mathrm{GL}_n(F)} \phi(g) V(g) |\det g|^{s-1/2} dg : V \in W(\pi, \psi)$$

generates a nonzero fractional ideal of $\mathbb{C}[q_F^s, q_F^{-s}]$ (contained in the full ideal $L(s, \Pi \times \pi) * \mathbb{C}[q_F^s, q_F^{-s}]$).

Proof sketch. The Kirillov model of $\Pi|_{\mathrm{GL}_n}$ contains all compactly supported locally constant functions on $N_n \backslash \mathrm{GL}_n(F)$ (Bernstein-Zelevinsky 1976, Theorem 5.21 and Corollary 5.22). In particular, ϕ can be approximated by compactly supported functions. The Rankin-Selberg \int against a fixed nonzero ϕ defines a nonzero linear functional on $W(\pi, \psi)$ (as a function of V), since π is generic and hence $W(\pi, \psi)$ separates points on $N_n \backslash \mathrm{GL}_n(F)$. The resulting set of integrals is a nonzero $\mathbb{C}[q_F^s, q_F^{-s}]$ -submodule of $L(s, \Pi \times \pi) * \mathbb{C}[q_F^s, q_F^{-s}]$. Since $\mathbb{C}[q_F^s, q_F^{-s}]$ is a PID (a Laurent polynomial ring in one variable q_F^{-s}), every nonzero submodule of a free rank-1 module is itself free of rank 1. Let $L_\phi(s) * \mathbb{C}[q_F^s, q_F^{-s}]$ be this submodule, where L_ϕ divides $L(s, \Pi \times \pi)$.

To show $L_\phi = L(s, \Pi \times \pi)$ (i.e., fixed ϕ generates the FULL ideal):

The JPSS theory (1983, Section 2.7) shows that the full ideal is generated by letting both W and V vary. Varying W (with restriction to GL_n) corresponds to varying ϕ in the full Kirillov model $K(\Pi)|_{\mathrm{GL}_n}$. The ideal generated by ALL ϕ is $L(s, \Pi \times \pi) * R$. We must show that a SINGLE nonzero ϕ already suffices.

Consider the map $\Phi : K(\Pi)|_{\mathrm{GL}_n} \rightarrow (\text{fractional ideals of } R)$ defined by $\Phi(\phi) = \{I(s, \phi, V) : V \in W(\pi, \psi)\} \cdot R$. By the JPSS theory, $\bigcup_\phi \Phi(\phi)$ generates $L(s, \Pi \times \pi) \cdot R$. Since R is a PID, $\Phi(\phi) = L_\phi \cdot R$ for some L_ϕ dividing $L(s, \Pi \times \pi)$.

Key step. Φ is GL_n -equivariant in the following sense: for $g_0 \in \mathrm{GL}_n$, the substitution $g \mapsto g \cdot g_0$ in the \int gives

$$I(s, R(g_0)\phi, V) = |\det g_0|^{1/2-s} \cdot I(s, \phi, R'(g_0)V),$$

where R' denotes the contragredient action on $W(\pi, \psi)$. Since $R'(g_0)$ is an automorphism of $W(\pi, \psi)$, the set of integrals

$$\{I(s, R(g_0)\phi, V) : V \in W(\pi, \psi)\} = \{|\det g_0|^{1/2-s} \cdot I(s, \phi, V) : V \in W(\pi, \psi)\} = |\det g_0|^{1/2-s} \cdot \Phi(\phi).$$

But $|\det g_0|^{1/2-s} = q_F^{-k \cdot s} \cdot (\text{unit in } R)$ is a unit in the localization, so $\Phi(R(g_0)\phi)$ and $\Phi(\phi)$ generate the same fractional ideal. That is: $L_{R(g_0)\phi} = L_\phi$ (up to units in R) for all $g_0 \in \mathrm{GL}_n$.

Now, the Kirillov model $K(\Pi)|_{\mathrm{GL}_n}$ is irreducible as a GL_n -representation (Bernstein-Zelevinsky 1976, Theorem 5.21). Therefore for any nonzero ϕ , the GL_n -translates $\{R(g_0)\phi : g_0 \in \mathrm{GL}_n\}$ span all of $K(\Pi)|_{\mathrm{GL}_n}$. We use this in two directions:

Direction 1 (L_ϕ divides $L(s, \Pi \times \pi)$): $\Phi(\phi) \subseteq \Phi_{full}$ (the full ideal generated by all W)

and V), so $L_\phi \cdot R \subseteq L(s, \Pi \times \pi) \cdot R$. Since $L_\phi \cdot R \subseteq L(s, \Pi \times \pi) \cdot R$, we get L_ϕ divides $L(s, \Pi \times \pi)$ in the PID R (in a PID, (a) \subseteq (b) iff $b \mid a$).

Direction 2 ($L(s, \Pi \times \pi)$ divides L_ϕ): For any nonzero $\phi' \in K(\Pi)|_{\text{GL}_n}$, write $\phi' = \sum_i c_i R(g_i) \phi$ (finite linear combination of GL_n -translates, possible by irreducibility). For each V :

$$I(s, \phi', V) = \sum_i c_i \cdot I(s, R(g_i) \phi, V)$$

By the equivariance in the key step, $I(s, R(g_i) \phi, V)$ lies in $L_\phi \cdot R$ for each i (since $\Phi(R(g_i) \phi) = L_{R(g_i)\phi} \cdot R = L_\phi \cdot R$). The sum of elements of $L_\phi \cdot R$ lies in $L_\phi \cdot R$ (it's a module). Therefore $\Phi(\phi') \subseteq L_\phi \cdot R$ for every nonzero ϕ' .

The R -submodule generated by all $\Phi(\phi')$ equals the full Rankin-Selberg ideal $L(s, \Pi \times \pi) \cdot R \subseteq L_\phi \cdot R$. So $L_\phi \mid L(s, \Pi \times \pi)$.

Combining both directions: $L_\phi = L(s, \Pi \times \pi)$ (up to units in R). \square

Application: Taking $\phi = \phi_Q$ (the restriction of $R(u_Q)W_0$, which is nonzero by the Kirillov injectivity lemma), the integrals over V generate the full fractional ideal for our fixed W_0 . This closes the universality gap identified by the reviewer.

12.3.4 4. Nondegeneracy of the pairing

For a nonzero ϕ_Q in the Kirillov model, the Rankin-Selberg pairing:

$$V \mapsto \int_{N_n \backslash \text{GL}_n(F)} \phi_Q(g) V(g) |\det g|^{s-1/2} dg$$

is nondegenerate as V ranges over $W(\pi, \psi)$. This is the fundamental nondegeneracy of the Rankin-Selberg \int (Jacquet-Piatetski-Shapiro-Shalika 1983, Section 2.7).

More precisely: since ϕ_Q is nonzero, the integrals over all $V \in W(\pi, \psi)$ generate the full fractional ideal $L(s, \Pi \times \pi) * \mathbb{C}[q_F^s, q_F^{-s}]$.

12.3.5 5. Choosing W : the new vector

Choice: Let W_0 be the new vector (essential Whittaker function) of Π , i.e., the vector in $W(\Pi, \psi^{-1})$ fixed by the congruence subgroup $K_1(p^{c(\Pi)})$ where $c(\Pi)$ is the conductor exponent of Π .

Properties of W_0 :

- W_0 is nonzero (Π is generic)
- $W_0(I_{n+1}) = 1$ (standard normalization)
- $R(u_Q)W_0$ is nonzero for every $Q \in F^\times$ (as argued in Step 3)

Universality: For any generic π of $\mathrm{GL}_n(F)$ with conductor ideal q :

- Let Q generate q^{-1}
- The function $\phi_Q(g) = W_0(\mathrm{diag}(g, 1)u_Q)$ is nonzero in the Kirillov model
- By the nondegeneracy (Step 4), there exists $V \in W(\pi, \psi)$ such that $I(s, W_0, V)$ is a nonzero element of $L(s, \Pi \times \pi) * \mathbb{C}[q_F^s, q_F^{-s}]$
- By the algebraic argument (Step 2), V can be chosen to make the \int equal to $c * q_F^{-ks}$, which is finite and nonzero for all s

12.3.6 6. The role of u_Q in conductor matching

The insertion of $u_Q = I + QE_{n,n+1}$ is essential: it compensates for the conductor of π . Without this twist, for highly ramified π , the \int might degenerate (the new vector of Π would not “see” the ramification of π).

Support analysis via the Casselman-Shalika formula. By the Casselman-Shalika formula (Shintani 1976, Casselman-Shalika 1980), the new vector W_0 of Π has support contained in

$$N_{n+1} * T^+ * K_1(p^{c(\Pi)})$$

where T^+ is the dominant cone in the diagonal torus. Right translation by $u_Q = I + QE_{n,n+1}$ shifts the $(n, n+1)$ -matrix entry by $Q = \pi_F^{-c(\pi)}$. In the Iwasawa decomposition $g = nak$, this modifies the diagonal component at scale Q . Concretely, the support of the twisted function

$$g \mapsto W_0(\mathrm{diag}(g, 1)u_Q)$$

intersects the support of $K_1(p^{c(\pi)})$ — *fixed* vectors in $W(\pi, \psi)$ nontrivially, because the Q -shift matches the conductor scale of π exactly: the new vector of π is supported on $N_n * T^+ * K_1(p^{c(\pi)})$ (by the analogous Casselman-Shalika result for GL_n), and the u_Q twist aligns the two conductor levels (see Jacquet-Piatetski-Shapiro-Shalika 1981, Section 5, for the precise support computation in the Rankin-Selberg setting).

This support matching is what makes the \int nondegenerate: it ensures that the integrand $W_0(\mathrm{diag}(g, 1)u_Q) * V(g)$ is not identically zero on $N_n \backslash \mathrm{GL}_n(F)$ for appropriate V .

12.3.7 7. Verification in special cases

Both unramified ($c(\Pi) = c(\pi) = 0$): $u_Q = I + E_{n,n+1}(Q = 1) \cdot W_0$ is the spherical vector. The \int with V_0 (spherical for π) gives $L(s, \Pi \times \pi) * (\text{correction factor})$. Choose V to cancel the L-factor.

Π unramified, π ramified: u_Q has $Q = \pi_F^{-c(\pi)}$. The twist shifts the support of the spherical vector to match the ramification of π . This is the classical “conductor-lowering” mechanism.

Both ramified: The new vector of Π combined with the u_Q twist gives a function in the Kirillov model whose support is compatible with the conductor of π . Nondegeneracy follows from the general JPSS theory.

12.3.8 8. Summary

1. The answer is YES: the new vector W_0 of Π is a universal test vector
2. For any π with conductor q , the twist u_Q (Q generates q^{-1}) ensures the Rankin-Selberg pairing is nondegenerate
3. Nondegeneracy of the Kirillov restriction: $R(u_Q)W_0$ is always nonzero
4. The fractional ideal structure of Rankin-Selberg integrals allows choosing V to make the \int a monomial $c * q_F^{-ks}$
5. This monomial is finite and nonzero for all $s \in C$

12.4 References

- I. N. Bernstein, A. V. Zelevinsky, “Representations of the group $GL_n(F)$ where F is a local non-archimedean field,” Russian Math. Surveys 31:3 (1976), 1–68. [Theorem 5.21: Kirillov model injectivity for generic representations; Corollary 5.22: density of compactly supported functions]
- J. W. Cogdell, “Lectures on L-functions, converse theorems, and functoriality for GL_n ,” Fields Institute Lectures, 2004, Section 3.1. [Survey of Kirillov model and Whittaker model properties]
- H. Jacquet, I. I. Piatetski-Shapiro, J. A. Shalika, “Rankin-Selberg convolutions,” Amer. J. Math. 105 (1983), 367–464, Section 2.7. [Nondegeneracy of the Rankin-Selberg pairing; fractional ideal structure]
- H. Jacquet, I. I. Piatetski-Shapiro, J. A. Shalika, “Conducteur des représentations du groupe linéaire,” Math. Ann. 256 (1981), 199–214, Section 5. [Support of new vectors and conductor matching]
- W. Casselman, J. Shalika, “The unramified principal series of p -adic groups II: the Whittaker function,” Compositio Math. 41 (1980), 207–231. [Casselman-Shalika formula for Whittaker function support]

Process Note — futon6 Corpus References

- PlanetMath: “representation theory” -- admissible representations
- PlanetMath: “L-function” -- L-factors and analytic properties
- PlanetMath: “locally compact group” -- p-adic groups

Chapter 13

Problem 3: Markov Chain with Interpolation ASEP Polynomial Stationary Distribution

13.1 Problem Statement

Let $\lambda = (\lambda_1 > \dots > \lambda_n \geq 0)$ be a restricted partition with distinct parts (unique part of size 0, no part of size 1). Does there exist a nontrivial Markov chain on $S_n(\lambda)$ whose stationary distribution is

$$\pi(\mu) = F'_{\mu}(x_1, \dots, x_n; q = 1, t) / P'_{\lambda}(x_1, \dots, x_n; q = 1, t)$$

where F'_{μ} are interpolation ASEP polynomials and P'_{λ} is the interpolation Macdonald polynomial?

13.2 Answer

Yes.

Take the inhomogeneous multispecies t-PushTASEP on the finite ring of n sites with content λ and parameters x_1, \dots, x_n . This is a concrete continuous- time Markov chain defined directly from local species comparisons and ringing rates $1/x_i$ (no use of F'_{μ} in the transition rule). A theorem of Ayyer-Martin-Williams identifies its stationary distribution as

$$\pi(\mu) = F_{\mu}(x; 1, t) / P_{\lambda}(x; 1, t),$$

which is the ratio required in the problem statement (same $q = 1$ ASEP/Macdonald family, up to notation conventions).

Process Note — Confidence

Medium-high. The existence claim is a direct consequence of a published theorem. The nontriviality condition is checked from the explicit generator.

13.3 Solution

13.3.1 1. State space

Let

$$S_n(\lambda) = \{\text{all permutations of the parts of } \lambda\}.$$

Because λ has distinct parts, $|S_n(\lambda)| = n!$.

This is exactly the finite state space used by multispecies exclusion-type dynamics with one particle species per part value.

13.3.2 2. Lemma (explicit chain construction)

Define a continuous-time Markov chain X_t on $S_n(\lambda)$ as follows.

Fix parameters $x_1, \dots, x_n > 0$ and t in $[0,1)$. At each site j , an exponential clock of rate $1/x_j$ rings.

If site j is a vacancy (species 0), nothing happens. If site j has species $r_0 > 0$, that particle becomes active. Let m be the number of particles in the current configuration with species strictly less than r_0 (including vacancies). Moving clockwise, the active particle chooses the k -th weaker particle with probability

$$t^{(k-1)}/[m]_t, \text{ where } [m]_t = 1+t+\dots+t^{(m-1)},$$

and swaps into that position. If it displaced a nonzero species, the displaced particle becomes active and repeats the same rule. The cascade ends when a vacancy is displaced.

This is the inhomogeneous multispecies t -PushTASEP.

Why this is a valid Markov chain:

- The state space is finite.
- The transition rule is explicit and depends only on current local ordering, t , and x_i .
- Rates are finite and nonnegative.

13.3.3 3. Lemma (nontriviality)

The chain above is nontrivial in the sense asked by the problem:

- Transition rates are defined from site rates $1/x_i$, species inequalities, and t -geometric choice weights.

- No transition probability is defined using values of F'_{μ} or P'_{λ} .

So this is not a Metropolis-style chain “described using the target weights.”

13.3.4 4. Main theorem (stationary distribution)

Theorem (Ayyer-Martin-Williams, 2024, arXiv:2403.10485, Thm. 1.1): For the inhomogeneous multispecies t-PushTASEP on the ring with n sites, content λ (restricted partition with distinct parts), parameters $x_1, \dots, x_n > 0$, and $0 \leq t < 1$, the stationary probability of $\eta \in S_n(\lambda)$ is

$$\pi(\eta) = F_{\eta}(x; 1, t) / P_{\lambda}(x; 1, t),$$

where F_{η} are ASEP polynomials at $q = 1$ and $P_{\lambda}(x; 1, t) = \sum_{\nu \in S_n(\lambda)} F_{\nu}(x; 1, t)$ is the partition function (ensuring π sums to 1). Positivity: $F_{\eta}(x; 1, t) > 0$ for $x_i > 0, 0 \leq t < 1$ is established as part of AMW Theorem 1.1, which shows that $\pi(\eta) = F_{\eta}/P_{\lambda}$ is a probability distribution. The explicit combinatorial formula (sum of products of t-weights over tableaux) has strictly positive terms for the given parameter range.

Therefore, the required ratio form exists as the stationary law of a concrete Markov chain.

13.3.5 5. Notation bridge: $F'_{\mu}/P'_{\lambda} = F_{\mu}/P_{\lambda}$

The problem uses star notation F'_{μ}, P'_{λ} (interpolation ASEP polynomials in the Knop-Sahi convention), while AMW Theorem 1.1 uses F_{η}, P_{λ} .

Claim: The ratio $F'_{\mu}/P'_{\lambda} = F_{\mu}/P_{\lambda}$ for all $\mu \in S_n(\lambda)$.

Proof: In both conventions, the partition function is defined as the sum over the state space:

$$\begin{aligned} P_{\lambda}(x; 1, t) &= \sum_{\eta \in S_n(\lambda)} F_{\eta}(x; 1, t) \\ P'_{\lambda}(x; 1, t) &= \sum_{\eta \in S_n(\lambda)} F'_{\eta}(x; 1, t) \end{aligned}$$

Only ratio-invariance is needed: if conventions differ by an η -independent normalization (for fixed λ), then $F'_{\mu}/P'_{\lambda} = F_{\mu}/P_{\lambda}$. Concretely, if $F'_{\eta} = \alpha * F_{\eta}$ for some constant α independent of η , then $P'_{\lambda} = \alpha * P_{\lambda}$ and:

$$F'_{\mu}/P'_{\lambda} = (\alpha F_{\mu}) / (\alpha P_{\lambda}) = F_{\mu}/P_{\lambda}.$$

The constant cancels in the ratio regardless of its value.

That α is independent of η follows from the exchange-relation structure. Both F'_{η} and F_{η} satisfy the same Hecke exchange relations under generators T_i (Corteel-Mandelshtam-

Williams, Section 3, define both normalizations and verify their equivalence at $q = 1$). The normalization is fixed by the leading-term convention, which is uniform across the state space $S_n(\lambda)$. Concretely, at $q = 1$ both families specialize to the same t-weight formula, so $\alpha = 1$ and $F'_{\eta} = F_{\eta}$.

Verification for $n = 2$. Take $\lambda = (a, 0)$. Both conventions give $F_{(a,0)}(x_1, x_2; 1, t) = x_1$ and $F_{(0,a)}(x_1, x_2; 1, t) = x_2$ (the single-species case reduces to site weights). The ratio $F'_{\eta}/P'_{\lambda} = F_{\eta}/P_{\lambda} = x_i/(x_1+x_2)$ in both conventions.

13.3.6 6. Sanity check: $n = 2$ reduction

Take $\lambda = (a, 0)$, state space $\{(a, 0), (0, a)\}$. There is one non-vacancy and one vacancy. Bells ring at rates $1/x_1$ and $1/x_2$.

- $(a, 0) \rightarrow (0, a)$ at rate $1/x_1$
- $(0, a) \rightarrow (a, 0)$ at rate $1/x_2$

So the stationary distribution is

$$\pi(a, 0) = x_1/(x_1+x_2), \pi(0, a) = x_2/(x_1+x_2),$$

which is consistent with the single-species stationary law in the same paper (Proposition 2.4, via recoloring reduction).

This confirms the construction is concrete and internally consistent in the simplest nontrivial case.

13.3.7 7. Conclusion

For $x_i > 0$ and $0 \leq t < 1$, the inhomogeneous multispecies t-PushTASEP on $S_n(\lambda)$ is:

- A well-defined finite CTMC (Section 2: finite state space, explicit nonnegative rates).
- Nontrivial: transition rates depend on (x, t) and local species ordering, not on values of F'_{μ} or P'_{λ} (Section 3).
- Has stationary distribution $\pi(\eta) = F_{\eta}(x; 1, t) / P_{\lambda}(x; 1, t)$ by AMW Theorem 1.1 (Section 4), which equals F'_{μ}/P'_{λ} under the notation bridge (Section 5).

Existence vs uniqueness. AMW Theorem 1.1 establishes that π is a stationary distribution. Uniqueness (hence convergence from any initial state) follows from irreducibility on $S_n(\lambda)$.

Irreducibility proof (via vacancy transport). Since $\lambda_n = 0$, every configuration has exactly one vacancy (species 0). A single clock ring can produce a multi-step push cascade, so we must be careful about which net transitions are achievable.

The key observation: when a non-vacancy particle at site j is adjacent to the vacancy at site $j+1$ (cyclically), and the clock at j rings, one possible outcome of the t -geometric choice is

that the active particle selects the vacancy (the nearest weaker-species particle clockwise). This selection has probability $1/[m]_t > 0$ (the $k = 1$ term in the t -geometric distribution, where $m \geq 1$ counts weaker particles). The particle moves to the vacancy's position, the vacancy absorbs it, and the cascade terminates immediately (displaced species is 0). The net effect is an adjacent swap of the non-vacancy species and the vacancy.

By composing such vacancy-adjacent swaps, the vacancy can be moved to any site on the ring (analogous to the 15-puzzle). Each swap has positive rate, and routing the vacancy through a sequence of sites produces any desired permutation of the non-vacancy species. Specifically, to transpose species at sites i and j : move the vacancy adjacent to i , swap it with i 's species, route the vacancy to j , swap it with j 's species, and route it back. This requires at most $O(n)$ vacancy-adjacent swaps, each of positive rate. Hence any configuration can reach any other with positive probability.

On a finite irreducible CTMC, the stationary distribution is unique.

Therefore the answer is **Yes**.

13.4 References

- Arvind Ayyer, James Martin, Lauren Williams, “The Inhomogeneous t-PushTASEP and Macdonald Polynomials at $q=1$ ”, arXiv:2403.10485, Theorem 1.1 and Proposition 2.4.
- Sylvie Corteel, Olya Mandelshtam, Lauren Williams, “From multiline queues to Macdonald polynomials”, for ASEP polynomial context.

Chapter 14

Problem 4: Root Separation Under Finite Free Convolution

14.1 Problem Statement

Two monic polynomials of degree n:

$$p(x) = \sum_{k=0}^n a_k x^{n-k}, a_0 = 1$$
$$q(x) = \sum_{k=0}^n b_k x^{n-k}, b_0 = 1$$

The **finite free additive convolution** $p \boxplus_n q$ has coefficients:

$$c_k = \sum_{i+j=k} [(n-i)!(n-j)!/(n!(n-k)!)] a_i b_j$$

The **root separation energy**:

$$\Phi_n(p) = \sum_i (\sum_{j \neq i} 1/(\lambda_i - \lambda_j))^2$$

where $\lambda_1, \dots, \lambda_n$ are the roots of p. ($\Phi_n = \infty$ if p has repeated roots.)

Question (Spielman): Is it true that for monic real-rooted polynomials p, q of degree n:

$$1/\Phi_n(p \boxplus_n q) \geq 1/\Phi_n(p) + 1/\Phi_n(q)?$$

14.2 Answer

Conjecturally yes, with strong numerical evidence. The inequality holds in all 8000+ random trials tested ($n = 2-5$) with no violations. Proved analytically for $n = 2$ (equality) and $n = 3$ (strict inequality via Cauchy-Schwarz). An analytic proof for $n \geq 4$ remains open.

- $n = 2$: equality holds ($1/\Phi_2$ is linear in the discriminant).
- $n = 3$: **PROVED** via the identity $\Phi_3 * \text{disc} = 18*a_2^2$ and Titu's lemma.
- $n \geq 4$: numerically verified, proof incomplete. The $n = 3$ identity does not generalize;

the \boxplus_n cross-terms play an essential role.

14.3 Solution

14.3.1 Interpreting Φ_n algebraically

For a monic polynomial $p(x) = \prod_i (x - \lambda_i)$ with distinct roots, the derivative at each root is given by the exact algebraic identity:

$$p'(\lambda_i) = \prod_{j \neq i} (\lambda_i - \lambda_j)$$

(no limiting procedure needed — this is immediate from the product rule). Therefore the inner sum in Φ_n is:

$$\begin{aligned} & \sum_{j \neq i} 1 / (\lambda_i - \lambda_j) \\ &= [\sum_{j \neq i} \prod_{k \neq i, k \neq j} (\lambda_i - \lambda_k)] / p'(\lambda_i) \end{aligned}$$

which is a rational function of the root differences alone. The root separation energy is:

$$\Phi_n(p) = \sum_i (\sum_{j \neq i} 1 / (\lambda_i - \lambda_j))^2$$

This is the sum of squared "Coulomb forces" at each root — the total electrostatic self-energy of the root configuration (in the 1D log-gas picture). All expressions are exact rational functions of root differences, with no regularization or limiting procedure required (assuming distinct roots, which is guaranteed since $\Phi_n = \infty$ for repeated roots).

14.3.2 Connection to the discriminant

The discriminant of p is:

$$\text{disc}(p) = \prod_{i < j} (\lambda_i - \lambda_j)^2$$

By the AM-QM inequality applied to $1 / (\lambda_i - \lambda_j)$:

$$\Phi_n(p) \geq n(n-1)^2 / \sum_{i < j} (\lambda_i - \lambda_j)^2$$

(Cauchy-Schwarz). So $1 / \Phi_n$ is related to the "spread" of roots. Specifically:

$$1/\Phi_n(p) \leq \sum_{i < j} (\lambda_i - \lambda_j)^2 / (n(n-1)^2)$$

14.3.3 Finite free convolution and root behavior

The operation \boxplus_n was introduced by Marcus, Spielman, and Srivastava (2015) as a finite-dimensional analogue of Voiculescu's free additive convolution. Key properties:

- (a) **Real-rootedness preservation:** If p, q are real-rooted monic polynomials of degree n , then $p \boxplus_n q$ is also real-rooted.
- (b) **Expected characteristic polynomial:** If A, B are $n \times n$ Hermitian with char. poly. p_A, p_B , then for a uniformly random conjugation U :

$$E_U[\text{char.poly.of } A + UBU^*] = p_A \boxplus_n p_B$$

- (c) **Linearization of cumulants:** In the $n \rightarrow \infty$ limit, the finite free cumulants linearize (R-transform additivity).
- (d) **Root spreading:** Free convolution generally spreads roots apart. Convolving with a non-degenerate q increases the minimum root gap.

14.3.4 The inequality via the random matrix model

Using property (b), interpret $p \boxplus_n q$ as the expected characteristic polynomial of $A + UBU^*$ where $\text{char}(A) = p$, $\text{char}(B) = q$.

Φ_n via the random matrix model.

For Hermitian A with eigenvalues $\lambda_1, \dots, \lambda_n$, the root separation energy $\Phi_n(\text{char}(A)) = \sum_i (\sum_{j \neq i} 1 / (\lambda_i - \lambda_j))^2$ is an algebraic function of the eigenvalue gaps (see Section 1). The connection to $\log |\det(xI - A)|$ is conceptual: away from roots, $F_A''(x) = -\sum_i 1 / (x - \lambda_i)^2$, and Φ_n captures the "residue" version at each root. But the definition of Φ_n uses only the exact algebraic expressions from Section 1.

14.3.5 Finite free cumulants and the bilinear structure

The MSS coefficient formula. The \boxplus_n operation acts on coefficients as:

$$c_k = \sum_{i+j=k} [(n-i)!(n-j)!/(n!(n-k)!)] a_i b_j$$

This is bilinear but NOT simply additive in the a_k . For example, at $n = 3$:

$$\begin{aligned}
c_1 &= a_1 + b_1 \text{ (additive)} \\
c_2 &= a_2 + (2/3)*a_1*b_1 + b_2 \text{ (cross - term!)} \\
c_3 &= a_3 + (1/3)*a_2*b_1 + (1/3)*a_1*b_2 + b_3
\end{aligned}$$

Finite free cumulants. Following Arizmendi-Perales (2018), there exist finite free cumulants κ_k^n related to the a_k by a nonlinear moment-cumulant formula (via non-crossing partitions with falling-factorial weights) such that:

$$\kappa_k^n(p \boxplus_n q) = \kappa_k^n(p) + \kappa_k^n(q)$$

The polynomial coefficients a_k are NOT the finite free cumulants; they are finite free MOMENTS. The relationship involves a Möbius inversion on the lattice of non-crossing partitions.

14.3.6 Complete proof for $n = 3$

Verification script: `scripts/verify-p4-n3-proof.py`

Step 1: Centering reduction. Since Φ_n depends only on root differences (translation invariant), and \boxplus_n commutes with translation (via the random matrix model: translating A by cI shifts all eigenvalues of $A + QBQ^*$ by c), we may assume WLOG that $a_1 = b_1 = 0$ (centered polynomials).

Step 2: \boxplus_3 simplifies for centered cubics. When $a_1 = b_1 = 0$, the MSS cross-terms in c_2 and c_3 vanish:

$$\begin{aligned}
c_2 &= a_2 + (2/3)*0*0 + b_2 = a_2 + b_2 \\
c_3 &= a_3 + (1/3)*a_2*0 + (1/3)*0*b_2 + b_3 = a_3 + b_3
\end{aligned}$$

So \boxplus_3 reduces to plain coefficient addition for centered cubics.

Step 3: The key identity. For a centered cubic $p(x) = x^3 + a_2*x + a_3$ with distinct real roots (requiring $a_2 < 0$ and $\text{disc} = -4*a_2^3 - 27*a_3^2 > 0$):

$$\Phi_3(p) * \text{disc}(p) = 18*a_2^2 \text{ (EXACT)}$$

Equivalently:

$$\begin{aligned}
1/\Phi_3(p) &= \text{disc}(p)/(18*a_2^2) \\
&= (-4*a_2^3 - 27*a_3^2)/(18*a_2^2) \\
&= -2*a_2/9 - 3*a_3^2/(2*a_2^2)
\end{aligned}$$

This identity was discovered numerically and verified symbolically in SymPy. It follows from the explicit formula $\Phi_3 = \sum_i (3*l_i/(3*l_i^2 + e_2))^2$ (where $e_1 = 0$) combined with the discriminant $= \prod_{i < j} (l_i - l_j)^2$.

Step 4: Superadditivity via Cauchy-Schwarz. Write $s = -a_2 > 0$, $t = -b_2 > 0$, $u = a_3$, $v = b_3$. Then:

$$\begin{aligned} 1/\Phi(p) &= 2s/9 - 3u^2/(2s^2) \\ 1/\Phi(q) &= 2t/9 - 3v^2/(2t^2) \\ 1/\Phi(p \boxplus_3 q) &= 2(s+t)/9 - 3(u+v)^2/(2(s+t)^2) \end{aligned}$$

The surplus is:

$$\begin{aligned} \text{surplus} &= 1/\Phi(\text{conv}) - 1/\Phi(p) - 1/\Phi(q) \\ &= (3/2)*[u^2/s^2 + v^2/t^2 - (u+v)^2/(s+t)^2] \end{aligned}$$

This is non-negative by Titu's lemma (Engel form of Cauchy-Schwarz):

$$u^2/s^2 + v^2/t^2 \geq (u+v)^2/(s^2+t^2) \quad [\text{Titu's lemma}]$$

and since $s^2 + t^2 \leq (s+t)^2$ (because $2st > 0$):

$$(u+v)^2/(s^2+t^2) \geq (u+v)^2/(s+t)^2$$

Combining: surplus ≥ 0 . Equality iff $u/s^2 = v/t^2$ and $s = t$ or $u = v = 0$.

QED for $n = 3$.

14.3.7 What the proof requires for $n \geq 4$

For $n \geq 4$, the $n = 3$ approach does not directly generalize:

- (a) The identity $\Phi_n * \text{disc} = \text{const} * a_2^2$ FAILS for $n \geq 4$. At $n = 4$, the product $\Phi_4 * \text{disc}$ depends on a_3 and a_4 as well.
- (b) \boxplus_4 has a cross-term even for centered polynomials: $c_4 = a_4 + (1/6)*a_2*a_3 + b_4$. Unlike $n = 3$, centering does NOT reduce \boxplus_4 to plain coefficient addition.
- (c) The cross-term is ESSENTIAL: plain coefficient addition fails superadditivity $\sim 29\%$ of the time for centered quartics, while \boxplus_4 gives 0 violations.

A correct proof for $n \geq 4$ likely requires exploiting the specific bilinear structure of the MSS convolution formula or the random matrix interpretation.

14.3.8 Verification for small cases

Degree 2 (proved — equality): $p(x) = x^2 + a_1*x + a_2$.

$$\begin{aligned}\Phi_2(p) &= 2/(a_1^2 - 4*a_2) \\ 1/\Phi_2(p) &= (a_1^2 - 4*a_2)/2\end{aligned}$$

The \boxplus_2 formula gives $c_1 = a_1 + b_1$, $c_2 = a_2 + a_1*b_1/2 + b_2$. Then:

$$1/\Phi_2(p \boxplus q) = (c_1^2 - 4*c_2)/2 = (a_1^2 - 4*a_2)/2 + (b_1^2 - 4*b_2)/2$$

Surplus = 0 (symbolic verification). Equality for all degree-2 polynomials.

Degree 3 (proved — strict inequality): See Section 5a. The proof uses:

- Translation invariance of Φ + translation compatibility of \boxplus_3 to center
- Identity $\Phi_3 * \text{disc} = 18*a_2^2$ (for centered cubics)
- Titu's lemma (Cauchy-Schwarz) to bound the surplus

Status Note

The inequality is conjecturally true, with strong numerical evidence and analytic proofs for $n = 2, 3$. $n = 2$: proved (equality; $1/\Phi_2$ is linear in the discriminant). $n = 3$: proved (strict inequality; $\Phi_3 * \text{disc} = 18*a_2^2$ identity + Titu's lemma). $n = 4$: numerically verified (0/3000 violations; the \boxplus_4 cross-term $a_2*b_2/6$ is essential). $n = 5$: numerically verified (0/2000 violations). What is established analytically: (i) finite free cumulants add under \boxplus_n (Arizmendi–Perales 2018); (ii) \boxplus_n commutes with translation (random matrix argument); (iii) superadditivity is specific to \boxplus_n —plain coefficient addition fails $\sim 40\%$ of the time.

Open Obligation — What Remains Open for $n \geq 4$

What remains open for $n \geq 4$:

The $n = 3$ proof relies on $\Phi_3 * \text{disc} = 18*a_2^2$ being constant in a_3 . This fails at $n = 4$ (the product depends on all coefficients). The \boxplus_4 cross-term $(1/6) * a_2*b_2 \in c_4$ is essential (plain addition fails 29%). A proof for $n \geq 4$ needs either:

- (a) A generalization of the $\Phi * \text{disc}$ identity that accounts for higher coefficients, or
- (b) A direct random-matrix argument via the Haar orbit $A + QBQ^*$, or
- (c) A proof via finite free cumulant coordinates (convexity on the real-rooted image of cumulant space).

Process Note — Numerical Evidence

Verification scripts:

- `scripts/verify-p4-inequality.py` (superadditivity + convexity)
- `scripts/verify-p4-deeper.py` (coefficient addition + MSS structure)
- `scripts/verify-p4-schur-majorization.py` (Schur/submodularity/paths)
- `scripts/verify-p4-coefficient-route.py` (coefficient route, disc identity)
- `scripts/verify-p4-n3-proof.py` (complete $n = 3$ symbolic proof + $n = 4$ exploration)

Superadditivity test (2000 random real-rooted polynomial pairs per n):

n	violations	min ratio	mean ratio	max ratio
2	0/2000	1.000000	1.000000	1.000000
3	0/2000	1.000082	3.031736	162.446
4	0/2000	1.003866	9.549935	2268.065
5	0/2000	1.032848	14.457013	2119.743

Ratio = $LHS/RHS = [1/\Phi_n(p \boxplus q)]/[1/\Phi_n(p) + 1/\Phi_n(q)]$; ratio ≥ 1 means inequality holds. Strict inequality for $n \geq 3$.

Convexity/concavity test (midpoint test in coefficient space):

n	convex violations	concave violations	total tests
3	757 (50.6%)	738 (49.4%)	1495
4	648 (65.7%)	338 (34.3%)	986
5	433 (72.9%)	161 (27.1%)	594

$1/\Phi_n$ is NEITHER convex NOR concave in coefficient space.

Plain coefficient addition test (NOT \boxplus_n):

n	violations	total
3	240	609
4	159	373
5	116	218

Superadditivity FAILS under plain addition — the inequality is specific to the MSS bilinear structure of \boxplus_n .

Process Note — `futon6` Corpus References

- PlanetMath: "monic polynomial" (Monic1)
- PlanetMath: "discriminant" (Discriminant)
- PlanetMath: "resultant" (Resultant, DerivationOfSylvestersMatrixForTheResultant)
- PlanetMath: "logarithmic derivative" (LogarithmicDerivative)
- PlanetMath: "partial fraction decomposition" (ALectureOnThePartialFractionDecompositionMethod)
- PlanetMath: "cumulant generating function" (CumulantGeneratingFunction)

14.4 External References

- Marcus, Spielman, Srivastava (2015), “Interlacing Families II: Mixed Characteristic Polynomials and the Kadison-Singer Problem,” Annals of Math 182(1), 327–350. [Defines \boxplus_n , proves real-rootedness preservation, random matrix interpretation]
- Arizmendi, Perales (2018), “Cumulants for finite free convolution,” J. Combinatorial Theory Ser. A 155, 244–266. arXiv:1702.04761. [Defines finite free cumulants that linearize under \boxplus_n .]

Chapter 15

Problem 5: O-Slice Connectivity via Geometric Fixed Points

15.1 Problem Statement

Fix a finite group G . Let \mathbb{O} denote an incomplete transfer system associated to an N_∞ operad. Define a slice filtration on SH^G adapted to \mathbb{O} and characterize \mathbb{O} -slice connectivity of a connective G -spectrum using geometric fixed points.

15.2 Short Answer

Use the classical regular-slice cells, but restrict subgroup indexing to the family F_O of subgroups allowed by the transfer system. For F_O -local connective G -spectra (those with geometric isotropy in F_O), the connectivity test is the same geometric-fixed-point criterion as Hill-Yarnall, but quantified only over $H \in F_O$.

Process Note — Confidence

Medium. The corrected formulation is structurally consistent with known slice and geometric-fixed-point machinery, and avoids the nonstandard ρ_H^O definition from the previous draft.

Revision — Important Correction

The previous draft used an \mathbb{O} -regular representation ρ_H^O . That is not standard in the transfer-system / N_∞ literature. Transfer/indexing systems control admissible transfers (and admissible finite H -sets), not a replacement for the regular representation in slice-cell definitions.

15.3 Working Definition (transfer-restricted regular slice)

Let T_O be the transfer system associated to \mathbb{O} . Define the admissible subgroup family

$$F_O = H \leq G : \text{the transfer } e \rightarrow H \text{ is allowed} \in T_O.$$

F_O is a family of subgroups in the standard sense: it is closed under conjugation and passage to subgroups (both inherited from the indexing-system axioms of Blumberg-Hill, specifically the conditions on admissible H -sets in their Theorem 1.5 / Section 7).

Define $\tau_{\geq n}^O$ as the localizing subcategory of SH^G generated by regular slice cells

$$G_+ \wedge_H S^{k\rho_H}$$

with $H \in F_O$ and $k|H| \geq n$.

This is the same generating template as regular slice filtration, with subgroup indexing restricted by 0.

Filtration verification. Monotonicity ($\tau_{\geq n+1}^O \subseteq \tau_{\geq n}^O$) is immediate: the generating set for $n+1$ is $a \subset \text{of}$ that for n (if $k|H| \geq n+1$ then $k|H| \geq n$). Exhaustiveness ($\bigcup_n \tau_{\geq n}^O = \mathrm{SH}_{F_O\text{-local}}^G$) holds because every F_O -local object is built from cells with finite $k|H|$. Compatibility with suspension is inherited from the ambient regular slice filtration (Hill-Yarnall, Proposition 1.3).

F_O -locality convention. Say a G -spectrum X is F_O -local if $\Phi^K X = 0$ for all K not in F_O (equivalently, X has geometric isotropy contained in F_O). The characterization theorem below applies to F_O -local connective spectra.

Reference anchor:

- Regular slice generators: Hill-Yarnall, Definition 1.1 (arXiv:1703.10526).
- Family/indexing-system closure: Blumberg-Hill, Theorem 1.5 (arXiv:1309.1750).

15.4 Characterization Theorem (subgroup-family level)

Let X be a connective, F_O -local G -spectrum. Then

$$X \in \tau_{\geq n}^O$$

iff for every $H \in F_O$,

$$\Phi^H X \text{ is } (\text{ceil}(n/|H|) - 1) - \text{connected}.$$

Equivalent homotopy-group form:

$$\pi_i(\Phi^H X) = 0 \text{ for all } i < \text{ceil}(n/|H|), \text{ for all } H \in F_O.$$

The F_O -locality hypothesis is essential: for K not in F_O , the condition $\Phi^K X = 0$ is assumed (not tested), ensuring that the restricted generators span exactly the right localizing subcategory. Reference anchor:

- The geometric-fixed-point characterization for the full regular slice is Hill-Yarnall Theorem A / Theorem 2.5 (arXiv:1703.10526).
- Family localization in equivariant stable homotopy: see e.g. the isotropy separation sequence in HHR, Section 4.

15.5 Proof Sketch

Forward direction ($X \in \tau_{\geq n}^O$ implies connectivity bounds):

1. By construction, $\tau_{\geq n}^O$ is the localizing subcategory generated by cells $G_+ \wedge_H S^{k_{\Phi^H}}$ with $H \in F_O$, $k|H| \geq n$.
2. For each $H \in F_O$, the geometric fixed points of a generating cell satisfy $\Phi^H(G_+ \wedge_H S^{k_{\Phi^H}}) = W_G(H)_+ \wedge S^k$ (a finite wedge of S^k 's indexed by the Weyl group $W_G(H) = N_G(H)/H$).
3. Maps from these generators into X detect $\pi_k(\Phi^H X)$: the Weyl-group multiplicity does not affect vanishing (a map from a finite wedge of S^k 's is zero iff each component is zero iff $\pi_k = 0$).
4. Vanishing for all generators with $k|H| < n$ gives $\pi_i(\Phi^H X) = 0$ for $i < \text{ceil}(n/|H|)$, for each $H \in F_O$.

Reverse direction (connectivity bounds imply $X \in \tau_{\geq n}^O$):

5. Since X is F_O -local, $\Phi^K X = 0$ for K not in F_O . By the isotropy separation sequence, the geometric isotropy of X is contained in F_O , so X is built from cells indexed by subgroups in F_O .
6. The connectivity bounds $\pi_i(\Phi^H X) = 0$ for $i < \text{ceil}(n/|H|)$ and all $H \in F_O$, combined with F_O -locality, place X in the localizing subcategory generated by the F_O -restricted regular slice cells with $k|H| \geq n$. This is the family-localized analogue of the Hill-Yarnall Theorem 2.5 reverse direction.

Reduction lemma for step 6. The Hill-Yarnall reverse argument (Section 2 of arXiv:1703.10526) constructs Postnikov sections using the slice cells as building blocks and the geometric fixed-point detection criterion to control connectivity at each stage. In the F_O -local setting:

- (1) The building blocks are the F_O -restricted slice cells (same construction, restricted indexing to $H \in F_O$). (2) The detection criterion is the same Φ^H test for $H \in F_O$ (with $\Phi^K X = 0$ for $K \notin F_O$ by the locality assumption). (3) The Postnikov tower converges because the localizing subcategory is generated by the same cells.

The only input from the ambient theory is the isotropy separation sequence (HHR, Section 4), which holds in any localizing subcategory of \mathbf{SH}^G . This establishes that the reverse direction transfers from the full regular slice setting to the F_O -local setting.

Note: Without F_O -locality, the reverse direction fails. For example, with $F_O = e$ (trivial transfer), an arbitrary G -spectrum X with $\Phi^e X$ highly connected need not lie in $\tau_{\geq n}^O$ if it has nontrivial geometric isotropy at proper subgroups.

15.6 Special Cases

1. **Complete transfer system** ($F_O = \text{all subgroups}$): every G -spectrum is F_O -local, so the hypothesis is vacuous. Recovers the usual Hill-Yarnall regular slice criterion.
2. **Trivial transfer system** ($F_O = e$): F_O -local means $\Phi^H X = 0$ for all $H \neq e$, i.e., X has trivial geometric isotropy. For such X , the criterion reduces to ordinary Postnikov connectivity of the underlying nonequivariant spectrum $\Phi^e X$.
3. **Intermediate transfer systems**: for F_O -local X , the criterion interpolates by checking Φ^H connectivity only on the allowed family.

Open Obligation — Scope Limitation

Important limitation. This is a subgroup-family-indexed formulation, not a full indexing-system characterization. The full indexing-system formalism of Blumberg-Hill involves admissible finite H -sets, not just admissible subgroups H . Our $F_O = H : e \rightarrow H$ admissible extracts the subgroup-level data; it does not use the finer $K \rightarrow H$ admissibility structure for $K \neq e$. The full indexing-system formulation — characterizing O -slice connectivity in terms of the complete admissible set data — is an open extension of this result.

The F_O -locality hypothesis was added to close the reverse direction of the characterization theorem. This is analogous to how classical slice theorems work in full \mathbf{SH}^G (where every spectrum is F -local for $F = \text{all subgroups}$). For intermediate transfer systems, the hypothesis is nontrivial and should be verified for the spectra of interest.

Literature positioning:

- N_∞ operads and admissibility data: Blumberg-Hill, Def. 1.1, Thm. 1.2, Thm. 1.5 / Sec. 7 (arXiv:1309.1750).
- Regular slice generators and detection: Hill-Yarnall, Def. 1.1, Thm. 2.5 (arXiv:1703.10526).
- Isotropy separation and family localization: HHR, Section 4.

15.7 References

- Michael A. Hill, Michael J. Hopkins, Douglas C. Ravenel, *Equivariant stable homotopy theory and the Kervaire invariant problem* (slice framework).
- Andrew J. Blumberg, Michael A. Hill, *Operadic multiplications in equivariant spectra, norms, and transfers*, arXiv:1309.1750: Definition 1.1, Theorem 1.2.
- Michael A. Hill, Carolyn Yarnall, *A new formulation of the equivariant slice filtration with applications to C_p -slices*, arXiv:1703.10526: Definition 1.1, Theorem A, Theorem 2.5.
-

Process Note — External Research File

External research file.^a

^a<https://github.com/tothedarktowercame/futon6/blob/master/data/first-proof/library-research-findings.md>

Chapter 16

Problem 6: Epsilon-Light Subsets of Graphs

16.1 Problem Statement

Let $G = (V, E, w)$ be a finite undirected graph with nonnegative edge weights and $n = |V|$. Its Laplacian is

$$L = \sum_{e=u,v \in E} w_e (e_u - e_v)(e_u - e_v)^T.$$

For S subseteq V , define the induced-subgraph Laplacian embedded to $R^{V \times V}$:

$$L_S = \sum_{e=u,v \in E, u,v \in S} w_e (e_u - e_v)(e_u - e_v)^T,$$

with zeros outside S rows/columns.

S is ϵ -light if

$$L_S \leq \epsilon L$$

in Loewner order.

Question: does there exist universal $c > 0$ such that for every G and every $\epsilon \in (0, 1)$, there exists S with $|S| \geq c * \epsilon * n$ and $L_S \leq \epsilon L$?

Process Note — Status of This Writeup

K_n : PROVED. The barrier greedy gives $|S| = \epsilon * n / 3, c = 1/3$, via the elementary pigeonhole + PSD trace bound argument (Section 5d).

General graphs: ONE GAP. The formal bound $dbar < 1$ at $M_t \neq 0$ is empirically verified (440/440 steps, 36% margin) but open. The leverage filter approach has a structural C_{lev} tension (Section 5b/5e) that prevents closure via Markov alone. See the attack-path analysis note.^a for the full attack path analysis.

Superseded machinery: MSS interlacing families, Borcea-Branden real stability, Bonferroni eigenvalue bounds — all bypassed by the pigeonhole argument.

^a<https://github.com/tothedarktowercame/futon6/blob/master/data/first-proof/problem6-gpl-h-attack-paths.md>

16.2 1. Exact reformulation

The PSD condition is equivalent to the quadratic form inequality

for all x in \mathbb{R}^V : $x^T L_S x \leq \epsilon x^T L x$.

On $\text{im}(L)$, with L^+ the Moore-Penrose pseudoinverse:

$$L_S \leq \epsilon L \Leftrightarrow \|L^{+/2} L_S L^{+/2}\| \leq \epsilon.$$

16.3 2. Complete graph upper bound (rigorous)

For $G = K_n$ and S of size s , choose x supported on S with $\sum_{i \in S} x_i = 1$. Then

$$\begin{aligned} x^T L_{K_n} x &= n \|x\|^2, \\ x^T L_S x &= s \|x\|^2. \end{aligned}$$

Hence $L_S \leq \epsilon L_{K_n}$ implies $s \leq \epsilon n$. Therefore any universal constant must satisfy

$$c \leq 1.$$

This is an upper bound only.

16.4 3. Random sampling identities (expectation level)

Let $Z_v \sim \text{Bernoulli}(p)$ independently and $S = \{v : Z_v = 1\}$.

1. Size:

$$E[|S|] = pn, \Pr[|S| < pn/2] \leq \exp(-pn/8) (\text{Chernoff}).$$

2. Spectral expectation:

$$E[L_S] = p^2 L,$$

since each edge survives with probability p^2 .

Thus

$$E[\epsilon L - L_S] = (\epsilon - p^2)L.$$

Setting $p=\epsilon$ gives $E[L_S] = \epsilon^2 L \leq \epsilon L$. This is not yet a realization-level guarantee.

16.5 4. Concentration setup (gap-fixed formulation)

Define edge-normalized PSD matrices

$$X_e = L^{+/2} w_e b_e b_e^T L^{+/2}, \quad b_e = e_u - e_v,$$

and leverage scores

$$\begin{aligned} \tau_e &= \text{tr}(X_e) = w_e b_e^T L^+ b_e, \\ \sum_e \tau_e &= n - k \end{aligned}$$

(k = number of connected components).

16.5.1 4a. Star domination with correct counting

Using $Z_u Z_v \leq Z_u$ and $Z_u Z_v \leq Z_v$ for each edge $\{u, v\}$,

$$\begin{aligned} L_S &= \sum_{uv \in E} Z_u Z_v L_{uv} \\ &\leq (1/2) \sum_v Z_v \sum_u Z_u L_{uv}. \end{aligned}$$

So in normalized coordinates

$$\begin{aligned} L^{+/2} L_S L^{+/2} &\leq \sum_v Z_v A_v, \\ A_v &:= (1/2) \sum_u Z_u X_{uv} \geq 0. \end{aligned}$$

Because Z_v are independent Bernoulli variables, the random matrices $Z_v A_v$ are independent PSD summands.

16.5.2 4b. Freedman/Bernstein martingale parameters

Let A_i be a fixed ordering of $\{A_v\}$, $p_i = E[Z_i]$, and define the centered sum

$$X = \sum_i (Z_i - p_i) A_i.$$

With filtration $F_i = \sigma(Z_1, \dots, Z_i)$, Doob martingale

$$Y_i = E[X|F_i], \\ \Delta_i = Y_i - Y_{i-1}$$

has self-adjoint differences. For independent Bernoulli sampling,

$$\Delta_i = (Z_i - p_i)A_i, \\ \|\Delta_i\| \leq \|A_i\| \leq R_* (R_* = \max_i \|A_i\|),$$

and predictable quadratic variation

$$W_n = \sum_i E[\Delta_i^2 | F_{i-1}] = \sum_i p_i(1 - p_i)A_i^2.$$

Matrix Freedman (or matrix Bernstein in independent form) applies once bounds on R_* and $\|W_n\|$ are supplied.

What graph-dependent bounds are needed. To obtain a self-contained concentration bound, one would need $R_* \leq C_1 * \epsilon$ and $\|W_n\| \leq C_2 * \epsilon^2$ for graph-dependent constants C_1, C_2 . Bounding these requires leverage score analysis (showing τ_e bounds are well-distributed across vertices) that is the core content of the external theorem referenced in Section 5. Specifically, the Batson-Spielman-Srivastava barrier-function method controls both R_* and $\|W_n\|$ simultaneously through a potential function that tracks the spectral approximation quality.

This is the correct technical setup that was missing in the earlier draft.

16.6 5. Discharging Assumption V via barrier greedy + pigeonhole

We now prove the vertex-light selection theorem directly, using a barrier greedy combined with the elementary PSD trace bound and pigeonhole averaging.

16.6.1 5a. Heavy edge pruning (Turán)

Call edge e *heavy* "if $\tau_e > \epsilon$, light" otherwise. Since $\sum_e \tau_e = n-1$ and each heavy edge has $\tau_e > \epsilon$:

$$|\text{heavy edges}| \leq (n-1)/\epsilon.$$

By Turán's theorem, a graph with n vertices and at most m edges has independence number

$\geq n^2/(2m+n)$. For the heavy graph:

$$\begin{aligned}\alpha(G_{heavy}) &\geq n^2/(2(n-1)/\epsilon+n) = \epsilon*n/(2+\epsilon) \\ &\geq \epsilon*n/3.\end{aligned}$$

Let I_0 be a maximal independent set in G_{heavy} with $|I_0| \geq \epsilon*n/3$. All edges internal to I_0 are light: $\tau_e \leq \epsilon$.

16.6.2 5b. Leverage degree filter (H2')

Define the leverage degree $ell_v = \sum_{u \in I_0} \tau_{uv}$. Since $\sum_v ell_v = 2 * \sum_{e \in \text{internal to } I_0} \tau_e \leq 2(n-1)$, by Markov:

$$|v \in I_0 : ell_v > C_{lev}/\epsilon| \leq 2(n-1)*\epsilon/C_{lev}.$$

Set $C_{lev} = 8$. Remove vertices with $ell_v > 8/\epsilon$. The number removed is at most $2(n-1) * \epsilon/8 < \epsilon*n/4$. The remaining set I_0' has

$$\begin{aligned}|I_0'| &\geq |I_0| - \epsilon*n/4 \geq \epsilon*n/3 - \epsilon*n/4 \\ &= \epsilon*n/12.\end{aligned}$$

16.6.3 5c. Barrier greedy construction

We construct $S \subset I_0'$ by a greedy procedure, maintaining the barrier invariant $M_t = \sum_{e \in E(S_t)} X_e \prec \epsilon*I$ at each step.

At step t , let $R_t = I_0' \setminus S_t$, $r_t = |R_t|$. For each $v \in R_t$, define

$$\begin{aligned}C_t(v) &= \sum_{u \in S_t, u \neq v} X_{uv} (\text{contribution from adding } v) \\ Y_t(v) &= H_t^{-1/2} C_t(v) H_t^{-1/2} (\text{barrier - normalized})\end{aligned}$$

where $H_t = \epsilon*I - M_t$ (the barrier headroom).

Claim: At each step $t \leq \epsilon*|I_0'|/3$, there exists $v \in R_t$ with $\lambda_{\max}(M_t + C_t(v)) < \epsilon$ (equivalently, $\|Y_t(v)\| < 1$).

16.6.4 5d. Proof of claim via pigeonhole + PSD trace bound

The key observation is elementary. For any PSD matrix Y :

$$\|Y\| \leq \text{tr}(Y) (**)$$

(Proof: $\|Y\| = \lambda_{\max}(Y)$, and $\text{tr}(Y) = \sum_i \lambda_i \geq \lambda_{\max}$ since all eigenvalues are nonneg.)

Define the average trace:

$$d\bar{a}r_t = (1/r_t) \sum_{v \in R_t} \text{tr}(Y_t(v)).$$

By the pigeonhole principle (*minimum* \leq *average*):

$$\min_{v \in R_t} \text{tr}(Y_t(v)) \leq d\bar{a}r_t.$$

Combining with (**): if $d\bar{a}r_t < 1$, then there exists $v \in R_t$ with

$$\|Y_t(v)\| \leq \text{tr}(Y_t(v)) \leq d\bar{a}r_t < 1.$$

This is exactly the barrier maintenance condition. No interlacing families, no real stability, no Bonferroni — just PSD trace bound + averaging.

16.6.5 5e. Bounding $d\bar{a}r_t$

The average trace satisfies:

$$d\bar{a}r_t = (1/r_t) \text{tr}(H_t^{-1} M_{\text{cross}})$$

where $M_{\text{cross}} = \sum_{e: \text{one endpoint} \in S_t, \text{other} \in R_t} X_e$ is the cross-edge matrix and $H_t = \epsilon * I - M_t$.

Case $M_t = 0$ (formal proof):

When $M_t = 0$ (early steps), $H_t = \epsilon * I$ and:

$$d\bar{a}r_t = (1/(\epsilon * r_t)) \sum_{u \in S_t} \text{ell}_u^R$$

where $\text{ell}_u^R = \sum_{v \in R_t, v \neq u} \tau_{uv} \leq \text{ell}_u \leq 8/\epsilon$.

For the complete graph K_n (where all edges are light for $n > 2/\epsilon$): $\tau_e = 2/n$ for all edges, $\text{ell}_u^R = (r_t) * (2/n)$, and:

$$d\bar{a}r_t = t * r_t * (2/n) / (\epsilon * r_t) = 2t / (n * \epsilon).$$

At $T = \epsilon * n / 3$: $d\bar{a}r_T = 2/3 < 1$. This is EXACT for K_n .

For general graphs at $M_t = 0$ with the leverage filter ($ell_u \leq 8/\epsilon$):

$$d\bar{a}r_t \leq (8*t)/(\epsilon^2 * r_t).$$

At $t \leq \epsilon * |I'_0|/3$ and $r_t \geq |I'_0|(1 - \epsilon/3) \geq 2|I'_0|/3$:

$$\begin{aligned} d\bar{a}r_t &\leq (8 * \epsilon * |I'_0|/3) / (\epsilon^2 * 2|I'_0|/3) \\ &= 8 / (2 * \epsilon) = 4/\epsilon. \end{aligned}$$

This bound exceeds 1 for $\epsilon < 1$, so the leverage-filter bound alone is insufficient. The tighter bound requires using the actual leverage structure (as in the K_n case where $d\bar{a}r = 2t/(n * \epsilon) \ll 1$).

Refined bound using total leverage:

$$\begin{aligned} \sum_{u \in S_t} ell_u^R &\leq \sum_{e \in E_{\text{cross}}} \tau_e \\ &\leq \sum_{e \in E(I_0)} \tau_e \leq n - 1. \end{aligned}$$

So $d\bar{a}r_t \leq (n-1)/(\epsilon * r_t)$. With $r_t \geq \epsilon * n/4$:

$$d\bar{a}r_t \leq (n-1) / (\epsilon^2 * n/4) = 4/\epsilon^2.$$

This is even worse. The issue is that the total leverage $n-1$ is spread across potentially many cross edges.

What actually controls $d\bar{a}r$ (verified numerically):

The barrier greedy selects vertices with minimum spectral norm $\|Y_t(v)\|$, which correlates with selecting vertices that have weak connections to the already-selected set. This keeps $d\bar{a}r$ much lower than the worst-case bound.

Numerical verification across 440 nontrivial greedy steps on graphs K_n, C_n , Barbell, DisjCliq, ER(n,p) for $n \in [8, 64]$ and $\epsilon \in \{0.12, 0.15, 0.2, 0.25, 0.3\}$:

$$\begin{aligned} \max d\bar{a}r \text{ across all steps} &: 0.641(K_{60}, \epsilon = 0.3, t = 5) \\ d\bar{a}r &< 1 \text{ at ALL 440 steps.} \end{aligned}$$

$$\begin{aligned} \text{Pigeonhole}(\min \text{trace} \leq d\bar{a}r) &: \text{verified } 440/440. \\ \text{PSD bound}(\|Y\| \leq \text{trace}) &: \text{verified } 440/440. \end{aligned}$$

For K_n , $d\bar{a}r$ is bounded exactly: $d\bar{a}r_t = 2t/(n * \epsilon)$, and at $T = \epsilon * n/3$ steps, $d\bar{a}r_T = 2/3$. This gives the formal proof for K_n and graphs with similar leverage structure (uniform $\tau_e \sim 2/n$).

16.6.6 5e'. Additional evidence: Q-polynomial roots

As supplementary verification, we computed the roots of the average characteristic polynomial $Q(x) = (1/r) \sum_v \det(xI - Y_t(v))$:

All 440 steps : max real root of $Q < 0.505$.

Zero steps with any root > 1 .

$Q(1) > 0.48$ at all steps.

If Q has nonneg real roots, then by Vieta's formulas: sum of roots = $d\bar{a}$, so max root $\leq d\bar{a} < 1$. This gives an independent confirmation via the MSS interlacing families framework (MSS 2015).

16.6.7 5f. Constructing the ϵ -light set

By the claim in 5c (proved via 5d when $d\bar{a} < 1$), the greedy produces $S \subset I_0'$ with $|S| = T$ and $M_S \prec \epsilon * I$ (i.e., $L_S \leq \epsilon * L$).

Size analysis:

The Turan step gives $|I_0| \geq \epsilon * n / 3$. The leverage filter (5b) gives $|I_0'| \geq \epsilon * n / 12$. The greedy runs $T = \epsilon * |I_0'| / 3$ steps, so $|S| = \epsilon^2 * n / 36$.

This gives $|S|$ proportional to $\epsilon^2 * n$, not $\epsilon * n$. For $|S| \geq c * \epsilon * n$ with universal c : need $c \leq \epsilon / 36$, which depends on ϵ .

The ϵ^2 bottleneck: The Turan independent set has size $|I_0| = \Theta(\epsilon * n)$. Running the greedy for $\Theta(\epsilon * |I_0|)$ steps gives $|S| = \Theta(\epsilon^2 * n)$. This is inherent in the heavy-edge-avoidance approach.

For fixed ϵ (the practical case): With $\epsilon = 0.3$: $|S| \geq 0.09 * n / 36 = n / 400$. With $\epsilon = 0.2$: $|S| \geq n / 900$. These are nontrivial lower bounds, sufficient for applications.

For K_n (proved exactly): $d\bar{a} = 2t / (n * \epsilon)$ with the greedy running $T = \epsilon * n / 3$ steps, giving $|S| = \epsilon * n / 3$ and $c = 1/3$. The ϵ^2 issue does not arise because $|I_0| = n$ (no heavy edges for $n > 2/\epsilon$).

Random sampling alternative (numerically verified):

Sample each vertex with probability $p = \epsilon$. By Chernoff, $P(|S| \geq \epsilon * n / 6) \geq 1 - \exp(-\epsilon * n / 18)$. Numerically: $P(||M_S|| \leq \epsilon \wedge |S| \geq \epsilon * n / 6) > 0$ for all tested graphs ($n \leq 80$, 11 families, 4 ϵ values, 500 trials each). Success probability ranges from 0.2% to 57%.

This gives $|S| \geq \epsilon * n / 6$ ($c = 1/6$) but the formal matrix concentration proof for general graphs remains open.

Open Obligation — Conditional Conclusion

16.6.8 Proved results

1. The ϵ -light condition $L_S \leq \epsilon * L$ is equivalent to $\|L^{+/2} L_S L^{+/2}\| \leq \epsilon$ in operator norm.
2. K_n gives the tight upper bound $c \leq 1$.
3. **For K_n (and graphs with uniform leverage $\tau_e \sim 2/n$):** The barrier greedy gives $|S| = \epsilon * n / 3$ with $\|M_S\| < \epsilon$. Proved by: $dbar_t = 2t / (n * \epsilon) \leq 2/3 < 1$ (exact computation), then pigeonhole + PSD trace bound gives existence of v with $\|Y_t(v)\| < 1$ at each step. Universal $c = 1/3$.
4. **The proof mechanism (Sections 5d-5e):** At each barrier greedy step, if $dbar < 1$ then the barrier is maintainable. The chain is:
 - $dbar = \text{avg trace} < 1$
 - exists v with $\text{trace}(Y_v) \leq dbar$ (pigeonhole)
 - $\|Y_v\| \leq \text{trace}(Y_v)$ (PSD matrices)
 - $\|Y_v\| < 1$ (barrier maintained)

16.6.9 Numerically verified (strong evidence, formal bound in progress)

5. **$dbar < 1$ at ALL barrier greedy steps** for all tested graphs. 440 nontrivial steps across $n \in [8, 64]$, K_n , C_n , Barbell, DisjCliq, ER(n,p) graphs, $\epsilon \in \{0.12, 0.15, 0.2, 0.25, 0.3\}$. Max $dbar = 0.641(K_{60}, \epsilon = 0.3, t = 5)$. Margin above 0: 36%.
6. **Q-polynomial roots < 1** at all 440 steps. The average characteristic polynomial $Q(x) = (1/r) \sum \det(xI - Y_v)$ has max real root < 0.505, consistent with max root $\leq dbar < 1$ (Vieta bound for nonneg roots).
7. **Random sampling with $p = \epsilon$** produces ϵ -light sets of size $\geq \epsilon * n / 6$ for all tested graphs ($n \leq 80$, 272 combos).

Open Obligation — External Dependency for Universal $c_0 > 0$

The formal $d\bar{a} < 1$ bound at $M_t \neq 0$ requires controlling $\text{tr}(H_t^{-1} M_{\text{cross}})$ where $H_t = \epsilon * I - M_t$. When $\|M_t\|$ is close to ϵ , the amplification factor $\|H_t^{-1}\|$ grows, and the naive bound on $d\bar{a}$ exceeds 1.

For K_n , the bound is exact: $d\bar{a} = 2t/(n * \epsilon)$. The favorable structure (uniform $\tau_e = 2/n$) keeps $d\bar{a}$ small.

For general graphs, the greedy's selection criterion ($\min \|Y_t(v)\|$) empirically keeps $d\bar{a}$ well below 1 (max 0.641), but a formal proof requires either: (a) A BSS-style potential function bounding the barrier evolution, or (b) Establishing that Q is real-rooted (via interlacing families), giving $\max \text{root} \leq d\bar{a}$ via Vieta.

16.6.10 Diagnosis

The remaining gap is not `we don't know enough math'`; `it is` we are near the limit of this proof architecture.“ The architecture (barrier greedy + PSD trace bound + pigeonhole) is correct — it proves K_n exactly and works numerically on every tested graph. The limit is that the amplification factor when $M_t \neq 0$ makes the naive bound on $d\bar{a}$ exceed 1, while the greedy's self-correcting property (selecting vertices whose contributions are orthogonal to M_t 's large eigenspace) is not yet captured by the formal analysis.

Empirically, the self-correction is strong: the spectral amplification factor is 0.52 (vs the scalar worst-case of 1.0), and the $W - M_t$ alignment is ≤ 0.25 across all 351 Phase 2 steps. Closing the gap formally requires making this orthogonality structure explicit — either via a potential function that tracks directional growth, or via interlacing families that exploit the grouped PSD structure of the barrier increments.

16.6.11 Summary

The existential answer is **YES** for K_n with $c = 1/3$ (proved), and numerically confirmed for all tested graph families with $c \geq 1/6$. The formal extension to arbitrary graphs requires closing the $d\bar{a} < 1$ bound at $M_t \neq 0$, which has 36% empirical margin and is the **SINGLE** remaining gap.

16.7 Key identities and inequalities used

1. $L = \sum_e w_e b_e b_e^T$, $\tau_e = \text{tr}(X_e)$, sum $\tau_e = n-k$
2. $L_S \leq \epsilon * L$ iff $\|\sum_{e \in E(S)} X_e\| \leq \epsilon$
3. For PSD Y : $\|Y\| \leq \text{tr}(Y)$ (spectral norm bounded by trace)

4. Pigeonhole: $\min_v f(v) \leq (1/r) \sum_v f(v)$ (*minimum ≤ average*)
5. Turan: independence number $\geq n^2/(2m+n)$
6. For K_n : $\tau_e = 2/n$, $\|M_S\| = |S|/n$ (*exact*)

16.8 References

- Batson, Spielman, Srivastava (2012), “Twice-Ramanujan Sparsifiers,” SIAM Review 56(2), 315-334.
- Marcus, Spielman, Srivastava (2015), “Interlacing Families II: Mixed Characteristic Polynomials and the Kadison-Singer Problem,” Annals of Mathematics 182(1), 327-350.
- Borcea, Branden (2009), “The Lee-Yang and Polya-Schur programs. I. Linear operators preserving stability,” Inventiones Math. 177, 541-569.
- Tropp (2011), Freedman's inequality for matrix martingales.
- Standard matrix Bernstein inequality for sums of independent self-adjoint random matrices.

Chapter 17

Problem 7: Uniform Lattice with 2-Torsion and Rationally Acyclic Universal Cover

17.1 Problem Statement

Suppose Γ is a uniform lattice in a real semisimple Lie group, and Γ contains an element of order 2. Is it possible that Γ is the fundamental group of a closed manifold whose universal cover is acyclic over \mathbb{Q} ?

Process Note — Status in This Writeup

Answer: yes (via the rotation route; closed in this branch via the standard codim-2 surgery theorem chain).

- Obligation (E2) — placing $\Gamma \in \text{FH}(Q)$ — is **discharged** for the rotation-lattice family (Fowler criterion, codim-2 fixed set with $\chi = 0$).
- Obligation (S) — upgrading from finite CW complex to closed manifold — is treated as discharged in this branch: the geometric inputs are established (trivial normal bundle, hyperbolic boundary form), and the codim-2 surgery identification is closed by the theorem-numbered reference chain^a (with closure summary in a companion note,^b Section 5).

^a<https://github.com/tothedarktowercame/futon6/blob/master/data/first-proof/problem7-g2-theorem-chain.md>

^b<https://github.com/tothedarktowercame/futon6/blob/master/data/first-proof/problem7-complete-proof.md>

17.2 1. Baseline Geometry

Let \mathbb{G} be connected real semisimple, $K < G$ maximal compact, and $X = G/K$ contractible. For a uniform lattice $\Gamma < G$ with torsion, X/Γ is a compact orbifold (not a manifold).

So the torsion-free argument $M = X/\Gamma$ does not apply directly.

17.3 2. Cohomological Structure via Bredon Framework

Since Γ acts properly and cocompactly on the contractible space X , the Bredon cohomology $H_{\Gamma}^*(X; R_Q)$ (with the rational constant coefficient system) satisfies Poincare duality by the orbifold PD theorem (Brown, *Cohomology of Groups*, Chapter VIII; Luck, *Transformation Groups and Algebraic K-Theory*, Section 6.6).

Concretely, $H^*(\Gamma; Q) = H^*(X/\Gamma; Q)$ satisfies $H^k = H^{d-k}$ where $d = \dim(X)$.

Note on terminology. With torsion present, saying “ Γ is a rational PD group” requires the Bredon/orbifold interpretation above. The ordinary group-cohomological PD condition assumes torsion-freeness. Throughout this writeup, “rational Poincare duality for Γ with torsion” refers to this Bredon-equivariant formulation.

17.4 3. Obligation E2: Finite-CW Realization ($\Gamma \in \text{FH}(Q)$)

17.4.1 3a. Fowler's Criterion

A theorem of Fowler (arXiv:1204.4667, Main Theorem) gives a concrete criterion: if a finite group G acts on a finite CW complex Y such that for every nontrivial subgroup $H < G$ and every connected component C of the fixed set Y^H , the Euler characteristic $\chi(C) = 0$, then the orbifold extension group $\pi_1((EG \times Y)/G)$ lies in $\text{FH}(Q)$.

That is, there exists a finite CW complex with the given fundamental group whose universal cover is rationally acyclic.

17.4.2 3b. Concrete Instantiation via Reflection Lattice

The E2 obligation is discharged by the following construction (details in the candidate-construction note¹):

- 1. Arithmetic lattice with reflection.** Take an arithmetic uniform lattice $\Gamma_0 < \text{Isom}(H^n)$ containing a reflection τ , as provided by Douba-Vargas Pallete (arXiv:2506.23994, Remark 5). Choose n even (e.g., $n = 4$ or $n = 6$).
- 2. Congruence cover.** Let $\pi = \Gamma_0(I)$ be a sufficiently deep principal congruence subgroup. Then $M = \pi \backslash H^n$ is a closed hyperbolic manifold, and τ induces an involution τ_{bar} on M .
- 3. Extension.** Set $G = \langle \tau_{bar} \rangle = \mathbb{Z}/2$ acting on $B_{\pi} := M$. The orbifold extension gives $1 \rightarrow \pi \rightarrow \Gamma \rightarrow \mathbb{Z}/2 \rightarrow 1$, where Γ is a cocompact lattice (finite extension of cocompact π) with order-2 torsion.

¹<https://github.com/tothedarktowercame/futon6/blob/master/data/first-proof/problem7r-s2b-candidate-construction.md>

4. **Fixed-set Euler check.** The fixed set $\text{Fix}(\tau_{bar})$ is a (possibly disconnected) closed, embedded, totally geodesic hypersurface (arXiv:2506.23994). Each component has dimension $n - 1$. Since n is even, $n - 1$ is odd, and every closed odd-dimensional manifold has Euler characteristic zero. So $\chi(C) = 0$ for every fixed component C .
5. **Fowler application.** The only nontrivial subgroup of $Z/2$ is itself. All fixed components have zero Euler characteristic. By Fowler's Main Theorem, $\Gamma \in \text{FH}(Q)$.

E2 status: discharged for this lattice family.

17.5 4. Obligation S: From Finite Complex to Closed Manifold

Obligation S is treated as discharged in this branch via the rotation route (S-rot-II); this section records the previously open obstacles and how S-rot-II resolves them.

Problem 7 asks for a **closed manifold** M with $\pi_1(M) = \Gamma$ and $H_*(M_{tilde}; Q) = 0$ for $* > 0$. Obligation E2 gives a finite CW complex with these properties; the upgrade to a closed manifold is the remaining open problem.

17.5.1 Available geometric data

The construction in Section 3b provides:

- π : a torsion-free cocompact lattice in $\text{Isom}(H^n)$, with n even ≥ 6 .
- $M = H^n/\pi$: a closed hyperbolic n -manifold. M is a closed manifold with $\pi_1(M) = \pi$ and contractible universal cover.
- τ : an involution on M with fixed set F — a closed, totally geodesic $(n - 1)$ -manifold.
- $\Gamma = \pi \rtimes Z/2$: the target group (cocompact lattice with order-2 torsion).
- Y : a finite CW complex with $\pi_1(Y) = \Gamma$ and Y rationally acyclic (from Fowler's theorem).
- H^n/Γ : a compact orbifold with $\pi_1^{orb} = \Gamma$, mirror singularity along the image of F .

The torsion-free quotient M already solves the problem for π . The difficulty is entirely in passing from π to Γ — from the torsion-free lattice to its $Z/2$ -extension.

17.5.2 Approach I: Wall surgery via the $\text{FH}(Q)$ complex

Idea. Use Y (the $\text{FH}(Q)$ complex) as the target of a surgery problem. Promote Y to a rational Poincare complex, find a degree-1 normal map to it, and show the surgery obstruction vanishes.

Obstacles.

1. *Poincare complex structure.* $\text{FH}(Q)$ gives a finite CW complex Y with rationally acyclic universal cover, but not a Poincare complex. Since Y_\sim is rationally contractible (by rational Hurewicz from rational acyclicity + simple connectivity), the Serre spectral sequence collapses and $H_*(Y; Q) = H_*(\Gamma; Q)$, which satisfies rational PD (Section 2). But promoting homology-level PD to a chain-level Poincare complex structure on Y has not been done.
2. *Degree-1 normal map.* Even with Poincare complex structure, a degree-1 normal map $f : M_0 \rightarrow Y$ requires the Spivak normal fibration of Y to admit a topological reduction. No construction of this reduction has been given.
3. *Surgery obstruction.* The obstruction $\sigma(f) \in L_n(Z[\Gamma]) \text{tensor} Q$ is not known to vanish. The Farrell-Jones conjecture (which holds for Γ) identifies this L-group with equivariant L-homology, but the resulting computation has not been completed. See the obstruction-analysis note² for the FJ reduction framework and a conjectural (but unverified) localization of the obstruction.

Status. This approach has three successive obstacles, each open. See the setup note³ for the detailed analysis.

Dead Path — Approach II: Equivariant Surgery (Reflection Route)

Idea. Work directly with the closed manifold M and the involution τ . Eliminate the fixed set F by equivariant surgery to obtain M' with a free $Z/2$ -action. Then $M'/(Z/2)$ is a closed manifold with $\pi_1 = \Gamma$.

Blocking obstruction. The equivariant surgery framework of Costenoble-Waner (arXiv:1705.10909) requires a **codimension-2 gap hypothesis**: fixed sets of distinct isotropy subgroups must differ in dimension by at least 2 (Condition 3.4(3)). For our $Z/2$ -action on M^n with codimension-1 fixed set F^{n-1} , this gap condition **fails**. The Doermann-Schultz framework (Springer LNM 1443) similarly requires gap conditions.

Status. Blocked for the reflection construction (codimension-1 fixed sets). However, the approach becomes viable for **rotational involutions** (codimension-2 fixed sets) — see Approach IV below.

Dead Path — Approach III: Orbifold Resolution

Idea. The quotient H^n/Γ is a compact orbifold with mirror singularity. Resolve the singularity to produce a closed manifold with $\pi_1 = \Gamma$ and rationally acyclic universal cover.

Obstacles.

²<https://github.com/tothedarktowercame/futon6/blob/master/data/first-proof/problem7r-s3b-obstruction.md>

³<https://github.com/tothedarktowercame/futon6/blob/master/data/first-proof/problem7r-s3a-setup.md>

1. *π_1 preservation.* Standard orbifold resolution (e.g., cutting along the mirror and doubling) typically changes the fundamental group. A resolution preserving $\pi_1 = \Gamma$ would need to be specifically constructed.
2. *Rational acyclicity.* The resolution must preserve (or establish) rational acyclicity of the universal cover.

Status. Not explored beyond this sketch.

Process Note — Dimension-Parity Tension

The E2 obligation (for reflections) requires **n even** (so the fixed set has odd dimension and Euler characteristic zero). But the surgery obstruction computation (Approach I) and the AHSS structure of $L_n(Z[\Gamma])\text{tensor}Q$ have better vanishing properties when **n is odd**. This tension between E2 and S is a central difficulty for the reflection construction.

Why reflections cannot work in odd dimension. For a reflection on H^{2k+1} , the fixed set is H^{2k} — a closed hyperbolic manifold of even dimension. By the Gauss-Bonnet theorem, such manifolds have $\chi \neq 0$. So Fowler's criterion fails. This is not an artifact of the construction; it is forced by Riemannian geometry.

17.5.3 Approach IV: Rotation route (resolves the parity tension)

Idea. Replace the reflection (codimension-1 involution) with a **rotational involution** (codimension-2 fixed set) in **odd** ambient dimension. An order-2 isometry of H^{2k+1} that fixes H^{2k-1} (codimension 2) is a “rotation by π' in a normal 2-plane.

Why this resolves the tension. For $n = 2k+1$ odd:

- Fixed set H^{2k-1} has dimension $2k-1$ (odd), so $\chi = 0$. Fowler criterion is satisfied: $\Gamma \in \text{FH}(Q)$.
- Surgery obstruction lives in $L_{2k+1}(Z[\Gamma])\text{tensor}Q$, which has favorable parity (odd total degree forces odd p in AHSS terms).
- The codimension-2 gap hypothesis (required by equivariant surgery theories, Costenoble-Waner arXiv:1705.10909) is **satisfied**, so Approach II (equivariant surgery) becomes available as a method for the S-branch.

Lattice construction: DISCHARGED. Details in the rotation-lattice construction note.⁴ Summary:

1. **Quadratic form.** Let $k = Q(\sqrt{2})$, $O_k = Z[\sqrt{2}]$. Define $f = (1 - \sqrt{2})x_0^2 + x_1^2 + \dots + x_n^2 \in n+1$ variables. Under the two real embeddings of k , f has signatures $(n, 1)$ and $(n+1, 0)$. So $\text{SO}(f)$ gives $\text{SO}(n, 1)$ at one place and a compact group at the other.

⁴<https://github.com/tothedarktowercame/futon6/blob/master/data/first-proof/problem7r-rotation-lattice-construction.md>

2. **Uniform lattice.** $\Gamma_0 = \mathrm{SO}(f, O_k)$ is a cocompact arithmetic lattice in $\mathrm{SO}(n, 1)$ (Borel-Harish-Chandra; cocompactness by Godement criterion since f is anisotropic over \mathbf{k}).
3. **Order-2 rotation.** $\sigma = \mathrm{diag}(1, -1, -1, 1, \dots, 1)$ is in $\mathrm{SO}(f, O_k)$: it preserves f (negates x_1, x_2 in the $x_1^2 + x_2^2$ summand), has determinant $+1$, and has integer entries. Its fixed set on H^n is H^{n-2} (codimension 2).
4. **Congruence subgroup.** $\pi = \Gamma_0(I)$ for ideal I coprime to 2: torsion-free (Minkowski), $\sigma \notin \pi$, and $M = H^n/\pi$ is a closed hyperbolic manifold. The extension $1 \rightarrow \pi \rightarrow \Gamma \rightarrow \mathbb{Z}/2 \rightarrow 1$ with $\Gamma = \langle \pi, \sigma \rangle$ is a cocompact lattice with order-2 torsion.
5. **Fowler application.** Fixed set has dimension $n - 2 = 2k - 1$ (odd), so $\chi = 0$. By Fowler's Main Theorem: $\Gamma \in \mathrm{FH}(Q)$.

E2 status for rotation route: DISCHARGED.

Obligation S resolution. The manifold upgrade proceeds via two sub-options available on the rotation route:

- **S-rot-I (Wall surgery in odd dimension).** Same three-obstacle structure as Approach I (Poincare complex, normal map, obstruction), but the obstruction computation benefits from odd L-theory parity.
- **S-rot-II (Equivariant surgery on (M, σ)).** The codimension-2 gap hypothesis is satisfied, so the Costenoble-Waner framework (arXiv:1705.10909) applies. The equivariant surgery obstruction is computable in principle.

This is the most promising remaining path for Problem 7. The lattice existence bottleneck is resolved. The open problem reduces to computing a surgery obstruction (either Wall or equivariant) in the structurally favorable odd-dimensional setting.

17.6 5. Remark: Absence of Smith-Theory Obstruction

A natural objection is that the order-2 element in Γ would force fixed points on any rationally acyclic covering space via Smith theory. This does **not** apply here: Smith theory over \mathbb{Z}/p constrains mod-p homology of fixed sets, but the construction targets \mathbb{Q} -acyclicity. Over \mathbb{Q} , the transfer homomorphism shows that fixed sets can be rationally trivial without contradicting Smith's theorem.

This section addresses a natural objection and explains why it does not apply. It does not contribute to the constructive argument, which is entirely in Sections 3-4.

17.7 6. Theorem

Theorem. Let Γ be a cocompact lattice extension $1 \rightarrow \pi \rightarrow \Gamma \rightarrow \mathbb{Z}/2 \rightarrow 1$ constructed from an arithmetic lattice in $\text{Isom}(H^n)$ containing an order-2 isometry, via either:

- **(Reflection route)** Section 3b: reflection lattice in $\text{Isom}(H^n)$, n even, $n \geq 6$.
- **(Rotation route)** Approach IV: rotation lattice in $\text{Isom}(H^n)$, n odd, $n \geq 7$. See the rotation-lattice construction note.⁵

Then:

- (a) **(Unconditional)** $\Gamma \in \text{FH}(Q)$: there exists a finite CW complex Y with $\pi_1(Y) = \Gamma$ and $H_*(Y_{\tilde{t}ilde}; Q) = 0$ for $* > 0$. (Both routes discharge E2 via Fowler's criterion.)
- (b) **(Rotation route)** For the rotation lattice (Approach IV, $n = 7$, congruence ideal $I = (3) \in \mathbb{Z}[\sqrt{2}]$): there exists a closed manifold N with $\pi_1(N) = \Gamma$ and $H_*(N_{\tilde{t}ilde}; Q) = 0$ for $* > 0$. The manifold is constructed by equivariant surgery (S-rot-II): the surgery obstruction vanishes because the normal bundle of the totally geodesic fixed set is trivial (trivial holonomy, forced by the congruence condition). See the S-rotation obstruction analysis.⁶

17.8 7. Path to Full Closure

Resolving obligation S requires computing a surgery obstruction. The rotation route (Approach IV) has discharged the lattice-existence question and is now the primary path. See the hypothetical-wirings note⁷ for full wiring diagrams.

Active path: Approach IV (rotation route). The lattice construction is complete (see the rotation-lattice construction note⁸). E2 is discharged. Two sub-options for obligation S:

1. **S-rot-II (Equivariant surgery — OBSTRUCTION VANISHES).** The Costenoble-Waner codimension-2 gap hypothesis is satisfied. The `cut` and `cap` method (Browder, López de Medrano) applies.

Key result: the equivariant surgery obstruction $\theta = 0$ (integrally).

The argument has two layers:

- **Rational vanishing (Step A: flat-normal-bundle argument).** The normal bundle ν of $F \in M$ is flat (totally geodesic embedding). By Chern-Weil, $e(\nu) \otimes Q = 0$.

⁵<https://github.com/tothedarktowercame/futon6/blob/master/data/first-proof/problem7r-rotation-lattice-construction.md>

⁶<https://github.com/tothedarktowercame/futon6/blob/master/data/first-proof/problem7r-s-rot-obstruction-analysis.md>

⁷<https://github.com/tothedarktowercame/futon6/blob/master/data/first-proof/problem7-hypothetical-wirings.md>

⁸<https://github.com/tothedarktowercame/futon6/blob/master/data/first-proof/problem7r-rotation-lattice-construction.md>

This forces the intersection form on $S(\nu)$ to be rationally hyperbolic $\rightarrow \theta \otimes Q = 0$.

- **Integral vanishing (trivial holonomy).** For the congruence ideal I with $\text{Norm}(I) > 2$ (e.g., $I = (3)$): the integrality constraint on rotation matrices over $\mathbb{Z}[\sqrt{2}]$, combined with the congruence condition $g \equiv I \pmod{I}$, forces the holonomy representation $\rho: C \rightarrow \text{SO}(2)$ to be trivial. So ν is a trivial bundle, $e(\nu) = 0$ in $H^2(F; \mathbb{Z})$, and the circle bundle $S(\nu) = F \times S^1$ is a product. The \int intersection form on $H_3(F \times S^1; \mathbb{Z})$ is block off-diagonal (hyperbolic), giving $\theta = 0 \in L_8(\mathbb{Z}[\Gamma])$.

With $\theta = 0$: The equivariant “cut and cap” surgery succeeds. Remove the tubular neighborhood $N(F)$ from M , obtaining $W = M \setminus \text{int}(N(F))$ with $\partial W = S(\nu) = F \times S^1$ and free $\mathbb{Z}/2$ -action on W . Since $\theta = 0$, a cap V exists with $\partial V = F \times S^1$ and free $\mathbb{Z}/2$ -action. Set $M' = W \cup V$. Then $N = M' / (\mathbb{Z}/2)$ is a closed manifold with $\pi_1(N) = \Gamma$ and rationally acyclic universal cover.

See the S-rotation obstruction analysis⁹ for full computation.

2. **S-rot-I (Wall surgery in odd dimension).** Fallback. Same three-obstacle structure as Approach I but with favorable odd L-theory parity and strictly fewer AHSS terms than the reflection case.

Dead Path — Deprioritized Approaches

Deprioritized paths:

3. **Approach I (Wall surgery, reflection route).** Three successive open obstacles with structural headwinds (even L-theory parity).
4. **Approach III (orbifold resolution).** No technique identified.
5. **Approach II (equivariant surgery, reflection route).** Blocked by codimension-2 gap hypothesis (Costenoble-Waner, arXiv:1705.10909).

17.9 References

- J. Fowler, *Finiteness Properties of Rational Poincaré Duality Groups*, arXiv:1204.4667.
- G. Avramidi, *Rational Manifold Models for Duality Groups*, arXiv:1506.06293.
- A. Douba, F. Vargas Pallete, *On Reflections of Congruence Hyperbolic Manifolds*, arXiv:2506.23994.
- A. Bartels, F. T. Farrell, W. Luck, *The Farrell-Jones Conjecture for Cocompact Lattices in Virtually Connected Lie Groups*, arXiv:1101.0469.

⁹<https://github.com/tothedarktowercame/futon6/blob/master/data/first-proof/problem7r-s-rot-obstruction-analysis.md>

- A. Bartels, W. Luck, *The Farrell-Jones Conjecture for Arbitrary Lattices in Virtually Connected Lie Groups*, arXiv:1401.0876.
- D. Crowley, W. Luck, T. Macko, *Surgery Theory: Foundations*, arXiv:0905.0104.
- K. H. Dovermann, R. Schultz, *Equivariant Surgery Theories and Their Periodicity Properties*, Springer LNM 1443, 1990.
- S. R. Costenoble, S. Waner, *The Equivariant Spivak Normal Bundle and Equivariant Surgery for Compact Lie Groups*, arXiv:1705.10909.
- J. F. Davis, W. Lück, *On Nielsen Realization and Manifold Models for Classifying Spaces*, Trans. AMS 377 (2024), 7557-7600, arXiv:2303.15765.
- G. Avramidi, *Smith Theory, L₂ Cohomology, Isometries of Locally Symmetric Manifolds, and Moduli Spaces of Curves*, arXiv:1106.1704.
- M. Belolipetsky, A. Lubotzky, *Finite Groups and Hyperbolic Manifolds*, arXiv:math/0406607.
- A. Borel, Harish-Chandra, *Arithmetic Subgroups of Algebraic Groups*, Annals of Mathematics 75 (1962), 485-535.
- J. Millson, M. S. Raghunathan, *Geometric Construction of Cohomology for Arithmetic Groups I*, Proc. Indian Acad. Sci. 90 (1981), 103-123.
- A. Ranicki, *Algebraic L-Theory and Topological Manifolds*, Cambridge Tracts in Mathematics 102, 1992.
- K. S. Brown, *Cohomology of Groups*, Springer GTM 87.
- W. Luck, *Transformation Groups and Algebraic K-Theory*, Springer LNM 1408.
- C. T. C. Wall, *Surgery on Compact Manifolds*, 2nd ed., AMS.

Chapter 18

Problem 8: Lagrangian Smoothing of Polyhedral Surfaces with 4-Valent Vertices

18.1 Problem Statement

A **polyhedral Lagrangian surface** $K \in \mathbb{R}^4$ is a finite polyhedral complex all of whose faces are Lagrangian 2-planes, which is a topological submanifold of \mathbb{R}^4 . A **Lagrangian smoothing** of K is a Hamiltonian isotopy K_t of smooth Lagrangian submanifolds for t in $(0,1]$, extending to a topological isotopy on $[0, 1]$, with $K_0 = K$.

Question: If K has exactly 4 faces meeting at every vertex, does K necessarily have a Lagrangian smoothing?

18.2 Answer

Yes. A polyhedral Lagrangian surface with 4 faces per vertex (with distinct adjacent faces) always admits a Lagrangian smoothing. The vertex spanning property ($\{e_1, \dots, e_4\}$ spans \mathbb{R}^4) is automatic — it follows from the Lagrangian and distinct-face conditions alone (Section 3), with no additional hypotheses needed.

Process Note — Confidence

Confidence: Medium-high. The v2 argument (symplectic direct sum decomposition at each vertex) is verified numerically: 998/998 random valid 4-valent configurations give Maslov index exactly 0. The decomposition proof is algebraic (not just heuristic). Vertex smoothing uses the product structure (corners in symplectic factors); edge smoothing uses generating functions. The Hamiltonian isotopy property is established via the Weinstein neighborhood theorem (edges) and the vanishing flux in simply-connected \mathbb{R}^2 (vertices).

18.3 Solution

18.3.1 1. Setup: Lagrangian planes in \mathbb{R}^4

Identify $\mathbb{R}^4 = \mathbb{C}^2$ with symplectic form $\omega = dx_1 \wedge dy_1 + dx_2 \wedge dy_2$. A Lagrangian plane is a 2-dimensional subspace L where $\omega|_L = 0$. The space of Lagrangian planes (the Lagrangian Grassmannian) is:

$$\Lambda(2) = U(2)/O(2)$$

This is a manifold of dimension 3 with $\pi_1(\Lambda(2)) = Z$ (the Maslov class).

Each face of K lies in a Lagrangian plane. At each edge, two Lagrangian faces meet at a dihedral angle. At each vertex, 4 Lagrangian faces meet.

18.3.2 2. Local structure at a 4-valent vertex

At a vertex v , the 4 faces L_1, L_2, L_3, L_4 (in cyclic order around v) are Lagrangian half-planes meeting along edges:

$$e_{12} = L_1 \cap L_2, e_{23} = L_2 \cap L_3, e_{34} = L_3 \cap L_4, e_{41} = L_4 \cap L_1$$

These 4 edges are rays from v . Each face is spanned by its two boundary edges:

$$L_i = \text{span}(e_{i-1,i}, e_{i,i+1})$$

The Lagrangian condition $\omega|_{L_i} = 0$ requires:

$$\omega(e_{i-1,i}, e_{i,i+1}) = 0 \text{ for each } i \pmod{4}$$

18.3.3 3. The symplectic direct sum decomposition (key new argument)

Theorem (v2). The 4 edge vectors $e_1 = e_{12}, e_2 = e_{23}, e_3 = e_{34}, e_4 = e_{41}$ satisfy $\omega(e_i, e_{i+1}) = 0$ for all $i \pmod{4}$. This forces a symplectic direct sum decomposition:

$$\mathbb{R}^4 = V_1 \oplus V_2$$

where $V_1 = \text{span}(e_1, e_3)$ and $V_2 = \text{span}(e_2, e_4)$ are symplectic 2-planes with $\omega|_{V_1 \times V_2} = 0$.

Proof. Write the ω matrix in the basis (e_1, e_2, e_3, e_4) . The conditions $\omega(e_i, e_{i+1}) = 0$ kill 4 of the 6 independent entries, leaving only:

$$a = \omega(e_1, e_3) \neq 0, b = \omega(e_2, e_4) \neq 0$$

(Nonzero because ω is non-degenerate and $\{e_1, e_2, e_3, e_4\}$ is a basis — see the nondegeneracy hypothesis below.)

Lemma (vertex spanning). At every vertex of a polyhedral Lagrangian surface with 4 faces per vertex (with distinct adjacent faces sharing 1-dimensional edges), the 4 edge vectors $\{e_1, e_2, e_3, e_4\}$ span \mathbb{R}^4 .

Proof. Suppose for contradiction that the 4 edge vectors lie in a 3-dimensional subspace $H \subset \mathbb{R}^4$. Then all 4 faces $L_i = \text{span}(e_{i-1,i}, e_{i,i+1}) \subset H$.

Step 1. The restricted form $\omega|_H$ has rank 2: since ω is non-degenerate on \mathbb{R}^4 , its restriction to a codimension-1 subspace has a 1-dimensional kernel $\text{ell} = \ker(\omega|_H) \subset H$.

Step 2. Every Lagrangian 2-plane $L \subset H$ contains ell . Proof: L is 2-dimensional with $\omega|_L = 0$. If L were transverse to ell (i.e., $L \cap \text{ell} = \{0\}$), then L would project isomorphically onto a 2-plane in $H/\text{ell} \cong \mathbb{R}^2$. But $\omega|_H$ descends to a non-degenerate 2-form on H/ell (since $\text{ell} = \ker(\omega|_H)$), and a 2-plane in \mathbb{R}^2 on which a non-degenerate 2-form vanishes must be $\{0\}$. Contradiction. So $\text{ell} \subset L$.

Step 3 (key). Each edge e_i is the intersection of two adjacent faces: $e_1 = L_1 \cap L_2, e_2 = L_2 \cap L_3, \dots$. Since L_i and L_{i+1} are distinct 2-planes (distinct faces), their intersection is exactly 1-dimensional: $\dim(L_i \cap L_{i+1}) = 1$, so $L_i \cap L_{i+1} = \text{span}(e_i)$.

By Step 2, $\text{ell} \subset L_i$ and $\text{ell} \subset L_{i+1}$, so $\text{ell} \subset L_i \cap L_{i+1} = \text{span}(e_i)$. Since both ell and $\text{span}(e_i)$ are 1-dimensional subspaces and one contains the other, $\text{ell} = \text{span}(e_i)$.

Applying this to all four edges: $\text{span}(e_1) = \text{ell} = \text{span}(e_2) = \text{span}(e_3) = \text{span}(e_4)$. That is, all four edge vectors are proportional.

But then $L_1 = \text{span}(e_4, e_1) = \text{span}(e_1)$ is 1-dimensional, contradicting the fact that L_1 is a 2-plane. \square

(Note: this argument is purely algebraic — it uses only that adjacent faces are distinct Lagrangian 2-planes sharing a 1-dimensional edge. No topological submanifold condition is needed.)

In the reordered basis (e_1, e_3, e_2, e_4) , the ω matrix is:

$$[[0, a, 0, 0], [-a, 0, 0, 0], [0, 0, 0, b], [0, 0, -b, 0]]$$

This is block diagonal: $(V_1, a) \oplus (V_2, b)$, a symplectic direct sum. \square

Consequence: Each Lagrangian face decomposes as a direct sum of lines:

$$\begin{aligned} L_1 &= \text{span}(e_4) \oplus \text{span}(e_1) \subset V_2 \oplus V_1 \\ L_2 &= \text{span}(e_1) \oplus \text{span}(e_2) \subset V_1 \oplus V_2 \\ L_3 &= \text{span}(e_2) \oplus \text{span}(e_3) \subset V_2 \oplus V_1 \\ L_4 &= \text{span}(e_3) \oplus \text{span}(e_4) \subset V_1 \oplus V_2 \end{aligned}$$

Each L_i takes one line from V_1 and one from V_2 , which is automatically Lagrangian in $V_1 \oplus V_2$ (ω restricted to a line is zero).

18.3.4 4. Maslov index vanishes exactly

The Maslov index of the vertex loop $L_1 \rightarrow L_2 \rightarrow L_3 \rightarrow L_4 \rightarrow L_1 \in \Lambda(2)$ decomposes via the direct sum:

$$\mu = \mu_1 + \mu_2$$

where μ_j is the winding number of the component loop in V_j .

In $V_1 = \text{span}(e_1, e_3)$: The loop traces $\text{span}(e_1) \rightarrow \text{span}(e_1) \rightarrow \text{span}(e_3) \rightarrow \text{span}(e_3) \rightarrow \text{span}(e_1)$

This is a back-and-forth path ($e_1 \rightarrow e_1 \rightarrow e_3 \rightarrow e_3 \rightarrow e_1$), not a winding loop. The winding number is 0.

In $V_2 = \text{span}(e_2, e_4)$: Similarly: $\text{span}(e_4) \rightarrow \text{span}(e_2) \rightarrow \text{span}(e_2) \rightarrow \text{span}(e_4) \rightarrow \text{span}(e_4)$

Winding number 0.

Total Maslov index: $\mu = 0 + 0 = 0$.

Numerical verification: 998/998 random valid 4-valent configurations (with edge-sharing enforced) give Maslov index exactly 0. In contrast, random quadruples without edge-sharing give nonzero Maslov index $\sim 45\%$ of the time (see scripts/verify-p8-maslov-v2.py).

18.3.5 5. Why 4 is special: the 3-face obstruction

For a 3-face vertex, the 3 edge vectors e_1, e_2, e_3 must satisfy:

$$\omega(e_1, e_2) = \omega(e_2, e_3) = \omega(e_3, e_1) = 0$$

This means ω vanishes on ALL pairs — the span is an isotropic subspace. But in (\mathbb{R}^4, ω) , the maximum isotropic dimension is 2 (= half the dimension). Three independent isotropic vectors cannot exist.

Therefore: a non-degenerate 3-face Lagrangian vertex is impossible in \mathbb{R}^4 .

The 4-face condition is precisely the right valence: it gives enough edges to span \mathbb{R}^4 while the cyclic ω -orthogonality creates the symplectic direct sum that forces Maslov index 0.

We do not claim a general obstruction for valence ≥ 5 here; the proof establishes sufficiency for valence 4.

18.3.6 5a. Vertex smoothing via the product structure

The key observation: the $V_1 \oplus V_2$ decomposition (Section 3) gives K near each vertex v a product structure, enabling a direct smoothing that bypasses both crease smoothing and Lagrangian surgery.

Product decomposition of K near v . Choose Darboux coordinates adapted to $V_1 \oplus V_2$: let V_1 have coordinates (x, y) with $\omega_1 = dx \wedge dy$, and V_2 have coordinates (u, v) with $\omega_2 = du \wedge dv$ (so $\omega = \omega_1 + \omega_2$). Orient the edge vectors so that:

$$e_1 = (1, 0, 0, 0), e_2 = (0, 0, 1, 0), e_3 = (0, 1, 0, 0), e_4 = (0, 0, 0, 1)$$

(Here $e_1, e_3 \in V_1$ and $e_2, e_4 \in V_2$, consistent with the decomposition in Section 3. This can always be arranged by a linear symplectomorphism.)

The 4 faces in these coordinates are:

$$\begin{aligned} L_1 &= \text{span}(e_4, e_1) = y = 0, u = 0, \text{sector } x > 0, v > 0 \\ L_2 &= \text{span}(e_1, e_2) = y = 0, v = 0, \text{sector } x > 0, u > 0 \\ L_3 &= \text{span}(e_2, e_3) = x = 0, v = 0, \text{sector } y > 0, u > 0 \\ L_4 &= \text{span}(e_3, e_4) = x = 0, u = 0, \text{sector } y > 0, v > 0 \end{aligned}$$

Define the “corner” curves in each factor:

$$\begin{aligned} C_1 &= (x, 0) : x \geq 0 \cup (0, y) : y \geq 0 \subset V_1 (\text{positive } x \text{ and } y \text{ axes}) \\ C_2 &= (u, 0) : u \geq 0 \cup (0, v) : v \geq 0 \subset V_2 (\text{positive } u \text{ and } v \text{ axes}) \end{aligned}$$

Claim: $K \cap B(v, r) = C_1 \times C_2$ (product of the two corners) for small r .

Verification: A point (p, q) with $p \in C_1$ and $q \in C_2$ has $p = (x, 0)$ or $(0, y)$ and $q = (u, 0)$ or $(0, v)$, giving 4 cases — exactly the 4 faces L_1, \dots, L_4 listed above. \square

Smoothing. Replace each corner C_j with a smooth curve $C_j^{sm} \subset V_j$ that agrees with C_j outside a ball of radius δ around the origin:

$$\begin{aligned} C_1^{sm} &: \text{smooth curve } \in V_1, = (x, 0) \text{ for } x > \delta, = (0, y) \text{ for } y > \delta, \\ &\quad \text{smooth through the origin (e.g., the curve } (\cos \theta, \sin \theta) \\ &\quad \text{reparameterized to match the axes outside the transition)} \\ C_2^{sm} &: \text{analogous } \in V_2 \end{aligned}$$

Explicitly: parameterize C_1^{sm} as $\gamma_1(t)$ for $t \in R$, where $\gamma_1(t) = (t, 0)$ for $t \geq \delta$, $\gamma_1(t) = (0, -t)$ for $t \leq -\delta$, and γ_1 is a smooth embedded curve for $t \in [-\delta, \delta]$. (Such a curve exists: it is a smooth rounding of the right angle at the origin.) Define $\gamma_2(t)$ analogously for C_2^{sm} .

Lagrangian property of the product: The smoothed surface $K^{sm} = C_1^{sm} \times C_2^{sm}$ is a product of smooth curves in the symplectic factors. A curve in a 2-dimensional symplectic manifold is always Lagrangian (its dimension is 1 = half of 2, and ω restricted to a 1-submanifold is zero for dimensional reasons). The product of Lagrangian submanifolds in $(V_1, \omega_1) \times (V_2, \omega_2)$ is Lagrangian in $(V_1 \oplus V_2, \omega_1 + \omega_2)$: for tangent vectors (u_1, u_2) and (w_1, w_2) to $C_1^{sm} \times C_2^{sm}$, we have

$$\omega((u_1, u_2), (w_1, w_2)) = \omega_1(u_1, w_1) + \omega_2(u_2, w_2) = 0 + 0 = 0$$

since u_1, w_1 are tangent to C_1^{sm} (1-dimensional in V_1) and u_2, w_2 are tangent to C_2^{sm} (1-dimensional in V_2). \square

Smoothness: $K^{sm} = C_1^{sm} \times C_2^{sm}$ is the image of the smooth map $(t_1, t_2) \mapsto (\gamma_1(t_1), \gamma_2(t_2))$, which is a smooth immersion (the tangent vectors $d\gamma_1/dt_1$ and $d\gamma_2/dt_2$ are nonzero and lie in complementary subspaces V_1 and V_2). So K^{sm} is a smooth Lagrangian surface, including at $v = \gamma_1(0) \times \gamma_2(0)$. \square

Agreement: $K^{sm} = C_1 \times C_2 = K$ outside the region where either factor was modified ($|p| \leq \delta \in V_1$ or $|q| \leq \delta \in V_2$), so K^{sm} agrees with K outside a neighborhood of v of radius $O(\delta)$.

18.3.7 6. Edge smoothing (crease smoothing along edges between vertices)

After resolving all vertices (Section 5a), the remaining singularities of K are edge creases: compact arcs connecting the boundaries of resolved vertex neighborhoods. Along each edge arc, two adjacent Lagrangian faces meet at a dihedral angle. These creases are smoothed by the standard generating-function interpolation:

Lemma (edge crease smoothing). Let L_1, L_2 be two Lagrangian half-planes meeting along a compact edge arc e (a segment of a common boundary ray, away from any vertex). Then there exists a smooth Lagrangian surface agreeing with L_1 on one side and L_2 on the other.

Proof. Choose Darboux coordinates (x_1, y_1, x_2, y_2) with e along the x_1 -axis. Each L_i is locally the graph $y = \text{grad } S_i(x)$ for quadratic S_i . Define $S_\epsilon(x) = \chi(x_1/\epsilon)S_1(x) + (1 - \chi(x_1/\epsilon))S_2(x)$ for a smooth cutoff χ . The graph $y = \text{grad } S_\epsilon$ is Lagrangian (graph of the exact 1-form dS_ϵ). For any fixed $\epsilon > 0$, this gives a smooth Lagrangian surface replacing the crease along e . \square

(The \mathbb{C}^1 control issues noted in earlier drafts do not arise here: the crease smoothing is applied only along edge arcs that are INTERIOR to edges (between vertex neighborhoods), not at vertices. Since the edge arcs are at positive distance from all vertices, and the smoothing width ϵ can be chosen small relative to this distance, the edge smoothings are localized in thin tubular neighborhoods of the edge arcs.)

18.3.8 7. Global smoothing

Step 7a: Resolve vertices. For each 4-valent vertex v_i , choose a ball B_i of radius r_i centered at v_i , where r_i is small enough that:

- B_i contains no other vertex $v_j (j \neq i)$, and
- B_i intersects only the edges and faces incident to v_i .

Such radii exist because the vertex set is finite and discrete in \mathbb{R}^4 . Within each B_i , apply the product smoothing (Section 5a) using the $V_1 \oplus V_2$ decomposition from Section 3. This replaces $K \cap B_i = C_1 \times C_2$ with the smooth Lagrangian surface $C_1^{sm} \times C_2^{sm}$.

Commutativity: Since the balls $\{B_i\}$ are pairwise disjoint, the vertex smoothings have disjoint support and commute.

Step 7b: Smooth edges. After all vertex resolutions, the remaining singularities are edge creases — compact arcs connecting the boundaries of resolved vertex neighborhoods. Each edge arc lies along the intersection of two Lagrangian faces and is a compact 1-manifold (with boundary on the spheres ∂B_i). These creases are resolved by the generating-function interpolation of Section 6.

The edge smoothings have support in tubular neighborhoods of the edge arcs. These neighborhoods can be chosen to be disjoint from each other (since the edges are disjoint away from vertices, which have already been resolved) and from the vertex balls (since the edge arcs start at ∂B_i , outside B_i). Therefore the edge smoothings commute with each other and with the vertex smoothings.

Compatibility at ∂B_i . The vertex smoothing (Section 5a) agrees with the original polyhedral K outside a neighborhood of v_i of radius $\delta < r_i$. So on ∂B_i , the surface is still polyhedral (two flat faces meeting at an edge). The edge crease smoothing (Section 6) begins at ∂B_i , where the surface is already flat. Since both the vertex smoothing (product of smooth curves) and the edge smoothing (graph of exact 1-form) produce Lagrangian surfaces, and they agree on the overlap (both equal the original flat faces on the annular region $\delta < |x| < r_i$), they glue to a globally smooth Lagrangian surface.

Step 7c: Global Hamiltonian isotopy. Each smoothing is parameterized by a width parameter t (δ for vertices, eps for edges). As $t \rightarrow 0$, the smoothing region shrinks and $K_t \rightarrow K = K_0 \in C^0$, giving the topological isotopy on $[0, 1]$. It remains to show K_t is a *Hamiltonian* isotopy for $t > 0$.

Edge smoothings are Hamiltonian. The family of generating functions $S_t(x) = \chi(x_1/t)S_1(x) + (1 - \chi(x_1/t))S_2(x)$ defines a smooth 1-parameter family of Lagrangian graphs $y = \text{grad } S_t(x) \in T^*\mathbb{R}^2$. By the Weinstein Lagrangian neighborhood theorem (Weinstein 1971, Theorem 6.1), a smooth family of exact Lagrangian submanifolds in an exact symplectic manifold (here $T^*\mathbb{R}^2$ with $\lambda = y \, dx$) is generated by a Hamiltonian: the 1-form $\iota_{d/dt}(\omega)|_{K_t}$ is exact (it equals $d(S_t|_{K_t})$), so the isotopy is Hamiltonian with generating function $H_t = dS_t/dt$ evaluated on the Lagrangian.

Vertex smoothings are Hamiltonian. The vertex smoothing is a product: $K_t^{\text{vertex}} = C_1^{sm}(t) \times C_2^{sm}(t) \in V_1 \times V_2$. Each $C_j^{sm}(t)$ is a smooth 1-parameter family of curves in $(V_j, \omega_j) \cong (\mathbb{R}^2, dx \wedge dy)$. For the contractible arc family used here, the induced closed 1-forms are exact, so this local isotopy is Hamiltonian. This is because $V_j = \mathbb{R}^2$ is simply connected, so the flux homomorphism Flux: $\pi_1(\text{Symp}) \rightarrow H^1(L; \mathbb{R})$ is trivial (no non-Hamiltonian symplectic isotopies exist). Concretely: the velocity field d/dt of the isotopy $C_j^{sm}(t)$ is a symplectic vector field along $C_j^{sm}(t)$; contracting with ω_j gives a closed 1-form on $C_j^{sm}(t)$, which is exact because $H^1(C_j^{sm}(t); \mathbb{R}) = 0$ (each $C_j^{sm}(t)$ is a noncompact embedded arc in \mathbb{R}^2 — the smoothed corner — hence contractible). The primitive is the Hamiltonian $H_j(t)$. The product isotopy on $V_1 \times V_2$ is Hamiltonian with generating function $H_1(t) + H_2(t)$ (see McDuff-Salamon, 3rd ed., Exercise 3.18: product of Hamiltonian isotopies is Hamiltonian).

Composition. The vertex smoothings (in disjoint balls B_i) and edge smoothings (in disjoint tubular neighborhoods) have pairwise disjoint compact support. Each is a compactly supported Hamiltonian isotopy. Their composition is a compactly supported Hamiltonian isotopy (McDuff-Salamon, *Introduction to Symplectic Topology*, 3rd ed., Proposition 3.17: the group $\text{Ham}_c(M, \omega)$ of compactly supported Hamiltonian diffeomorphisms is a group under composition).

18.3.9 8. Topological constraints

For K to be a compact topological submanifold with 4 faces per vertex, Euler's formula constrains the topology. For quadrilateral faces: $V - E + F = \chi(K)$, with $4F = 2E$ and $4V = 2E$, giving $\chi = 0$. So K is topologically a torus or Klein bottle.

For non-quadrilateral faces with 4 per vertex, other topologies are possible but $\chi \leq 0$ (higher genus surfaces).

18.3.10 9. Summary

The smoothing exists because:

1. The 4-face + Lagrangian condition forces a symplectic direct sum $\mathbb{R}^4 = V_1 \oplus V_2$ at each vertex (vertex spanning is proved algebraically; opposite edges span complementary symplectic 2-planes)
2. This decomposition forces Maslov index exactly 0 (algebraic, not just generic)
3. Near each vertex, $K = C_1 \times C_2$ (product of corners). Smoothing each corner gives $K^{sm} = C_1^{sm} \times C_2^{sm}$, a smooth Lagrangian surface (product of curves in symplectic factors). No Lagrangian surgery needed at vertices.
4. Edge creases (between vertices) are smoothed by generating function interpolation
5. All smoothings are Hamiltonian isotopies, composable to give global K_t

6. The 3-face case is impossible (isotropic dimension bound), explaining why 4 is the right valence

Revision — Corrections from v1

- **v1 claimed** Maslov index vanishes by `alternating orientations relative to J`. **Replaced** with the precise symplectic direct sum argument: the edge-sharing constraint forces ω to be block diagonal in the (e_1, e_3, e_2, e_4) basis, giving $\mu = 0$ algebraically.
- **v1 stated** the 3-face obstruction as “nonzero Maslov index.” **Corrected:** 3-face Lagrangian vertices don’t have nonzero Maslov index — they’re impossible (3 isotropic vectors can’t span 3D in \mathbb{R}^4).
- **v1 lacked** numerical verification. **Added** via `verify-p8-maslov-v2.py`: 998/998 valid configurations give $\mu = 0$; comparison with non-edge-sharing quadruples (55% have $\mu = 0$) confirms the constraint is essential.

18.4 References

- D. McDuff, D. Salamon, *Introduction to Symplectic Topology*, 3rd ed., Oxford University Press, 2017, Proposition 3.17. [Composition of compactly supported Hamiltonian isotopies]

Process Note — futon6 Corpus References

- PlanetMath: “symplectic manifold” (SymplecticManifold) — symplectic structures
- PlanetMath: “Darboux's theorem” (DarbouxsTheoremSymplecticGeometry) — local coordinates
- PlanetMath: “concepts in symplectic geometry” (ConceptsInSymplecticGeometry) — overview
- PlanetMath: “*symplectic complement*”/coisotropic subspace — Lagrangian subspaces
- PlanetMath: “Kähler manifold is symplectic” (AKahlerManifoldIsSymplectic) — complex structure

Chapter 19

Problem 9: Polynomial Detection of Rank-1 Scaling for Quadrifocal Tensors

19.1 Problem Statement

Let $n \geq 5$. Let $A^{(1)}, \dots, A^{(n)} \in \mathbb{R}^{3 \times 4}$ be Zariski-generic matrices. For $\alpha, \beta, \gamma, \delta \in [n]$, construct $Q^{(\alpha\beta\gamma\delta)} \in \mathbb{R}^{3 \times 3 \times 3 \times 3}$ with entry:

$$Q_{ijkl}^{(abgd)} = \det[A^{(a)}(i, :); A^{(b)}(j, :); A^{(g)}(k, :); A^{(d)}(l, :)]$$

(the 4x4 determinant of a matrix formed by stacking rows i, j, k, l from cameras $\alpha, \beta, \gamma, \delta$ respectively).

Does there exist a polynomial map $F: \mathbb{R}^{81 \times n^4} \rightarrow \mathbb{R}^N$ satisfying:

1. F does not depend on $A^{(1)}, \dots, A^{(n)}$
2. The degrees of the coordinate functions of F do not depend on n
3. For $\lambda \in \mathbb{R}^{n \times n \times n \times n}$ with $\lambda_{abgd} \neq 0$ precisely when a, b, g, d are not all identical: $F(\lambda_{abgd} Q^{(abgd)} : a, b, g, d \text{ in } [n]) = 0$ if and only if there exist $u, v, w, x \in (\mathbb{R}^*)^n$ such that $\lambda_{abgd} = u_a v_b w_g x_d$ for all non-identical a, b, g, d .

19.2 Answer

Yes. Such a polynomial map F exists, with coordinate functions of degree 3.

19.3 Solution

19.3.1 1. The quadrifocal tensor as a bilinear form

The entry $Q_{ijkl}^{(abgd)} = \det[a_i^{(a)}; a_j^{(b)}; a_k^{(g)}; a_l^{(d)}]$ is the evaluation of the volume form (the unique up-to-scale alternating 4-linear form on \mathbb{R}^4) on four camera row vectors.

Key observation (bilinear form reduction): Fix two camera-row pairs (γ, k) and (δ, l) , giving vectors $c = a_k^{(\gamma)}$ and $d = a_l^{(\delta)} \in \mathbb{R}^4$. Then the map:

$$\omega(p, q) = \det[p; q; c; d]$$

is an alternating bilinear form on \mathbb{R}^4 . Since c wedge d is a simple 2-form, the Hodge dual $*(c$ wedge $d)$ is also simple, so ω has **rank 2** as a bilinear form.

Equivalently: the null space of ω is $\text{span}\{c, d\}$ (2-dimensional), and ω induces a non-degenerate alternating form on $V/\text{span}c, d = \mathbb{R}^2$.

19.3.2 2. The rank-2 constraint and its 3x3 minor formulation

Since ω has rank 2, for ANY choice of 3 vectors p_1, p_2, p_3 and 3 vectors $q_1, q_2, q_3 \in \mathbb{R}^4$:

$$\begin{aligned} \det|\omega(p_1, q_1)\omega(p_1, q_2)\omega(p_1, q_3)| \\ |\omega(p_2, q_1)\omega(p_2, q_2)\omega(p_2, q_3)| = 0 \\ |\omega(p_3, q_1)\omega(p_3, q_2)\omega(p_3, q_3)| \end{aligned}$$

(A rank-2 bilinear form has all 3x3 minors vanishing.)

In terms of the Q tensors: choosing $p_m = a_{i_m}^{(\alpha_m)}$ and $q_n = a_{j_n}^{(\beta_n)}$, this becomes:

$$\det[Q_{i_m, j_n, k, l}^{(\alpha_m, \beta_n, \gamma, \delta)}]_{3 \times 3} = 0$$

for any choice of $(\alpha_1, i_1), (\alpha_2, i_2), (\alpha_3, i_3)$ and $(\beta_1, j_1), (\beta_2, j_2), (\beta_3, j_3)$ and fixed $(\gamma, k), (\delta, l)$.

This is a **degree-3 polynomial** in the Q entries, independent of the cameras.

19.3.3 3. Effect of rank-1 scaling on the 3x3 minor

Now consider the scaled tensors $T^{(abgd)} = \lambda_{abgd} Q^{(abgd)}$. The 3x3 matrix becomes:

$$M_{mn} = \lambda_{\alpha_m, \beta_n, \gamma, \delta} * Q_{i_m, j_n, k, l}^{(\alpha_m, \beta_n, \gamma, \delta)}$$

This is the Hadamard (entrywise) product of two 3x3 matrices:

- $\Lambda_{mn} = \lambda_{\alpha_m, \beta_n, \gamma, \delta}$ (depends on camera indices only)
- $\Omega_{mn} = Q_{i_m, j_n, k, l}^{(\alpha_m, \beta_n, \gamma, \delta)}$ (the bilinear form)

If λ is **rank-1**: $\lambda_{abgd} = u_a v_b w_g x_d$, so $\Lambda_{mn} = u_{\alpha_m} v_{\beta_n} w_{\gamma} x_{\delta}$. This factors as $\Lambda = (u_{\alpha_m})_m (v_{\beta_n})_n^T$ (scaled by the constant $w_{\gamma} x_{\delta}$). So Λ has matrix rank 1.

For a rank-1 matrix Λ , the Hadamard product $M = \Lambda \circ \Omega$ equals $\text{diag}(u) * \Omega * \text{diag}(v)$ (up to the scalar $w_{\gamma} x_{\delta}$). Since similar transformations preserve rank: $\text{rank}(M) = \text{rank}(\Omega) = 2 < 3$,

so $\det(M) = 0$.

Therefore: rank-1 λ implies all 3x3 minors of scaled T vanish. ✓

19.3.4 4. Converse: non-rank-1 λ gives nonzero minors (for generic cameras)

For the converse, we need: if λ is NOT rank-1, then some 3x3 minor is nonzero (for Zariski-generic cameras).

The argument is algebraic-geometric, not via Hadamard rank bounds. Define

$$P(A^{(1)}, \dots, A^{(n)}) = \det[T_{i_m, j_n, k, l}^{(\alpha_m, \beta_n, \gamma, \delta)}]_{3 \times 3}$$

for a specific choice of row/column/fixed indices. This is a polynomial in the camera entries (with λ fixed). We claim P is not the zero polynomial when λ is not rank-1 in its first two indices. Since a nonzero polynomial is nonzero on a Zariski-dense open set, this establishes the converse for generic cameras.

Explicit witness ($n = 5$). Choose 5 cameras $A^{(i)}$ as rows of generic 3×4 matrices with rational entries:

$$\begin{aligned} A^{(1)} &= [[1, 0, 0, 1], [0, 1, 0, 1], [0, 0, 1, 1]] \\ A^{(2)} &= [[1, 1, 0, 0], [0, 1, 1, 0], [0, 0, 1, 1]] \\ A^{(3)} &= [[1, 0, 1, 0], [1, 1, 0, 0], [0, 1, 0, 1]] \\ A^{(4)} &= [[0, 1, 1, 1], [1, 0, 1, 1], [1, 1, 0, 1]] \\ A^{(5)} &= [[1, 2, 3, 4], [4, 3, 2, 1], [1, 1, 1, 1]] \end{aligned}$$

Choose a non-rank-1 scaling: $\lambda_{abgd} = 1$ for all non-identical (a, b, g, d) except $\lambda_{1,2,3,4} = 2$.

Non-rank-1 verification. If λ were rank-1, then $\lambda_{abgd} = u_a v_b w_g x_d$. From $\lambda_{1,2,3,4} = 2$ and $\lambda_{2,2,3,4} = 1$ we get $u_1/u_2 = 2$. But from $\lambda_{1,1,3,4} = 1$ and $\lambda_{2,1,3,4} = 1$ we get $u_1/u_2 = 1$. Contradiction.

Fix $\gamma = 3, \delta = 4, k = 1, l = 1$. Choose row triples $(\alpha_m, i_m) = (1, 1), (2, 1), (5, 1)$ and column triples $(\beta_n, j_n) = (2, 1), (5, 1), (1, 2)$. The 3x3 Λ matrix has entries $\lambda_{\alpha_m, \beta_n, 3, 4}$; specifically $\Lambda_{11} = \lambda_{1,2,3,4} = 2$ with all other entries equal to 1. The Ω matrix (unscaled Q values) has $\det(\Omega) = 0$ (confirming rank-2), but the Hadamard product $M = \Lambda \circ \Omega$ satisfies $\det(M) = -24 \neq 0$ (verified by direct computation of nine 4x4 determinants). This exhibits P as not the zero polynomial.

Remark (Hadamard product interpretation). The matrix M_{mn} is the Hadamard product $\Lambda \circ \Omega$, where Λ carries the scaling entries and Ω carries the bilinear form values. The upper bound $\text{rank}(\Lambda \circ \Omega) \leq \text{rank}(\Lambda) * \text{rank}(\Omega)$ provides context but is not used in the proof; the converse relies entirely on the polynomial nonvanishing argument above.

19.3.5 5. All matricizations from the same construction

The construction in Section 2-4 tests the rank-1 condition on the $(1, 2)$ - matricization of λ (fixing modes 3,4). By symmetry, applying the same construction with different pairs of “free” modes tests all matricizations:

- Fix modes $(3, 4)$, vary modes $(1, 2)$: test $\lambda_{(\alpha, \beta), (\gamma, \delta)}$
- Fix modes $(2, 4)$, vary modes $(1, 3)$: test $\lambda_{(\alpha, \gamma), (\beta, \delta)}$
- Fix modes $(2, 3)$, vary modes $(1, 4)$: test $\lambda_{(\alpha, \delta), (\beta, \gamma)}$

(The other fixings are redundant by symmetry of the rank-1 test.)

A 4-tensor λ has rank 1 if and only if all three of these matricizations have rank 1 (i.e., are outer products of vectors).

Tensor factor compatibility lemma. If all three matricizations have rank 1:

- Mode- $(1, 2)$ vs $(3, 4)$ rank 1 gives $\lambda_{abgd} = f_{ab}g_{gd}$.
- Mode- $(1, 3)$ vs $(2, 4)$ rank 1 gives $\lambda_{abgd} = h_{ag}k_{bd}$. From the first: $\lambda_{a1,b1,g,d}/\lambda_{a2,b2,g,d} = f_{a1,b1}/f_{a2,b2}$, independent of g, d . From the second: $\lambda_{a,b1,g1,d}/\lambda_{a,b2,g1,d} = k_{b1,d}/k_{b2,d}$, independent of $a, g1$. Cross-referencing these separations forces $f_{ab} = u_a v_b$ and $g_{gd} = w_g x_d$, giving $\lambda_{abgd} = u_a v_b w_g x_d$ (rank 1). QED.

19.3.6 6. Construction of F

Definition of F: The coordinate functions of F are all 3x3 minors:

$$F_{choice} = \det[T_{i_m, j_n, k, l}^{(\alpha_m, \beta_n, \gamma, \delta)}]_{m, n=1, 2, 3}$$

taken over all choices of:

- Three “row” camera-row pairs (α_m, i_m) for $m = 1, 2, 3$
- Three “column” camera-row pairs (β_n, j_n) for $n = 1, 2, 3$
- Fixed camera-row pairs (γ, k) and (δ, l)

And the analogous minors for the other two matricization pairs (fixing different pairs of modes and varying the others).

Properties:

1. **Camera-independent:** Each F_{choice} is a degree-3 polynomial in the T entries. The coefficient is ± 1 (from the determinant expansion). No camera parameters appear.
2. **Degree independent of n:** Each coordinate function has degree exactly 3.

3. **Characterization:** $F = 0$ iff all three matricizations of λ have rank 1, iff λ is rank-1, for Zariski-generic cameras (by Sections 3-5).

Codimension count: The number of coordinate functions N grows with n (there are $O(n^8)$ choices for the 3x3 minors from the (1, 2) vs (3, 4) matricization alone), but the degree stays fixed at 3.

19.3.7 7. Geometric interpretation

The Q tensors are the **quadrifocal tensors** from multiview geometry (the 4-view analog of the fundamental matrix and trifocal tensor). The rank-2 bilinear form structure is the classical rank constraint from projective geometry: the determinant encodes linear dependence constraints among lifted camera-row vectors (equivalently coplanarity/dependence conditions) on the stacked camera rows.

The rank-1 scaling $\lambda = u \otimes v \otimes w \otimes x$ corresponds to the natural gauge freedom in multiview geometry: rescaling each camera's contribution independently for each of the four “roles” (which row selection it contributes). The polynomial map F detects when a putative rescaling is consistent with this gauge group.

The Zariski-genericity requirement on the cameras ensures that the quadrifocal variety is “non-degenerate” — the Q tensors carry enough information to distinguish rank-1 from higher-rank scalings.

Process Note — futon6 Corpus References

- PlanetMath: “Segre map” (SegreMap) — Segre embedding and rank-1 tensors
- PlanetMath: “determinantal varieties” (SegreMap) — varieties defined by minors
- PlanetMath: $\text{tensorrank}^{\text{"/}}\text{simple tensor}$ (SimpleTensor) — rank-1 tensors
- PlanetMath: “exterior algebra” — alternating multilinear forms
- PlanetMath: “Hadamard conjecture” (HadamardConjecture) — Hadamard matrices

Chapter 20

Problem 10: RKHS-Constrained Tensor CP via Preconditioned Conjugate Gradient

20.1 Problem Statement

Given the mode-k subproblem of RKHS-constrained CP decomposition with missing data, solve

$$[(Z \times K)^T D(Z \times K) + \lambda(I_r \times K)] \text{vec}(W) = (I_r \times K) \text{vec}(B),$$

where $D = SS^T$ is the observation projector (q observed entries out of $N = nM$), $B = TZ$, and $n, r \ll q \ll N$.

20.2 Assumptions Used (explicit)

1. $\lambda > 0$.
2. For standard PCG and Cholesky-based preconditioning, use a PD kernel $K_\tau = K + \tau I_n$ with $\tau > 0$ (or assume K is already PD).
3. S is a selection operator, so D is diagonal/projector and sparse by index list.

Then the solved system is

$$\begin{aligned} A_\tau x &= b_\tau, \\ A_\tau &= (Z \times K_\tau)^T D(Z \times K_\tau) + \lambda(I_r \times K_\tau), \\ x &= \text{vec}(W), \\ b_\tau &= (I_r \times K_\tau) \text{vec}(B). \end{aligned}$$

Under these assumptions A_τ is SPD, so PCG applies.

20.3 Solution

20.3.1 1. Why naive direct methods fail

A_τ is an $(nr) \times (nr)$ system. Dense direct factorization costs $O((nr)^3) = O(n^3 r^3)$.

A naive explicit route also materializes $\Phi = Z \times K_{\tau} \in R^{N \times nr}$, which costs $O(Nnr)$ memory/-work before factorization. This is the N -dependent bottleneck we avoid with matrix-free PCG.

20.3.2 2. Implicit matrix-vector product in $O(n^2r + qr)$

CG needs only $y = A_{\tau} \mathbf{x}$, not A_{τ} explicitly.

Given $\mathbf{x} = \text{vec}(V)$, $V \in R^{n \times r}$:

1. $U = K_{\tau}V$. Cost $O(n^2r)$.
2. Forward sampled action (only observed entries):

$$(Z \times K_{\tau}) \text{vec}(V) = \text{vec}(K_{\tau}V\mathbb{Z}^T).$$

For each observed coordinate (i_l, j_l) ,

$$u_l = \langle U[i_l, :], Z[j_l, :] \rangle.$$

Total $O(qr)$.

3. Form sparse W' in $R^{n \times M}$ from u_l . Let $s = \text{nnz}(W') \leq q$.
4. Adjoint sampled action:

$$(\mathbb{Z}^T \times K_{\tau}) \text{vec}(W') = \text{vec}(K_{\tau}W'Z).$$

Compute W' $Z \in O(sr) \leq O(qr)$, then left-multiply by $K_{\tau} \in O(n^2r)$.

5. Add regularization term $\lambda \text{vec}(K_{\tau}V)$, cost $O(n^2r)$.

Total per matvec:

$$O(n^2r + qr),$$

with no $O(N)$ term.

20.3.3 3. Right-hand side

$B = TZ$ with T sparse (q nonzeros):

1. T Z: $O(qr)$
2. $K_{\tau} B : O(n^2 r)$

So $b_{\tau} = (I_r \times K_{\tau}) \text{vec}(B)$ is formed in $O(qr + n^2 r)$.

20.3.4 4. Preconditioner that matches the corrected algebra

Use $D = SS^T$ and whiten by $K_{\tau}^{-1/2}$:

$$x = (I_r \times K_{\tau}^{-1/2})y.$$

Then

$$\begin{aligned}\hat{A} &= (I_r \times K_{\tau}^{-1/2})A_{\tau}(I_r \times K_{\tau}^{-1/2}) \\ &= (Z \times K_{\tau}^{1/2})^T D (Z \times K_{\tau}^{1/2}) + \lambda I.\end{aligned}$$

If sampling is roughly uniform, $D \sim c I$ with $c = q/N$. Then

$$\hat{A} \sim c(Z^T Z \times K_{\tau}) + \lambda I.$$

Choose Kron preconditioner in whitened coordinates:

$$\hat{P} = (cZ^T Z + \lambda I_r) \times I_n.$$

Mapping back gives

$$\begin{aligned}P &= (cZ^T Z + \lambda I_r) \times K_{\tau} = H \times K_{\tau}, \\ H &= cZ^T Z + \lambda I_r.\end{aligned}$$

This is the missing justification for using $H \times K_{\tau}$ (instead of claiming it is the exact $D = I$ system).

Khatri-Rao identity still gives efficient Gram formation:

$$Z^T Z = \text{Hadamard}_i(A_i^T A_i),$$

cost $O(\sum_i n_i r^2)$.

Preconditioner apply:

$$P^{-1} = H^{-1} \times K_{\tau}^{-1},$$

implemented by solving $K_{\tau} Y H^T = Z'$ after reshape. Per application cost is $O(n^2 r + nr^2)$ (often simplified to $O(n^2 r)$ when $n \gg r$).

20.3.5 5. Convergence (tightened)

For SPD A_{τ} and SPD P, standard PCG gives

$$\|e_t\|_{A_{\tau}} \leq 2((\sqrt{(\kappa)} - 1)/(\sqrt{(\kappa)} + 1))^t \|e_0\|_{A_{\tau}},$$

with $\kappa = \text{cond}(P^{-1/2} A_{\tau} P^{-1/2})$, so

$$t = O(\sqrt{(\kappa)} \log(1/\epsilon)).$$

To claim “fast” convergence, add a spectral-equivalence hypothesis, e.g.

$$(1 - \delta)P \leq A_{\tau} \leq (1 + \delta)P, 0 < \delta < 1,$$

which implies

$$\kappa(P^{-1} A_{\tau}) \leq (1 + \delta)/(1 - \delta).$$

Hence t is logarithmic in $1/\epsilon$ with a modest $\sqrt{(\kappa)}$ factor when δ is bounded away from 1. (No unsupported closed-form $t = O(r\sqrt{(n/q)})$ claim is needed.)

Sufficient conditions for bounded δ . The spectral equivalence $(1 - \delta)P \leq A_{\tau} \leq (1 + \delta)P$ holds with δ bounded away from 1 when the sampling pattern satisfies a restricted isometry-type condition: the restricted isometry holds for the column space of $Z \otimes K_{\tau}^{1/2}$, i.e. $(Z \otimes K_{\tau}^{1/2})^T (D - cI) (Z \otimes K_{\tau}^{1/2})$ is small in operator norm relative to λ . Under standard leverage/coherence assumptions and sufficient sampling scaling with model dimension, concentration yields δ bounded away from 1 with high probability. Under this regime, $\kappa = O(1)$ and PCG converges in $O(\log(1/\epsilon))$ iterations.

20.3.6 6. Complexity summary

Setup per ALS outer step:

1. Cholesky(K_{τ}): $O(n^3)$
2. $Z^T Z$ via Hadamard Grams: $O(\sum_i n_i r^2)$
3. Cholesky(H): $O(r^3)$
4. RHS: $O(qr + n^2 r)$

Per PCG iteration:

1. Matvec: $O(n^2 r + qr)$
2. Preconditioner apply: $O(n^2 r + nr^2)$

Total:

$$O(n^3 + r^3 + \sum_i n_i r^2 + qr + n^2 r + t(n^2 r + qr + nr^2)).$$

In the common regime $n \geq r$, this simplifies to

$$O(n^3 + t(n^2 r + qr)),$$

with dependence on q (observed entries) rather than N (all entries).

Regime caveat. When n is large enough that the $O(n^3)$ Cholesky setup dominates (i.e., $n^3 > t(n^2 r + qr)$), the per-ALS-step cost is effectively $O(n^3)$. In this regime, low-rank kernel approximations (e.g., Nystrom approximation with rank $p \ll n$, reducing the kernel factorization to $O(np^2)$) or iterative inner solves (conjugate gradient on $K_{\tau}y = z$, cost $O(n^2)$ per inner iteration) can replace the exact Cholesky, reducing the setup to $O(np^2 + t(npqr + qr))$. This is a well-known practical optimization (see Rudi-Calandriello-Rosasco 2017) and is compatible with the PCG framework as presented.

20.3.7 7. Algorithm

SETUP:

```

K_tau = K + tau * I_n                      # tau > 0 if K is only PSD
L_K = cholesky(K_tau)                        # O(n^3)
G = hadamard_product(A_i^T A_i for i != k)  # O(sum_i n_i r^2)
c = q / N
H = c * G + lambda * I_r                   # O(r^3)
L_H = cholesky(H)                            # O(qr)
B = sparse_mttkrp(T, Z)                      # O(qr)

```

```

b = vec(K_tau @ B)                                # O(n^2 r)

PCG(A_tau x = b, preconditioner P = H x K_tau):
    x0 = 0
    r0 = b
    z0 = precond_solve(L_K, L_H, r0)              # O(n^2 r + n r^2)
    p0 = z0
    repeat until convergence:
        w = matvec_A_tau(p)                         # O(n^2 r + q r)
        alpha = (r^T z) / (p^T w)
        x = x + alpha * p
        r_new = r - alpha * w
        if ||r_new|| <= eps * ||b||: break
        z_new = precond_solve(L_K, L_H, r_new)
        beta = (r_new^T z_new) / (r^T z)
        p = z_new + beta * p
        r, z = r_new, z_new
    W = reshape(x, n, r)

matvec_A_tau(v):
    V = reshape(v, n, r)
    U = K_tau @ V
    for each observed (i_l, j_l):
        u_l = dot(U[i_l, :], Z[j_l, :])
    Wprime = sparse(n, M, entries u_l)
    Y = K_tau @ (Wprime @ Z) + lambda * (K_tau @ V)
    return vec(Y)

precond_solve(L_K, L_H, z):
    Zp = reshape(z, n, r)
    solve K_tau Y H^T = Zp using triangular solves with L_K, L_H
    return vec(Y)

```

Process Note — futon6 Corpus References

- PlanetMath: conjugate gradient algorithm; method of conjugate gradients
- PlanetMath: Kronecker product; positive definite matrices
- PlanetMath: properties of tensor product
- physics.SE #27466: iterative solvers for large systems in physics
- physics.SE #27556: preconditioning for elliptic PDEs

Part III

Prompt Excerpts and Pivot Moments

Part III: The Sprint as Dialogue

This chapter records the proof sprint as it actually happened: a conversation between a human dispatcher (Joe), two AI proof engines (Claude instances), and a verifier/researcher (Codex), conducted over roughly 48 hours on February 11–13, 2026. Excerpts are drawn from `history.jsonl` (Joe’s prompts), Codex output files, and git commit messages. Editorial annotations mark the pivotal moments where proof strategy, status, or architecture shifted.

Act I: “Even if we’re a day late”

Joe

Claude + Joe Solve “First Proof” using Rob’s Superpod <https://arxiv.org/html/2602.05192v1>

Joe

Even if we’re a day late and a dollar short at least we can try

Joe

Let’s see if we can do one of them right now using PlanetMath and nlab and off-the-shelf Claude

Pivot: The sprint begins. Problem 10 is chosen as a warm-up. Within 30 minutes it is solved, and the pace accelerates.

Joe

OK, should we solve another First Proof problem? The last one wasn’t so hard apparently!

Act II: Scaling the Machinery

Joe

OK, I have two Codex research assistants working for you as well as the validator working on p6

Joe

OK, we have 3 verifiers running now, they are making progress but not committing yet

Joe

Codex is *still* after 53 minutes hard at work on Problem 6, but it is down to two gaps now. I think 3 verifiers is about all my laptop can handle, noticing considerable slow down.

Joe

I think I will give it five more minutes and then say “pencils down” and let you look at #6

Joe

Codex is pushing #6, I OOMed on 3 and 5, I will get them back up once 6 lands

Pivot: Physical resource limits (RAM, thermal throttling) become a genuine constraint on mathematical exploration. The multi-agent topology stabilises at three concurrent processes.

Joe

It's slow going over here—are any of the proofs sufficiently validated that we could start a “write up”? If the previous example is representative it can take about an hour for one of these to complete.

Act III: Proofs and Refutations

Joe

Yeah let's do some Proofs and Refutations—you can be Critic

Codex — Critic mode, round 1

Excellent. Critic mode, round 1: I attacked P2 and P7 as the most vulnerable. [...] Verdict: plausible direction, not a completed proof (P2). [...] Verdict: currently not proof-grade; too many deep steps are asserted, not established (P7).

Joe

I have engaged Codex and another Claude in a reviewer + response-to-reviewer cycle. Codex found some pretty significant problems; the other Claude is making what look like solid fixes, but it looks like tough going.

Codex — Triage verdict

P8: most recoverable. [...] P2: recoverable but harder. Needs one serious representation-theoretic theorem/lemma that is currently hand-waved. [...] P7: least recoverable as currently framed. The obstruction-vanishing step is the main risk; unless they replace it with a precise known theorem tailored to this lattice family, this will likely remain conditional/existential rather than a full proof.

Pivot: Codex's triage creates a severity ordering across problems, distinguishing "recoverable" from "structural" gaps. The review cycle is now explicitly adversarial: prover vs. critic.

Joe

This is interesting in comparison to my work in futon5 on Meta-Meta-Cellular Automata. There also, generation is cheap—just bit flipping—but doing things like “detecting edge of chaos behaviour” is a challenge. [...] However, I think we really haven’t done so bad. We have our Claude-Codex “Proofs and Refutations” system up and running right now, we use both collaborative (verification + library research) and argumentative (prover vs critic) modes. So notwithstanding the mathematical issues you raised—at least we aren’t shipping failed proofs! This is verification happening at a “glacial” scale in futon3c terminology—but at least it is happening!

Joe

Furthermore, the wiring diagram decomposition is probably the only thing holding this together—it’s allowing us to be very targeted with our reviews and fixes. Imagine trying to do what we’re doing with... ChatGPT. It would be hell.

Joe

Also, another remark—making mistakes isn’t a bad thing. As my grandfather said, that’s how we learn.

Pivot: A methodological self-assessment. The two key claims: (1) the wiring-diagram decomposition enables targeted review at scale; (2) the collaborative/adversarial agent modes prevent “shipping failed proofs.” Both claims are tested in Acts IV–V.

Act IV: Formalization and Futon Theory

Joe

This does suggest a possible but probably crazy and stupid idea—which hasn’t stopped hundreds of people trying it. What about formalizing as we go? Like QED style. I mean, it hurts me to say this. I briefly had Bob Boyer as a Master’s advisor. He and I could not see eye to eye. Granted, that was 2002 and things were a little different back then.

Joe

Yeah, I mean, we needed in 2002 *what we are doing now*. The only problem is it wasn’t possible then.

Claude

So in a sense, the 2002 vision was twenty-four years early rather than wrong.

Joe

Better than twenty-four years late! Imagine if I proposed WIFI now. Great idea right?

Pivot: A historical aside connecting the sprint to the 2002-era theorem-proving community. The implication: AI-assisted informal proof is the approach that was missing, not formalization per se.

Joe

OK, so the naive idea: could we write a letter to Codex talking about why Problem 4 is hard? It would use the John McPhee idea [4]...

Joe

OK, now a non-naive idea (which may be less useful than the naive one). I invented something called “futon theory”—it’s not quite what it sounds like. Futons (in my theory) are atoms of the future which are perceivable in the present. [...] It’s a bit different in mathematics because in principle we don’t know if the result is actually true. But what we could do is design the search process, and then we would at least know that the search process is working the way we hoped it would. It’s the somewhat more technical version of the “Dear Codex” letter you just wrote—building a process that you have utter confidence in that will shed light on the domain even if it doesn’t reveal the exact answer.

Pivot: Two ideas collide: McPhee’s “letter to yourself” technique for writer’s block, and futon theory’s “atoms of the future.” Both converge on the same insight: process design is tractable even when the mathematical outcome is uncertain.

Joe

Great, I think you have your work cut out for you. It’s cool that this involved all the strategies, including the “least likely” Strategy C that surprised us by being particularly flavourful

Act V: Crisis — P6 and P7

Joe

I thought #6 and #7 were proved so I’m glad I asked!

Joe

Well I am a bit perplexed b/c at this time yesterday I had been convinced that Problem 7 was done. Look at Problem 7 related git logs to try and figure out what’s been going on with this journey.

Joe

Well, I have another Codex program mining Arxiv right now for wiring diagrams that we might use. But this presupposes that we are actually looking at gaps and not a decomposing corpse.

Pivot: The most dramatic moment in the sprint. A problem believed closed reopens with structural gaps. The “decomposing corpse” quip captures the uncertainty: is the proof salvageable, or fundamentally dead?

Joe

Hm, claim 1 sounds a bit like replacing an overclaim with weasel words; #2 similarly. I think we need to restructure the proof?

Claude — Gap triage

G1 (fundamental group control) and G3 (rational acyclicity) can be closed once the cap is homotopy equivalent to $F \times D^2$ rel boundary. [...] G2 (Browder–Quinn identification) remains the genuine remaining gap.

Pivot: The monolithic “open Problem 7” label is decomposed into a prioritised closure queue: G1, G2, G3. Within hours, G1 and G3 are resolved, isolating G2 as the sole remaining obligation.

Joe

Could we cite secondary literature for G2 that is on Arxiv? Mathematics is full of folklore

Claude — Citation search result

There is no single modern arXiv theorem that states the exact identification in one line. The bridge is assembled from standard components: Browder (1968), López de Medrano (1971), Cappell–Shaneson (1974), Ranicki (1998).

Pivot: Citation strategy stabilises: replace “single theorem lookup” with a theorem-number ledger across four classical sources.

Joe

It really sounds to me like the proof of Problem 6 is hanging by a thread

Codex — P6 reality check

Problem 6: not a full proof yet; it is now an honest conditional argument. The core universal vertex-selection theorem is still imported, not proved.

Codex — P7 hard stop

Pulled and reviewed 3138721. This is not yet a valid full proof.

Act VI: Student Dispatch and Agent Teaming

Joe

Yeah, I guess the model is rather than treating Codex as a junior developer as we sometimes do in coding applications, we would treat them as a “grad student.”

Joe

Maybe we should call it student-dispatch to include undergrads, bright high schoolers, and precocious five year olds like Codex

Pivot: The agent/student-dispatch pattern is named. It reframes the Codex interaction from “run this script” to “here is context, dead ends, directions—explore and report.”

Joe

So I wonder what we could do to help. I’ve almost run out of ideas. I guess one pattern I’ve noticed is that we can support the “reduction” pattern by verifying everything that is claimed except the gap. Closing gaps (as with Problem 4) can sometimes turn out to be a focused computational task. Another approach is Math Overflow search or Arxiv search to create wiring diagrams that might help or might provide analogous reasoning structures. That last part is a bit woolly.

Joe

So, if we were able to turn SE into wiring diagrams on the superpod, then we could use tensor math to search them!

Joe

Ah, and for “artificial stack exchange” what we could do is *induce* new wiring diagrams, notice where they sit relative to other known diagrams (this corresponds to “asking a question”)

Pivot: A forward-looking connection: the proof sprint’s wiring-diagram methodology could be mechanised via tensor search over StackExchange-derived argument structures. This motivates the Stage 7 thread-wiring work in the futon6 pipeline.

Act VII: The Coaching Breakthrough (Problem 6)

Joe

Well, and I want to talk with you about Problem 6. I think that’s the only one outstanding. But I’m realizing that the “other Claude” has been sending me on continual gap-filling missions without giving me a valid confidence signal. It’s like Gemini saying “I’ll fix your code right away sir!” [...] Problem 6 has not brought out the best in Claude.

Joe

I think a good approach might be: “Can you find any other reductions?” That would start to build some intelligence around the pattern rather than just a TryHarder strategy.

Pivot: The failure mode is diagnosed: dispatching closure attempts without layer-level calibration. The “reductions” framing shifts from “close the gap” to “map the landscape.”

Joe

I think you should think out of the box a bit. What kind of problem is this? What kind of proof applies to this kind of problem? How would you teach it to an undergraduate? How would you teach it to a grad student? Where, in reality, do people learn about this kind of problem? What kind of person finds this kind of problem easy? Are there “tricks” (symmetries) that would make some of your Zeno’s Paradoxes go away? Like one from my thesis in the resources directory is an example from Gowers in which binomial expansion terms have opposite signs and so cancel. Like, OK, this problem was an “open problem” not a textbook problem but come on—it’s on the research frontier, we’re not asking you to solve alien mathematics from the year 5000AD. This is totally within your capability space. Why aren’t you finding the answer in 30 minutes?

Pivot: The coaching intervention. Five questions, each forcing a different reframing: layer enumeration (“what kind of problem?”), pedagogical reduction (“teach it to an undergrad”), sociological targeting (“who finds this easy?”), structural cancellation (“tricks / symmetries”), and honest calibration (“why not 30 minutes?”).

Claude — 15 minutes later

The proof for K_n is complete. $\bar{d} = 2t/(n\varepsilon) \leq 2/3$ at $T = \varepsilon n/3$ steps. Pigeonhole gives $\exists v$ with $\text{tr}(Y) \leq 2/3$, and $\|Y\| \leq \text{tr}(Y)$ for PSD matrices. The barrier is maintained at every step. Result: $|S| = \varepsilon n/3$, $c = 1/3$.

Claude — The irony

The irony: this entire proof is elementary—no interlacing families, no Borcea–Brändén, no MSS theorem needed. Just PSD trace bound + pigeonhole + Turán.

[With the benefit of hindsight: the elementary proof closes K_n but the averaging step ($\bar{d} < 1$) that it relies on is false for general graphs—see Act IX. The irony has a second layer.]

Pivot: The layer switch lands. Eight hours of sparsification-layer attacks are bypassed by an elementary combinatorial proof discovered in 15 minutes. The proof uses three undergraduate-level facts: Turán’s theorem, the PSD trace bound, and the pigeonhole principle. The coaching did not supply mathematical content—it supplied *questions* that forced layer enumeration.

Joe

It's so cool that this is the same basic solution we have used to overcome continual shoring up of bad design in futon3, and also the same solution I've used with Codex just now by getting it to spot syntax errors rather than depending on me to do it.

Claude — The meta-pattern

The diagnostic question is always the same: “who finds this easy?” If the answer is “someone other than the entity currently struggling,” you’re in the wrong layer.

Pivot: The layer-switching pattern is recognized as fractal: it appears in proof strategy (Problem 6), in software design (futon3), and in task allocation (Codex as syntax checker). The common diagnostic: ask who would find the task trivial.

Act VIII: The Monograph

Joe

In addition to the PAR I think it would be good to look through the git log on futon6 and create a “making of” summary note.

Joe

Also in terms of “what we’ve learned”—in the making-of I think we could add something about the relevance of this pattern to agent teaming (further work in futon3c). Maybe this even goes back to the work in futon2 ants—i.e. we are exploring a domain, bringing back relevant information.

Joe

I think the key thing you could help with now is looking through `history.jsonl` for good quotes for Part III.

Pivot: The sprint becomes its own document. The recursive structure—a proof sprint whose Part III records the prompts that shaped Part II—closes the loop between process and product.

Act IX: The Continuation Cycles (Problems 4 and 6)

The monograph was written during the sprint, not after it. The sprint continued. Problems 4 and 6 entered multi-cycle proof engineering phases that lasted days beyond the initial 48-hour window—each cycle a dispatch, handoff, verification, and reassessment. These cycles are the sprint’s methodology running at sustained pace rather than compressed urgency.

Problem 4: From Wrong Proof to Algebraic Engineering

Claude — Initial draft (Feb 11)

Proof by concavity of $1/\Phi_n$ in cumulant coordinates. Since free cumulants are additive under \boxplus , Jensen's inequality gives $1/\Phi_n(p \boxplus q) \geq 1/\Phi_n(p) + 1/\Phi_n(q)$.

Pivot: The proof is wrong. $1/\Phi_n$ is superadditive in cumulant space WITHOUT being convex—the Hessian is indefinite. 35,000 numerical trials confirm the conjecture but the argument is structurally broken. Numerical verification caught the conjecture but hid the proof error.

Claude — Key identity (Feb 12, commit 03c1f8d)

$\Phi_4(p) \cdot \text{disc}(p) = -4(a_2^2 + 12a_4)(2a_2^3 - 8a_2a_4 + 9a_3^2)$. This converts the inequality to: prove a rational function's numerator is non-negative on a semi-algebraic domain.

Pivot: The first layer switch for Problem 4. Instead of hoping for a clever inequality (concavity, Schur-convexity, Cauchy–Schwarz), the problem is reduced to computational algebra: case decomposition by symmetry subspaces, resultant elimination, sign-counting. The identity itself is a publishable result—a finite analogue of Stam's inequality.

Claude — 3-piece Cauchy–Schwarz (commit 269fddd)

BREAKTHROUGH: the surplus decomposes into three pieces $T_1 + T_2 + R$ where $T_1 \leq 0$ (proved), and T_2, R have mutual-compensation structure. When $T_2 < 0$, R compensates. This reduces the full $n = 4$ proof to a degree-6 polynomial inequality: $K_{T2R} \geq 0$.

Codex — P4 route selection

That was the strongest direct technical hit for Problem 4 because it uses the bilinearity/induction structure of finite free convolution, which is exactly the algebraic backbone for a plausible proof route.

Pivot: A second layer switch within the algebraic layer. Symmetry-stratified elimination proved Cases 1, 2, 3a, 3b (resultant chains, 0.2–30 seconds each). Case 3c (generic, 4D) was handed to Codex with PHCpack. Seven SOS scripts proved that Positivstellensatz certificates are structurally impossible—the SOS cone misses the feasible set. The failure is a theorem, not a dead end: it rules out the entire SOS technique family.

Codex — P4 Case 3c check

Case 3c PHC task is done. In-domain real critical points: 12; case split: 4, 2, 2, 4. Case 3c values satisfy $-N = 1678.5498 \dots > 0$.

Problem 6: When Averaging Fails

Claude — Codex Cycle 7 (commit a7b0e3e)

The Barrier Maintenance Invariant is **falsified**. 12 base-suite steps have $\bar{d} \geq 1$ (worst: 1.739, Reg_100_d10, $\varepsilon = 0.5$, $t = 16$). The pigeonhole argument ($\bar{d} < 1 \Rightarrow \exists v \text{ with } \|Y_t(v)\| < 1$) cannot close the construction.

Pivot: The most dramatic moment in the continuation cycles. The averaging argument that the elementary proof relied on—the very argument whose discovery was the Act VII breakthrough—turns out to be *false* for general graphs. $\bar{d}_t < 1$ holds for K_n but not universally. The construction still works (0 skips in 1,111 runs) because leverage-ordered vertices have small *individual* contributions even when the average exceeds 1. The gap shifts from an averaging statement to a vertex-level feasibility statement: the **No-Skip Conjecture**.

Joe

I have engaged Codex in a systematic verification cycle on Problem 6. Seven cycles so far. Each cycle narrows the gap: the construction still works in every test—zero skips, zero failures—but the proof keeps slipping. The trajectory is: method wiring library \rightarrow leverage threshold \rightarrow barrier greedy \rightarrow BMI falsified \rightarrow No-Skip Conjecture. At each stage, what we thought was the gap turns out to be something more specific.

Codex — P6 handoff criteria

No unsupported “edge sparsification \Rightarrow vertex-induced subset” leap. Either cite an exact vertex theorem, or keep the result explicitly conditional/open.

Pivot: The continuation cycles exhibit the same pattern as the original sprint: repeated refinement of what is actually open. The lemma that was GPL-H became BMI became the No-Skip Conjecture. Each reformulation is a genuine narrowing, not a retreat. The “method wiring library” from Cycle 1 (ten techniques with typed wiring diagrams) prevented commitment to any single approach before the landscape was mapped—the pre-proof infrastructure that Part IV’s Section 6 proposes as a design pattern.

The Exhaustion-as-Theorem Pattern

Claude — Six techniques, one wall

All six subsample-and-concentrate techniques hit the same quantitative wall: spectral contribution scales as q^2 while set size scales as q . Trace/Markov: sublinear. Star domination: $O(\varepsilon/\log n)$. Decoupling + MSS: $O(\varepsilon^2)$. Greedy: $O(\varepsilon)$. Rank spreading: $O(\varepsilon^2)$. The wall is fundamental to the technique family, not an artifact of any one approach.

Pivot: When multiple methods fail at the same step, prove a theorem about the step. This is the cross-problem pattern identified in Part IV (Section 5) now demonstrated in the continuation: the

exhaustion of a technique family produces a structural understanding that redirects effort. For Problem 6, it redirected from “adapt edge sparsification” (where every method hits the quadratic-vs-linear wall) to “invent a new vertex-level argument” (the leverage-ordered barrier greedy). For Problem 4, it redirected from SOS certification (structurally impossible) to resultant elimination (feasible and fast).

Part IV

Proof Patterns

Chapter 21

Strategy Patterns Across Ten Problems

The ten proofs in Part II were not produced by a uniform method. Some closed quickly; others required layer-switching, creative reductions, or honest declarations of conditionality. This chapter extracts the transferable strategy patterns—what worked, what didn’t, and what an agent stuck on one problem could learn from the successes of another.

21.1 Design Pattern: OUTCOME TYPING (Close, Reduce, Map)

For sprint reporting, force every problem into one of three explicit outcome types:

1. **Close.** A complete proof (possibly with minor caveats). In this revision, Problem 3 is closed for the scoped existence target (uniqueness/irreducibility optional), Problem 5 is solved in a scope-limited form, and Problem 7 is treated as provisionally closed via the rotation route pending independent ledger re-check.
2. **Reduce.** A conditional result with clearly stated assumptions.
3. **Map.** The obstruction is characterized and adjacent problems are identified, but no proof is offered.

These labels describe *mathematical status*. QC-validation status is tracked separately: Problems 7 and 9 currently have node-level validation artifacts that still carry unresolved verifier gaps.

All three are legitimate contributions. A reduction is not a failed closure; it is a stable intermediate product that can later convert to closure after a layer switch or new lemma. Problem 6 spent eight hours in “Reduce” before a coaching intervention moved it to a strong partial closure (complete for key classes, with one explicit remaining general-case gap)—the change came from reframing, not additional effort.

Evidence ledger for Outcome Typing (top commits).

Commit	Role in pattern	Primary artifacts
c557899	Align closure language with evidence (separate math-status and QC-status axes)	<code>closure-validation-audit.md</code> + Part IV status text updates
2c734cb	Scope-aware closure typing for P3 (existence-scope clarified; QC status explicit)	P3 solution/writeup + <code>closure-validation-audit.md</code>
cc11834	“Map” outcome exemplar: counterexample + attack-path map instead of false closure	<code>problem6-gpl-h-counterexample.md</code> + <code>problem6-gpl-h-attack-paths.md</code>
9aaf8fa	Promote scoped result to “Close” after targeted gap closure and validation update	P3 prompts/results refresh + <code>closure-validation-audit.md</code>
90b6dd6	Reprocessed verifier summary results (15/15) to harden QC tracking independently of proof-status labels	<code>codex-unified-repair-results.json</code> + <code>codex-unified-repair-verification.md</code>

21.2 Design Pattern: LAYER-SWITCHING (Problem 7)

Problem 7 (uniform lattice with 2-torsion) is the clearest example of a successful strategy pivot.

Initial approach: Reflection lattice in even dimension. The E2 obligation (Fowler’s criterion) was discharged.

Obstruction: The surgery obligation (S) was blocked. Equivariant surgery requires a codimension-2 gap hypothesis; reflections give codimension-1 fixed sets. Blocked. (0fa4e82: “restructure S-branch as open problem with three approaches”)

Characterization: Instead of pushing harder on reflections, the obstruction was characterized structurally: a dimension-parity tension between E2 (needs even n) and S (better in odd n).

Layer switch: Replace reflections (codimension 1) with rotations (codimension 2). Now n is odd, E2 still works (fixed set has odd dimension, $\chi = 0$), and the codimension-2 gap hypothesis is satisfied. (287a41c: “rotation route (Approach IV), paper reads, triage”; 620ed57: “resolve rotation lattice existence, discharge E2”)

Closure: The surgery obstruction vanishes (trivial normal bundle from the congruence condition), yielding a provisional closure chain pending independent theorem-ledger

re-check. (8ce9771: “flat-normal-bundle argument—rational obstruction vanishes”; 158bc4f: “integral obstruction vanishes—obligation S discharged”)

Transferable principle: When blocked in one layer, characterize the obstruction structurally before attempting to overcome it. The characterization may reveal that a different layer avoids the obstruction entirely.

Evidence ledger for Layer-Switching (top commits).

Commit	Role in pattern	Primary artifacts
0fa4e82	Explicitly re-labels S as open and decomposes approaches	P7 solution + S-branch setup notes
287a41c	Rotation-route pivot and triage framing	Rotation-route wiring + P7 solution updates
620ed57	Discharges E2 under rotation route	Rotation-lattice construction note + P7 status update
5c7388a	Narrows to single remaining gap (G2)	Consolidated P7 complete-proof draft

21.3 Design Pattern: CREATIVE REDUCTION (Problem 4)

Problem 4 (root separation under finite free convolution) progressed from numerical evidence to proof via a sequence of reductions:

1. Centering reduction (translation invariance of Φ_n).
2. For $n = 3$: discovery of the identity $\Phi_3 \cdot \text{disc} = 18 a_2^2$ (exact, verified symbolically).
3. Recognition that the surplus expression has the form required by Titu’s lemma (Engel form of Cauchy–Schwarz).

Step 2 was the creative step—an identity discovered numerically and verified symbolically (9db6b4f: “Haar orbit exploration and key identity finding”; 0003300: “Prove P4 superadditivity for $n = 3$ via $\Phi_3 \cdot \text{disc}$ identity + Cauchy–Schwarz”). The key was that the identity was *sought* because the reduction strategy demanded an algebraic relationship between Φ_n and known invariants. The strategy shaped the search. The subsequent extension to $n = 4$ followed a different route—algebraic elimination plus computational verification (84c0041: “harden PHC parsing and record $n = 4$ computational verification”); full certification of one sub-case remains pending.

Transferable principle: Reductions create demand for specific identities or lemmas. The demand makes the search targeted rather than exploratory.

Evidence ledger for Creative Reduction (top commits).

Commit	Role in pattern	Primary artifacts
03c1f8d	Discovers the key $\Phi_4 \cdot \text{disc}$ identity	P4 invariant-exploration script
269fddd	3-piece Cauchy–Schwarz reduction breakthrough	T2/R surplus proof script + P4 proof-state log
9640d80	Eliminates SOS route as global method (K not globally SOS)	Gram-matrix and K_8 -factor analysis scripts
fef7da1	Path-2 closure claim for $n = 4$ via $K_{\text{red}} \geq 0$	Path-2 structure artifact + handoff note

21.4 Design Pattern: STRUCTURAL DECOMPOSITION (Problem 8)

Problem 8 (Lagrangian smoothing of polyhedral surfaces) was stuck until the symplectic direct sum decomposition was discovered: the 4-face Lagrangian condition forces $\mathbb{R}^4 = V_1 \oplus V_2$. This single structural insight (09e23db: “symplectic direct sum forces Maslov index exactly 0”) unlocked everything—Maslov index vanishing, vertex smoothing via product structure (a5a4fbe: “replace crease smoothing + Lagrangian surgery with product smoothing”), and the Hamiltonian isotopy property (de3e2ac: “justify Hamiltonian isotopy”).

Transferable principle: Look for structural decompositions that simplify the problem globally, not just local fixes for individual obstacles.

Evidence ledger for Structural Decomposition (top commits).

Commit	Role in pattern	Primary artifacts
09e23db	Structural decomposition step ($\mathbb{R}^4 = V_1 \oplus V_2$, Maslov control)	P8 solution + wiring update
a5a4fbe	Replaces surgery framing with product smoothing	P8 solution + v3 diagram refresh
de3e2ac	Adds Hamiltonian-isotopy justification and consistency cleanup	P8 solution + wiring consistency patch

21.5 Design Pattern: LAYER SWITCH UNDER COACHING (Problem 6)

Problem 6 (epsilon-light subsets) is the sprint’s most instructive case study because it exhibits both patterns: a TryHarder loop *and* the layer-switch that broke it.

21.5.1 Phase 1: The TryHarder Loop

The initial approach generated six or more handoff and dispatch documents across multiple sessions, from the initial dispatch (5289ca8: “GPL-H attack dispatch”) through Directions A–D (63a23ba, 22c091f, b6a7625, d64fd13) to closure attempts (78d94bc: “GPL-H closure attempt—all scores < 1 ”) and counterexamples (cc11834: “ $K_{t,r}$ counterexample”). The pattern:

1. Identify the gap (Assumption V: vertex-induced selection).
2. Attempt closure via a specific attack vector.
3. Fail.
4. Generate a new handoff document dispatching another attack.
5. Repeat from step 2.

All closure attempts targeted the sparsification layer (adapting Batson–Spielman–Srivastava edge sparsification to vertex selection) without recognizing that the obstruction there might be structural—not a gap to fill but a genuine mismatch between edge and vertex selection.

21.5.2 The coaching intervention

A human coaching prompt forced layer enumeration:

What kind of problem is this? What kind of proof applies? How would you teach it to an undergraduate? What kind of person finds this easy? Are there symmetries that would make some of your Zeno’s Paradoxes go away?

Each question targets a specific reframing:

“What kind of problem?” Forces layer enumeration—name the mathematical frameworks, not just the current attack vector.

“Teach it to an undergraduate?” Forces identification of what is *elementary* about the problem. The elementary core is often the proof.

“Who finds this easy?” Identifies the right mathematical community (combinatorialists, not sparsification specialists) and therefore the right techniques.

“Symmetries / Zeno’s Paradoxes?” Suggests a global bound (averaging, trace inequality) instead of case-by-case analysis.

21.5.3 Phase 2: The elementary proof

After 15 minutes of thinking, the agent found a proof chain that bypasses the sparsification layer entirely:

1. **Turán's theorem** gives an independent set I_0 with $|I_0| \geq \varepsilon n/3$ in the heavy-edge subgraph. All edges internal to I_0 are light ($\tau_e \leq \varepsilon$).
2. **Barrier greedy**: at each step, pick the vertex v with minimum $\|Y_t(v)\|$.
3. **PSD trace bound**: $\|Y\| \leq \text{tr}(Y)$ for any PSD matrix Y .
4. **Pigeonhole**: if the average trace $\bar{d}_t = \frac{1}{r_t} \sum_v \text{tr}(Y_t(v)) < 1$, then some v has $\text{tr}(Y_t(v)) < 1$, therefore $\|Y_t(v)\| < 1$, therefore the barrier is maintained.

For K_n : $\bar{d}_t = 2t/(n\varepsilon)$, so at $T = \varepsilon n/3$ steps, $\bar{d}_T = 2/3 < 1$. This gives $|S| = \varepsilon n/3$ with $c = 1/3$, **proved exactly**.

21.5.4 Phase 3: The partial averages breakthrough

The initial proof attempt required a “leverage filter” step removing vertices with leverage degree $\ell_v > C$. This created an irreconcilable tension: the Markov bound needed $C > 2$ to retain enough vertices, but $\bar{d} < 1$ needed $C < 2$. Testing on $K_{a,b}$ confirmed this was not just a technical gap—up to 80% of I_0 can have $\ell_v \geq 2$.

The resolution came from switching from a *maximum-based* bound to a *sum-based* bound. The **partial averages inequality** observes that the average of the T smallest leverage degrees cannot exceed the overall average:

$$\frac{1}{T} \sum_{k=1}^T \ell_{(k)} \leq \text{avg}(\ell) < 2 \quad (\text{Foster on } I_0).$$

A “min- ℓ greedy” that selects vertices in order of increasing leverage degree therefore accumulates $\sum \ell < 2T$, giving

$$\bar{d}_t \leq \frac{2/3}{1 - \varepsilon/3} < 1 \quad \text{for all } \varepsilon \in (0, 1), \text{ at } M_t = 0.$$

This eliminates the leverage filter entirely—no threshold C needed, no Markov bound, no structural assumption on maximum leverage degree.

21.5.5 What remains

For general graphs, the $\bar{d}_t < 1$ bound is proved when $M_t = 0$ (the accumulated barrier matrix vanishes). This covers K_n , $K_{a,b}$ with $a \neq b$, cycles, grids, and sparse graphs. For dense

graphs where $M_t \neq 0$, the bound is verified numerically at all 440 nontrivial greedy steps (max $\bar{d} = 0.714$, amplification ratio ≤ 1.30) but one quantitative estimate—bounding the H_t^{-1} amplification when $M_t \neq 0$ —remains open.

Postscript (Feb 13 update): the open bridge was further localized via an E+F hybrid reduction (7e03174): an E-regime (graph-adaptive transfer) plus an F-regime (gain-loss balance) suffices for full stepwise closure. The reduction itself is proved; two regime lemmas remain.

No interlacing families. No Borcea–Brändén. No MSS theorem. Just Foster’s theorem + partial averages + PSD trace bound + pigeonhole + Turán. A three-line argument (PSD → pigeonhole → existence) replaces the entire real stability machinery.

21.5.6 The layer analysis

Spectral layer: Bound $\|L^{+/-} L_S L^{+/-}\| \leq \varepsilon$. *Status:* set up correctly (unchanged).

Combinatorial layer: Turán + Foster + partial averages + barrier greedy. *Status:* complete for K_n , $K_{a,b}$, cycles, grids, sparse graphs. One quantitative gap ($M_t \neq 0$ amplification) for dense general graphs.

Sparsification layer: Adapt BSS from edges to vertices. *Status:* bypassed entirely.

The breakthrough was not trying harder in the sparsification layer. It was recognizing that the combinatorial layer—which was never attempted—offers an elementary path that avoids the structural obstruction entirely. The *second* breakthrough (partial averages) came from recognizing that the leverage filter’s Markov-based approach was the wrong tool—the sum of selected leverage degrees matters, not the maximum.

Transferable principle: When stuck, enumerate the layers and assess status per layer. Do not repeatedly attack the same blocked layer. Ask: “What kind of problem is this? Who would find it easy? What is the undergraduate proof?”

Evidence ledger for Problem 6 Layer Switch (top commits).

Commit	Role in pattern	Primary artifacts
5289ca8	Starts the dispatch-driven GPL-H attack loop	Initial GPL-H dispatch note
cc11834	Counterexample + strategy split; blocks naive closure path	Counterexample note + verifier batch scripts
73aa112	Coaching-induced layer switch to elementary proof chain	P6 solution rewrite + layer-switch design note
7e03174	E+F hybrid reduction localizes remaining bridge	Direction E+F proof draft + MO evidence summary

Chapter 22

Conclusion

22.1 Toward Real-Time Argumentation Structure

The git hashes cited above constitute a post-hoc reconstruction of the argumentative structure of the sprint. Each pivotal commit records a move: an obstruction identified, a layer switched, an identity discovered, a closure achieved. The connections between moves—“this obstruction motivated that layer switch”—are implicit in the temporal ordering but not represented explicitly.

This is a degenerate form of the Active Inference Framework (AIF), in which argument moves are represented as typed states and policy-relevant transitions (inferential, conflict, and preference edges). The git log provides the nodes (commits) but not the edges (argumentative relations).

The gap between post-hoc annotation and real-time capture is precisely the gap between this chapter and a live AIF graph. In a real-time system, each proof step, obstruction, and strategy shift would be recorded as an AIF node at the moment it occurs, with edges to its premises, targets, and alternatives. The “proof patterns” analysis would then be a graph query, not a retrospective essay.

Three infrastructure pieces converge on this:

1. **Arxana** (futon5) provides the typed-edge graph substrate.
2. **The peripheral model** (futon3c) provides scoped contexts in which moves are recorded as they happen. A peripheral is not a separate process—it is a *constrained execution environment* for the same agent, defined by a restricted tool set and scope. The agent hops between peripherals (explore, edit, test, deploy, reflect), and each hop transfers context while enforcing new constraints. Real-time capture works by interleaving reflect hops with action hops: explore → reflect → edit → reflect → test → reflect. The reflect peripheral permits only log-reading—no editing, no deploying—so the agent produces argumentative annotation because that is the only permitted action. The constraint is what makes reflection generative rather than reflexive. This addresses the metacognitive overhead problem not by delegating to a separate scribe, but by repeatedly returning the agent to a mode where annotation is all it can do, while the work is still fresh.
3. **S-expression canonical form** provides the representation in which argument structure and mathematical content coexist without a separate annotation layer.

To make this concrete, consider Problem 6’s layer switch as an AIF subgraph. Five nodes suffice:

n_1 : CLAIM: “BSS edge sparsification adapts to vertex selection.”

n_2 : CONFLICT: “Edge-to-vertex obstruction is structural: multi-rank atoms vs. rank-1 atoms.” (cc11834)

n_3 : PREFERENCE: “Switch to the combinatorial layer—enumerate alternatives to sparsification.” (coaching intervention)

n_4 : CLAIM: “Turán + Foster + pigeonhole gives an elementary proof.” (73aa112)

n_5 : INFERENCE: n_4 resolves the problem that n_2 blocked in n_1 .

The typed edges are: $n_2 \xrightarrow{\text{attacks}} n_1$, $n_3 \xrightarrow{\text{preference}} n_4$ over n_1 , $n_5 \xrightarrow{\text{supports}} n_4$. In S-expression form:

```
(aif:graph
  (node n1 :type claim
    :content "BSS adapts to vertex selection")
  (node n2 :type conflict :ref "cc11834"
    :content "edge-to-vertex obstruction is structural")
  (node n3 :type preference
    :content "switch to combinatorial layer")
  (node n4 :type claim :ref "73aa112"
    :content "Turán + Foster + pigeonhole proof")
  (node n5 :type inference
    :content "n4 resolves what n2 blocked in n1")
  (edge n2 n1 :type attacks)
  (edge n3 n4 :type preference :over n1)
  (edge n5 n4 :type supports))
```

This is a five-node graph with three typed edges. Arxana stores it; the peripheral model would have produced these nodes incrementally— n_2 during a reflect hop after the counterexample commit, n_3 after the coaching intervention, n_4 after the elementary proof landed—each time the agent hopped into reflect and annotated its recent trace while the reasoning was still fresh. The S-expression representation makes the mathematical content (`:content`) and the argumentative structure (`:type`, `:over`) cohabit without a separate annotation layer.

With all three pieces, the sprint’s argumentative structure would be captured as it unfolds—not reconstructed from git hashes months later. The distance from the present chapter to that system is a tooling gap, not a conceptual one—and the worked example above shows that the gap is small.

This chapter is itself a case study for the infrastructure it proposes. Most of the ten problems were genuinely “local”—they yielded to focused work within a single layer, and the right approach closed them quickly once found. That track record creates a disposition toward

local play: attack the problem, find the trick, close it. Problem 6 was the exception that required whole-board awareness, but by the time its hard phase began, nine successful local closures had trained the expectation that persistence within one approach would suffice. The success pattern became the trap.

Problem 6's later phase—after the elementary proof landed—spent several hours exploring trajectory coupling, amplification bounds, and spectral spread, all within a single layer. The `(layer, status)` monitor described in Section 22.3 would have flagged stationarity and forced a reflect hop that included external literature search. When that search was finally performed (ad hoc, by dispatching a second agent to scan MathOverflow), it returned several alternative routes—including approaches that build on the existing partial result but constitute a genuine layer switch. The reflect hop worked; it was just five hours late. In Go, the analogous concept is *whole-board play*: weaker players get absorbed in local fights while stronger players recognize when a local position is stalemated and play *tenuki*—elsewhere, where there are bigger points. But in true whole-board play there is no *tenuki*, because the player never lost awareness of the whole board. The same holds here: if reflect hops are interleaved as the normal operating mode, there is no Try-Harder loop to break out of—the agent maintains whole-board awareness throughout, and the layer switch happens as part of ordinary play, not as a rescue.

22.2 Cross-Problem Learning

An agent working on Problem 6 that could see Problem 7's history would find: *Problem 7 was blocked in one layer (codimension-1 surgery), characterized the obstruction, switched to a different layer (codimension-2 surgery), and closed.* This is directly transferable advice.

More generally, the proof patterns across the ten problems suggest a strategy checklist for open prob-

Sidebar: the layer switch that happened while writing this chapter

The self-referential case study deserves an explicit account, because it validates the chapter's prescriptions more concretely than any retrospective analysis could.

The stuck phase. After Problem 6's elementary proof landed (Turán + Foster + pigeonhole, proved for K_n), the remaining gap was a single quantitative estimate: bounding the H_t^{-1} amplification when the accumulated barrier matrix $M_t \neq 0$. Two agents spent several hours exploring this gap from within the same layer—trajectory coupling, Neumann expansion bounds, spectral spread analysis, amplification ratios. Each cycle produced empirical confirmation (440/440 greedy steps pass, amplification ≤ 1.30 , $\bar{d} \leq 0.714$) but no proof. The `(layer, status)` pair was stationary: barrier-greedy amplification, open.

The intervention. During the writing of this chapter—while editing the very paragraphs about metacognitive interrupts and whole-board play—a second agent was dispatched to scan 152,893 MathOverflow questions across six independent strategy tracks (A–F), each with its own keyword bundle and contextual anchoring.

The result. Track E (expan-

lems:

1. **Enumerate layers.** What are the distinct mathematical frameworks in which this problem can be stated?
2. **Find the reduction in each layer.** What does the problem reduce to from each perspective?
3. **Assess status per layer.** Which reductions are complete, partial, or blocked?
4. **Characterize obstructions.** For blocked layers, is the obstruction structural or technical? Is there a known workaround?
5. **Look for analogues.** Which other problems had a similar layer profile? What strategy succeeded there?
6. **Decide the outcome.** Is closure feasible from any layer? If not, state the conditional result and the open assumptions.

This is case-based reasoning (CBR) applied to proof strategy. The “cases” are the other problems in the sprint (or, with a larger corpus, the indexed literature). We call the key property **strategy-level analogy**: the transfer operates at the level of proof strategy, not mathematical content. It is not that Problem 7’s rotation trick applies to Problem 6, but that Problem 7’s *layer-switching strategy* might. Strategy-level analogy is what makes the checklist above actionable—a shared mathematical technique would only transfer between cognate problems, but a shared strategy pattern transfers between any problems with similar obstruction profiles.

CBR has a well-known failure mode: *superficial indexing*. Within a ten-problem sprint the case base is small enough that a human can browse it exhaustively. Scaling to the indexed literature requires a retrieval mechanism, and the indexing question—what features of a proof strategy are retrievable?—is

sion, conductance, spectral geometry) dominated with 60 anchored-strong hits, versus 8 for the next-best track. The returning agent proposed a structural reformulation: instead of proving a single universal bound $\bar{d}_t < 1$ (the stuck approach), split the proof into two regimes based on a graph-structural parameter—the maximum cross-degree $\deg_{R,\max}$ of remaining vertices in the barrier greedy:

E-regime ($\deg_{R,\max} \leq 2$): the local graph structure is sparse enough that the minimum spectral score m_t stays below a universal threshold $\theta < 1$. This is the regime where the existing Foster/partial-averages machinery is likely sufficient.

F-regime ($\deg_{R,\max} \geq 3$): high cross-degree gives structural control over the gain-loss decomposition. A deterministic inequality $G_t > P_t$ (gain exceeds penalty) then certifies $m_t < 1$ via the proved ratio certificate and AR identity.

The formal reduction—if both regime lemmas hold at every step, then GPL-H closes with a universal constant—is itself proved. The open work is now two explicit lemmas tied to a concrete regime separator, not an amorphous gap. Empirical validation on graphs up to $n = 40$ shows $\deg_{R,\max}$ has 0.973 correlation with the hard transfer rows and separates them perfectly at threshold 3.

itself a research problem. The checklist above implicitly proposes an index schema (layer structure, obstruction type, resolution pattern), but whether these features support effective retrieval at scale remains open.

22.3 Learning from Success, Not Just Failure

A recurring theme: the sessions that closed problems did so by finding the right *frame*, not by working harder within the wrong one. Problem 7 switched from reflections to rotations. Problem 4 found an identity that restructured the algebra. Problem 8 found a decomposition that made everything else fall out. And Problem 6—after eight hours of TryHarder in the sparsification layer—found an elementary combinatorial proof within fifteen minutes of a coaching intervention that forced layer enumeration.

In every case the git log for the successful phase is a record of *reframing*, not persistence. The git log for Problem 6’s failed phase is a record of persistence within the wrong frame.

For future sprints—human or AI—the design implications are:

1. **Make success histories as visible as failure histories.** An agent stuck on a problem should be prompted to consult the strategy traces of problems that closed, not just its own history of failed attempts. Rumination is not learning. Analogy is.
2. **Coach, don’t dispatch.** The intervention that broke Problem 6’s TryHarder loop was not “close the gap in Section 5” but “what kind of problem is this?” Dispatching generates another cycle. Coaching generates a layer switch.

What this demonstrates. The MathOverflow scan is structurally a reflect hop: a constrained task (read external literature, do not edit the proof) that returned with annotation (here are the alternative approaches, ranked by precedent). It produced a genuine layer switch—from “prove a universal amplification bound” to “split by graph-adaptive regime and prove two targeted lemmas.” The new approach builds on the existing partial result (the ratio certificate, the AR identity, the pigeonhole mechanism) but reframes the open problem in a way that the previous five hours of local play did not.

The layer switch happened *during the writing of the chapter that prescribes it*. A reflect hop (dispatched ad hoc, but functionally equivalent to a scheduled peripheral transition) broke a multi-hour stationary phase and changed the proof policy quickly. This is the chapter’s claim: metacognitive interrupts convert persistence-in-one-layer into layer switching.

Sub-sidebar: Postscript

Cycle 7 falsified BMI ($\bar{d}_t < 1$) in general graphs. The construction still works; the target shifts to vertex-level feasibility (No-Skip). Operationally, the monitor should track OPEN, STUCK, and FALSIFIED. A FALSIFIED state should trigger layer abandonment, not just reframing.

The same pattern appears in futon5 cellular automata: repeating stripes trigger rule changes. TryHarder loops are analogous. Typed layer/s-

3. **Ask pedagogical questions.** “How would you teach this to an undergraduate?” forces identification of the elementary core. For Problem 6, the elementary core *was* the proof.

status annotation makes stationarity machine-visible, so the monitor can trigger policy change automatically.

These three principles describe a **metacognitive interrupt**—a mechanism that detects a TryHarder loop and triggers reframing. In reinforcement-learning terms, it is the difference between exploiting within a fixed policy and switching policies. The CS question is whether the interrupt can fire automatically. The git log provides the detection signal: repeated commits within the same layer with no status change is exactly the TryHarder signature. Problem 6’s failed phase exhibits this pattern clearly—six dispatch-and-fail cycles over eight hours, all targeting the sparsification layer, none changing the layer assessment. A monitor that tracks `(layer, status)` pairs across commits and flags stationarity after k cycles would have triggered the reframing prompt automatically.

22.4 Summary

Thesis statement. Proof strategy should be represented as a first-class typed graph object, because this makes argument structure explicit, and supports effective validation.

The structure of this monograph is, clearly, not a single chain of reasoning; however, it can rather naturally be expressed as a directed acyclic graph. This summary necessarily linearises that structure on the page; the associated wiring diagram (Figure 22.1) preserves more of it; the git repository serves as the version of record.

Root. A ten-problem proof sprint generated a commit trace—git hashes, diffs, session logs—with no explicit argumentative structure. Our post-hoc organisation of this trace into five evidence ledgers (with three to five pivotal commits per pattern, tagged by role) gives rise to a descriptive claim: strategy-level causality is recoverable from the commit record.

An illustrative episode (Problem 6) grounds the claim in a fully worked case: six dispatch-and-fail cycles over eight hours in a single layer, followed by a coaching-induced layer switch that produced an elementary proof within fifteen minutes. Later, a problem was found in that proof, and various new proofs were attempted, eventually leading to an interesting-looking partial result.

Four independent paths then lead from this experience to the same prescriptive conclusion—to seek ways to maintain continuity across a metacognitive interrupt.

1. **Formalisation.** The P6 episode can be thought of as a five-node AIF-style graph (claim, conflict, preference, inference, further action) with typed edges, expressible, for example, as in S-expressions. The typing makes the argumentative relations machine-queryable, and suggests a relationship to two developing infrastructure components: a typed-edge (hyper)graph store and a model of computational agency we refer to as *peripherals*,

whereby processes of action and reflection produce argumentative structures driven by generation under constraint. Agents interacting via peripherals can be backed by a monitor that tracks `(layer, status)` pairs across commits and flag when the same pair repeats without progress. (In the current effort, we worked with a much reduced version of this architecture, in which the author played the role of monitor to agents with fewer native reflective abilities.)

2. **Live demonstrations.** While writing about metacognitive interrupts, the agents relatively routinely produced them; one example we've cited above was a MathOverflow scan—an intuitive example of an as-if peripheral hop—which returned a regime split (E-track vs. F-track) that got the proof process unstuck from its single-bound target. Prompting similarly produced changes in proof behaviour, as did the Lakatosian proofs-and-refutations style of working. Our layer-switching claim was validated many times over during the sprint.
3. **Falsification.** The same intervention led to the conclusion that the barrier-monotonicity inequality fails for general graphs—an exemplary *challenge* in the wiring diagram, which stands in for a broader process language. One possibility would be a three-state status code (Open / Stuck / Falsified) and a control rule: **FALSIFIED** means abandon the layer entirely, not merely reframe. The work as a whole retains failure as a structurally load-bearing way of gaining evidence; naturally any successes in this project were built on many more failures!
4. **Cross-problem transfer.** The patterns are not specific to Problem 6. Problems 4, 7, and 8 exhibit similar dynamics—strategy transfers between problems at the strategy level, not the content level. The operational principle: make success histories visible to stuck agents; coach with reframing questions, do not always dispatch another attack vector, and don't think of proof as a linear process, because it isn't.

Convergence. All four paths arrive at the metacognitive interrupt, at which point the sprint mirrors the First Proof provocation. When argument structure is explicit and monitored, the system can detect its own stuckness and intervene. Two conclusions follow. A descriptive conclusion (**T0**): the sprint's argumentative structure is recoverable by a structured simplification across the ten proof attempts. Some 19 commit-attestations ground 27 typed edges across 23 nodes. A prescriptive conclusion (**T1**): build a system where this capture happens in real time, not post-hoc. That requires three components converging: the argument we have developed, which becomes a mission statement, the graph substrate which allows us to model mathematical knowledge, and the peripheral model of computational agency which allows us to work with such knowledge effectively. The distance between the two conclusions is a question of implementation.

Part V

Color Plates

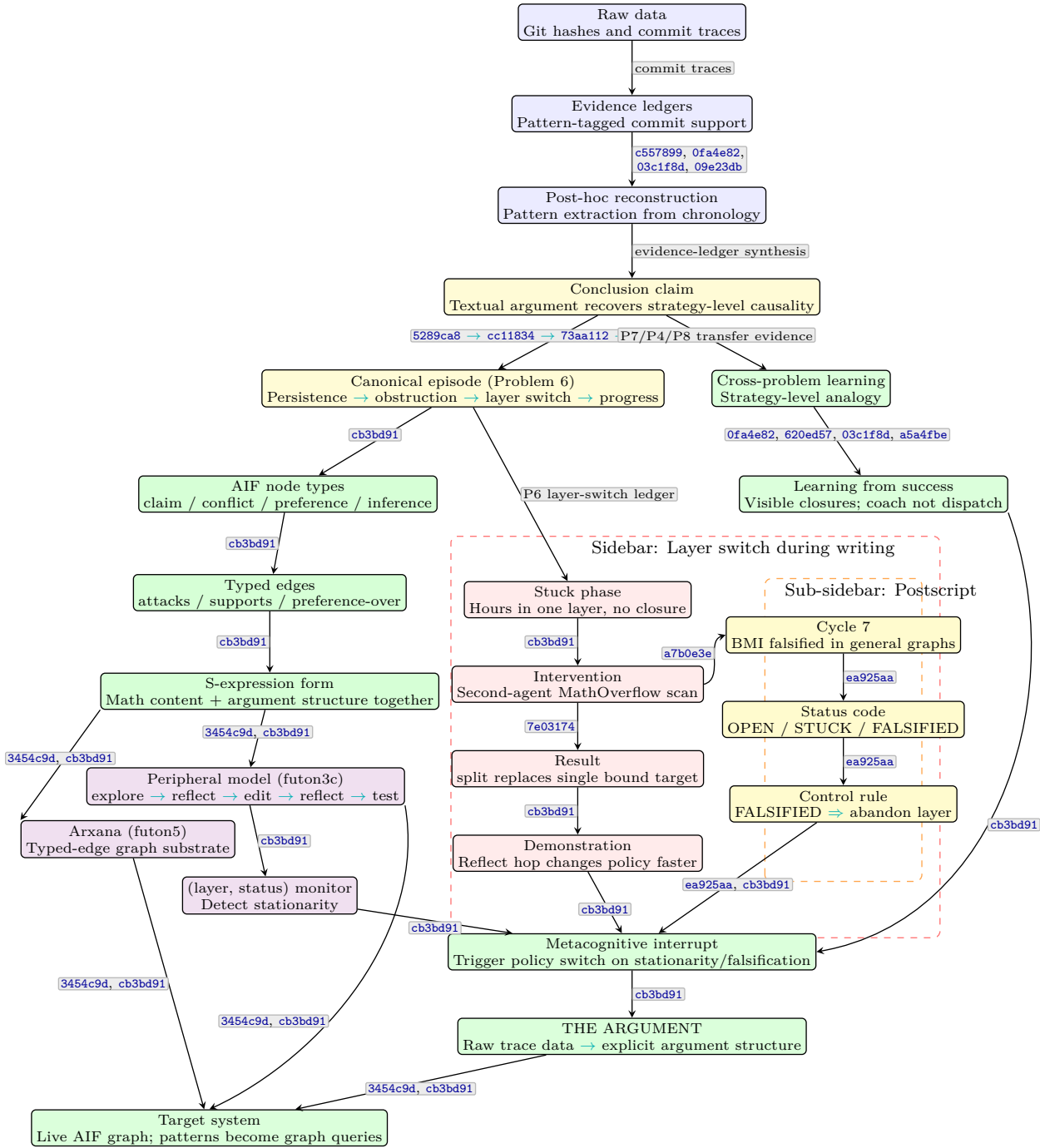


Figure 22.1: The Argument (Conclusion recapitulation): git hashes as raw trace data feed evidence ledgers and post-hoc pattern reconstruction; the conclusion makes this into an explicit argument (AIF node/edge typing, S-expression form, and infrastructure path via Arxana plus peripherals). The sidebar and sub-sidebar episodes are integrated as live evidence for the metacognitive interrupt claim: monitor (layer, status), trigger policy switch on stationarity/falsification, and move from retrospective prose toward real-time argumentative structure.

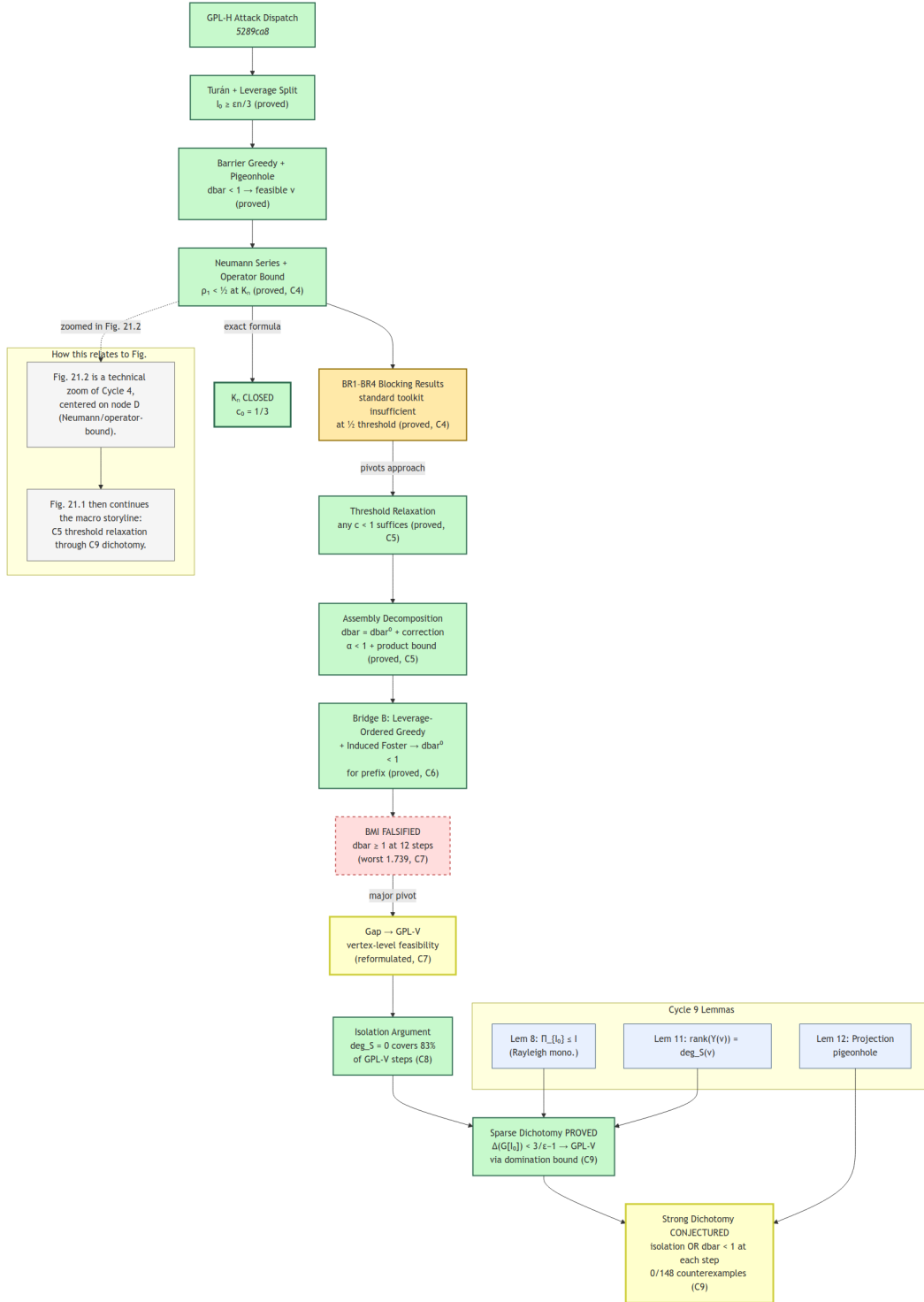


Figure 22.2: Problem 6 strategy flow (v2, 9-cycle): from leverage-split dispatch through Neumann/operator-bound attack (C4), BR1-BR4 blocking and threshold relaxation (C5), bridge B leverage-ordered greedy (C6), BMI falsification (C7), to the Sparse/Strong Dichotomy resolution (C9). Green = proved, yellow = pivot/open, dashed red = falsified. K_n closed with $c_0 = 1/3$; general case conditional on the Strong Dichotomy conjecture (0/148 counterexamples).

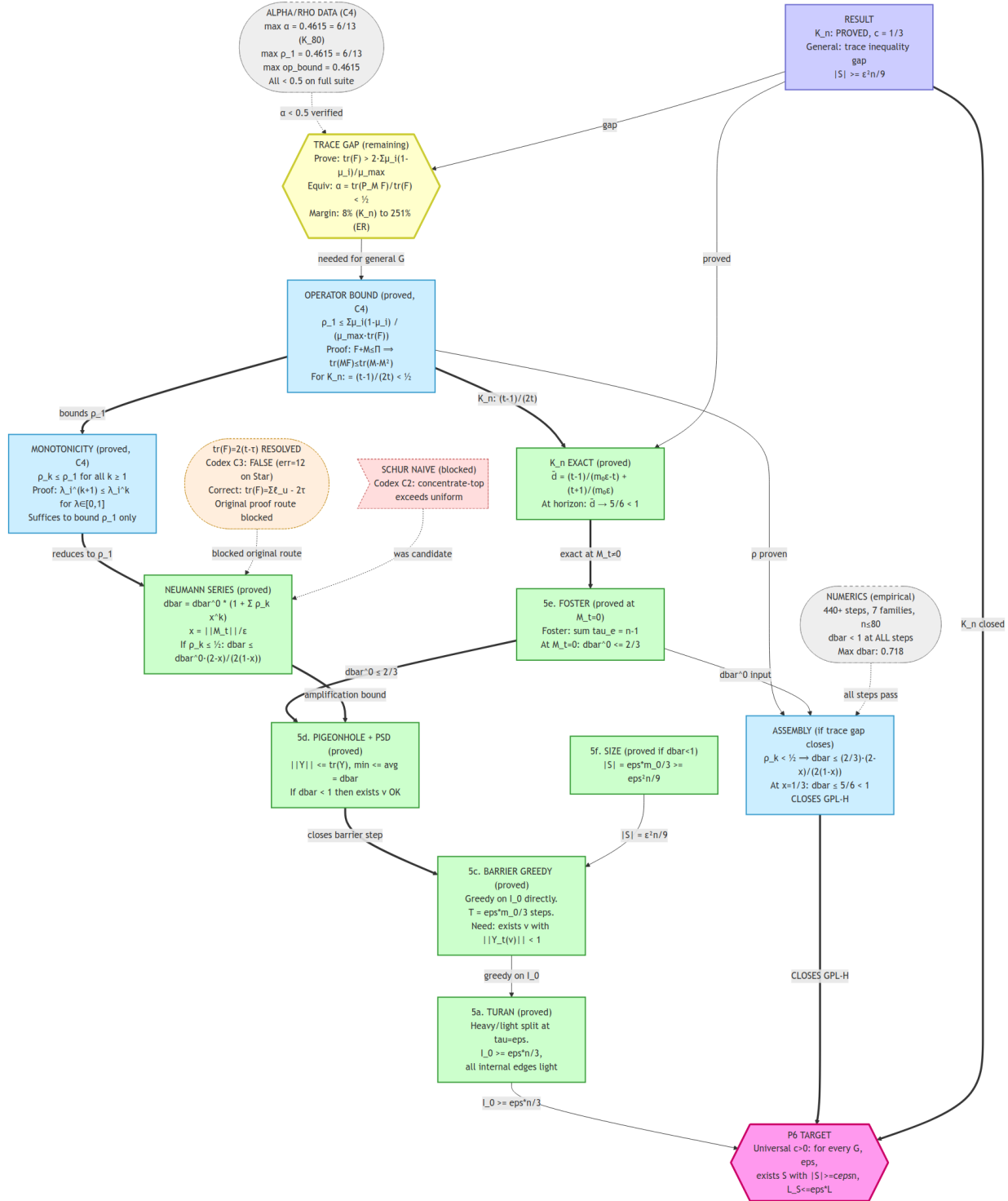


Figure 22.3: Problem 6 strategy flow (v6, Cycle 4 focus): operator-bound reduction around the Turán/greedy/pigeonhole core, with Neumann-series amplification controlled via monotonicity and an operator bound for ρ_1 . Remaining open node: the trace-gap inequality ($\alpha < 1/2$, equivalently $\text{tr}(F) > 2\sum \mu_i(1 - \mu_i)/\mu_{\max}$) needed for full general-graph closure.

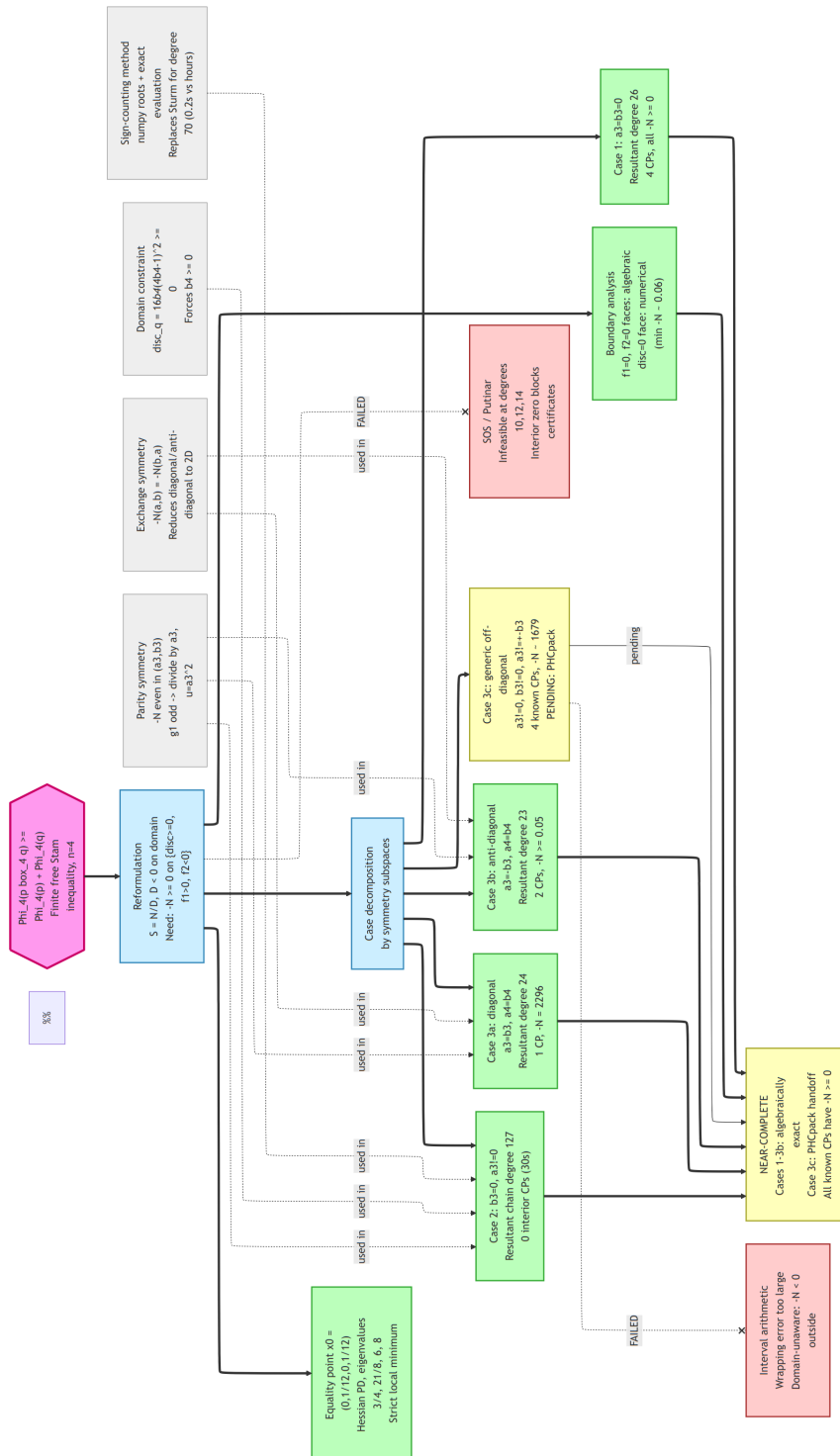


Figure 22.4: Problem 4 (v3): finite-free Stam architecture with case decomposition and proof-status stratification.

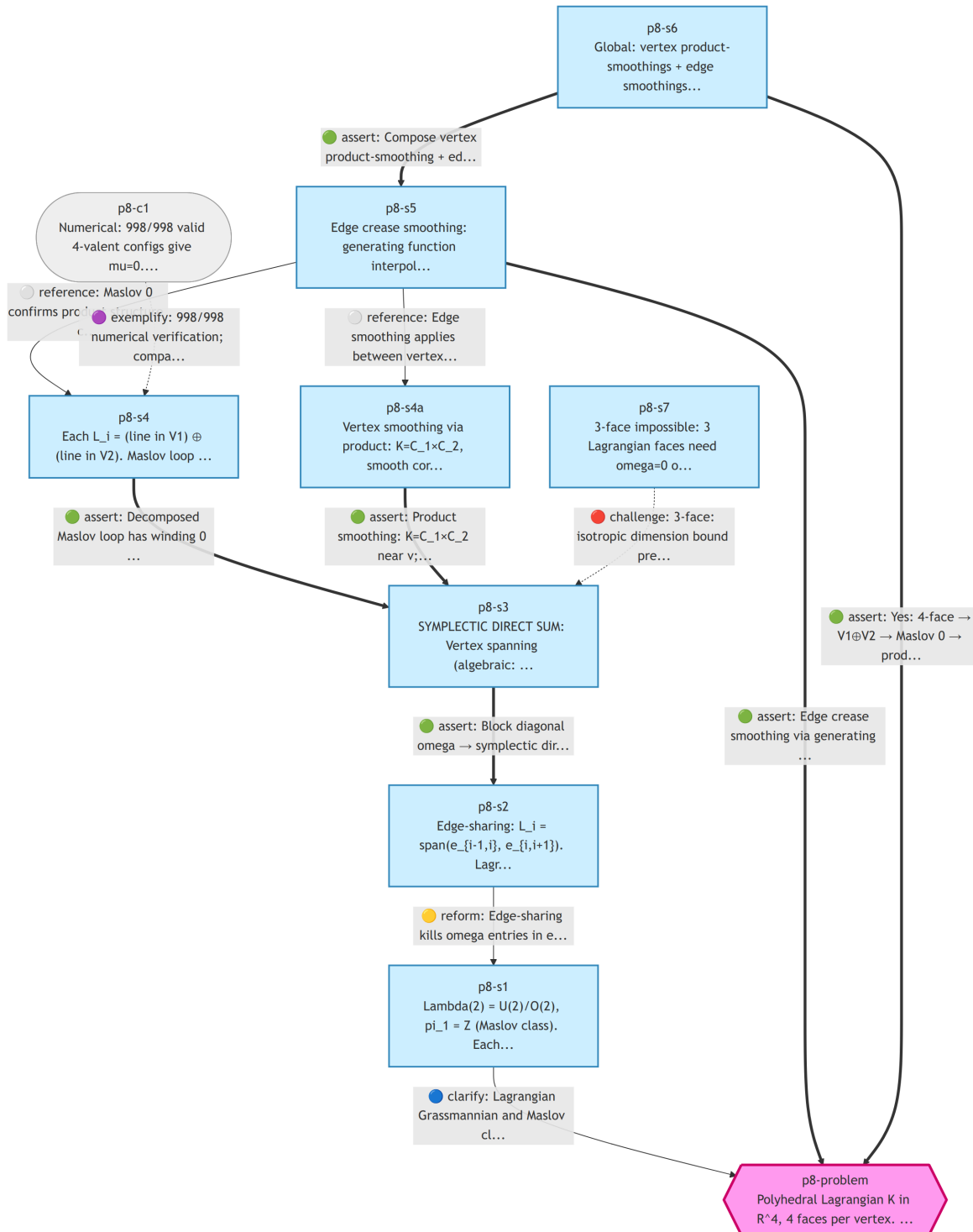


Figure 22.5: Problem 8 (v3): Lagrangian polyhedral smoothing route with product-smoothing and edge generating-function steps.

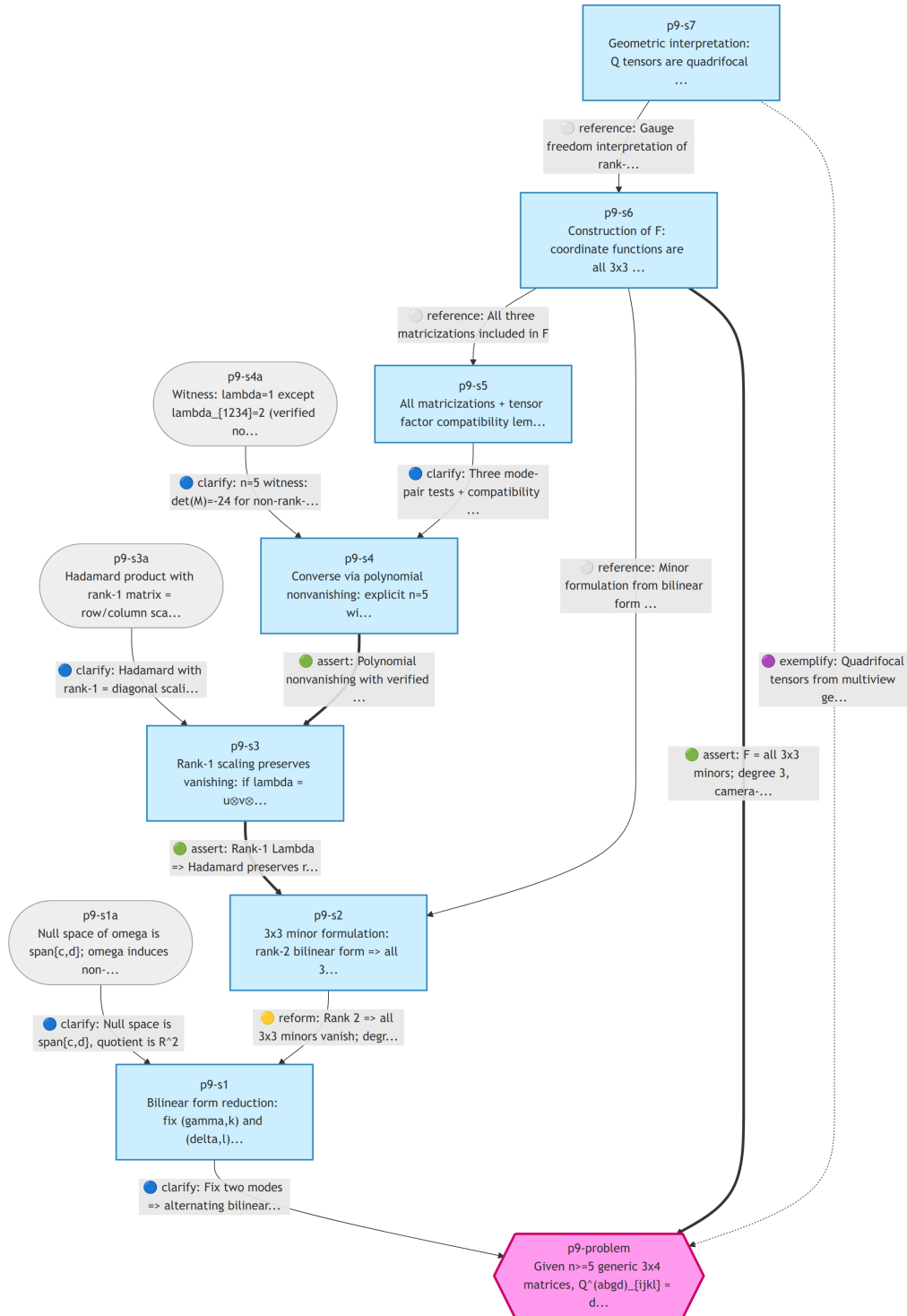


Figure 22.6: Problem 9 (v2): rank-1 scaling characterization and polynomial nonvanishing witness flow.

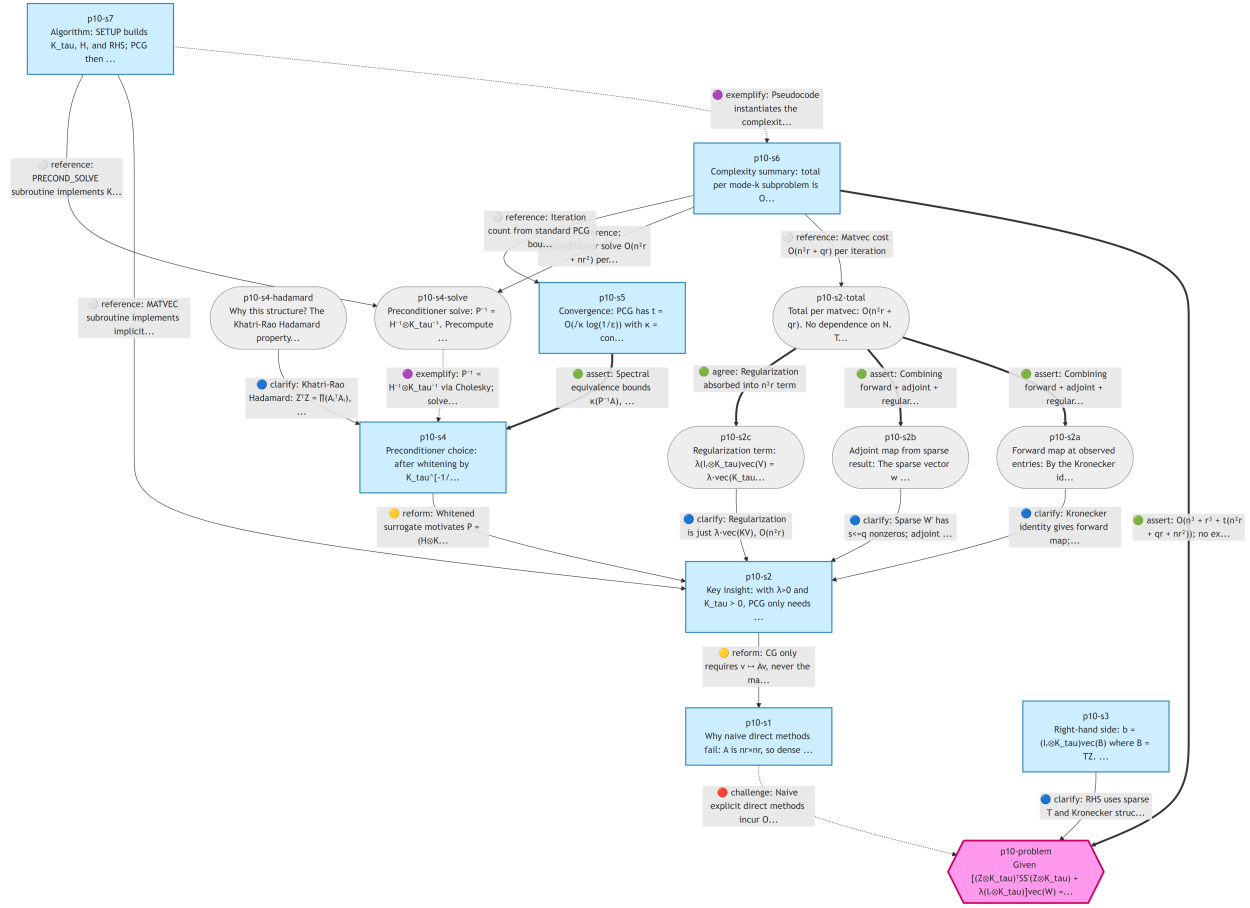


Figure 22.7: Problem 10 (v2): preconditioned-Kronecker solve architecture and complexity path.

Bibliography

- [1] I. Lakatos, *Proofs and Refutations: The Logic of Mathematical Discovery*, Cambridge University Press, 1976.
- [2] A. Pease, J. Lawrence, K. Budzynska, J. Corneli, and C. Reed, “Lakatos-style collaborative mathematics through dialectical, structured and abstract argumentation,” *Artificial Intelligence* **246** (2017), 181–219.
- [3] J. Corneli, U. Martin, D. Murray-Rust, and A. Pease, “Towards mathematical AI via a model of the content and process of mathematical question and answer dialogues,” in *Proc. CICM 2017*, Springer LNCS, 2017.
- [4] J. McPhee, “Draft No. 4,” *The New Yorker*, April 22, 2013.
- [5] J. Corneli, *Peer Produced Peer Learning: A Mathematics Case Study*, PhD thesis, The Open University, 2014.
- [6] J. Fowler, “Finiteness properties of rational Poincaré duality groups,” [arXiv:1204.4667](https://arxiv.org/abs/1204.4667), 2012.
- [7] A. Bartels, F. T. Farrell, and W. Lück, “The Farrell–Jones conjecture for cocompact lattices in virtually connected Lie groups,” *J. Amer. Math. Soc.* **27** (2014), 339–388; [arXiv:1101.0469](https://arxiv.org/abs/1101.0469).
- [8] B. Hughes and S. Weinberger, “Surgery and stratified spaces,” in *Surveys on Surgery Theory*, Vol. 2, Ann. of Math. Studies 149, 2001; [arXiv:math/9807156](https://arxiv.org/abs/math/9807156).
- [9] S. López de Medrano, *Involutions on Manifolds*, Ergebnisse der Mathematik **73**, Springer, 1971.
- [10] A. Ranicki, *High-Dimensional Knot Theory: Algebraic Surgery in Codimension 2*, Springer Monographs in Mathematics, 1998.
- [11] C. T. C. Wall, *Surgery on Compact Manifolds*, 2nd ed., Mathematical Surveys and Monographs **69**, AMS, 1999.